Chapter 5. Modifications of Polyethyleneimine with Short Chain Aliphatic acids and ω-Amino Aliphatic acids as Gene Carrier

I. INTRODUCTION

Delivery of exogenous gene in to target eukaryotic cell has been extensively studied using viral and non-viral vectors. Various viral vectors such as adenovirus, adeno-associated virus and retrovirus vectors have very high transfection efficiency but suffer from various drawbacks such as generation of immune or toxic reactions and insertional mutagenesis within host (1). To avoid such drawbacks during gene delivery various non-viral gene delivery vectors viz. cationic polymer based vectors (Polyplexes) and cationic lipid based vectors (lipoplexes) are developed. Ever since the design of Lipofection by Felgner et al in 1987 and formulation of lipoplexes (2), the focus of researcher worldwide has remarkably shifted towards non-viral vectors for gene delivery. Non viral vectors are relatively safer but have low transfection efficiency; unlike viral vectors which due to evolution of many years have excellent ability to overcome various cellular and intracellular barriers including nuclear barriers (3, 4).

Polyethyleneimine PEI, a cationic polymer, was first studied by boussif et al for functional gene delivery ability (5). PEI has very high cationic charge density as every third atom in PEI is ionisable nitrogen which is attributed to its ability to overcome various gene delivery barriers (6). PEI, like other cationic lipids and cationic polymers, forms complex with anionic pDNA by electrostatic interaction which leads to condensation of pDNA in form of nano to micro sized particles known as polyplexes. This electrostatic interaction between PEI and pDNA leads to neutralization of ~90% anionic charge of pDNA which in turn prevents repulsion that occurs between naked pDNA and negatively charged cell membrane, and hence enhance its internalization. Polymeric mass and hydrodynamic volume of branched PEI is much higher than that of linear PEI for same molecular backbone. As a consequence, branched PEIs have higher charge density compared to linear PEI. Ever since the discovery of PEI as gene delivery vector, various researchers have attempted to elucidate the mechanism of PEI mediated gene transfer.

Linear PEIs contain primary and secondary amine groups and have approximately 50% of the amine group protonated at pH = 7.4 (7); whereas, Branched PEIs have primary, secondary and tertiary amino groups in 1: 2: 1 ratio in its structure. The pKa value of these three types of amino groups spread across whole physiological pH range due to which PEI never remain fully protonated at physiological pH. Degree of

protonation of these amino groups increase from approximately 20% up to 45%, as surrounding pH decreases from 7.4 (cytosol) to 5 (endosomal compartment) (8, 9). This increased protonation is responsible for buffering inside endosome and is known as Proton Sponge Effect. Initially, proton sponge effect hypothesis was based on theroy that PEI leads to osmotic rupture due to its buffer capacity and then subsequent escape in lysosome (10). However, later on, Godbey et al. found that the buffering process lacks lysosomal involvement during proton sponge. From their study it was found that buffering process leads to osmotic rupture of endosome prior to its fusion with lysosome (11). Another study confirmed this observation and in which it was found that due to protonation of PEI, acidification of vesicles occurs which in turn increases chloride ion uptake inside endosome and subsequently increase water intake which furthermore leads to swelling of endosomes and subsequent lysis. Collectively, these two latterly discovered observations of proton sponge mechanism are widely accepted in the field (12).

Molecular weight of PEI has effect on transfection efficiency as well as toxicity. Morimoto et al elucidated that high molecular weight (HMW) PEI possess high transfection efficiency but at the same time high cyotoxicity also. Whereas, low molecular weight PEI (LMW PEI) possess low transfection efficiency as well as toxicity compared to HMW PEI (13). Due to low toxicity of LMW PEIs they are more suitable for medical applications; given their transfection efficiency is improved. LMW PEIs are modified using endosome disruptive agent lysine-histidine peptide conjugated to 6-bromo hexanoic acid using ethylene diamine as a linker (14), poly(ε-caprolactone) to form diblock copolymer (15), lipoic acid to form reduction triggered conjugate (16), and other hydrophobic modification of LMW PEIs performed using Carboxylic acid NHS ester (17) and folate NHS ester (18), 1-iodo dodecane and 1-iodo hexadecane (19), fatty acid chlorides (20-22). Pluronic (23-25), PPO-PEO (polypropylene oxide- polyethylene oxide) (26), poly-γ-benzyl-L-GLuatamate (27), Cholesteryl chloroformate (28-33), and aliphatic acids such as caprylic acid, myristic acid, palmitic acid, stearic acid, oleic acid and linoleic acid (21). But issue related to low transfection efficiency of LMW PEI is not addressed well. In a previous study by Neamnark et al, LMW PEI, 2KDa, was modified using aliphatic acids such as using caprylic acid, myristic acid, palmitic acid, stearic acid, oleic acid and linoleic acid (21). Modification by long chain aliphatic acids causes reduction in solubility of PEI and hence preparation of their formulation in aqueous

phase becomes difficult. So as to avoid this difficulty and maintain high aqueous solubility of PEI 10KDa modifications using short chain aliphatic acids was performed. Additionally, PEI 10KDa was also modified using ω-amino group containing same aliphatic acid for comparison with short aliphatic acid modified PEI.

Therefore, in present investigation we have modified branched LMW PEI 10KDa so as to increase its transfection efficiency but at the same time maintaining its low cytotoxicity. PEI 10KDa has been modified using hexanoic acid, octanoic acid, ω-amino hexanoic acid and ω-amino octanoic acid. We have also investigated whether change in number of amino groups in PEI have any effect on transfection efficiency by comparing hexanoic acid and octanoic acid modified PEI with ω-amino hexanoic acid and ω-amino octanoic acid.

II. MATERIALS AND METHODS

A. Materials

POLYETHYLENEIMINE (Cat#: 19850, MW 10 000 99% Polysciences, Inc.), Hexanoic acid and Octanoic acid (Himedia, India), Boc-6-amino-hexanoic acid (BOC-6-AHX-OH, T15395, Sigma-Aldrich, St Louis, MO,USA), ω-amino-octanoic acid (BOC-8-AOC-OH, 14972, Sigma-Aldrich, St Louis, MO,USA), N,N'-Dicyclohexylcarbodiimide (DCC, HiMedia laboratories, India), N-Hydroxysuccinimide (NHS, HiMedia laboratories, India), 2,4,6-Trinitrobenzenesulfonic acid (TNBS, Sigma–Aldrich, St. Louis, MO, USA), Sodium dodecyl sulfate (SDS, Sigma–Aldrich, St. Louis, MO, USA), DMSO (Cell culture grade, HiMedia laboratories, India), Ampicillin (Cell culture grade, HiMedia laboratories, India), Kanamycin (Cell culture grade, HiMedia laboratories, India), Ethanolamine, EDTA, Tris·Cl (HiMedia laboratories, India), Agarose and Gel loading buffer (HiMedia Lic, India), DMSO (Cell culture grade, HiMedia laboratories, India), Ampicillin (Cell culture grade, HiMedia laboratories, India), Kanamycin (Cell culture grade, HiMedia laboratories, India), Ethanolamine, EDTA, Tris·Cl (HiMedia laboratories, India), Agarose and Gel loading buffer (HiMedia Lic, India), 4',6-diamidino-2-phenylindole (DAPI, Sigma–Aldrich, St. Louis, MO, USA), TriZol (Invitrogen Life Technologies), Triton® X-100 (ThermoFisher Scientific), PEG 8000 (Sigma–Aldrich). Other chemicals such as ethyl ether, methylene dichloride, Tetrafluroacetic acid, triethylamine, hydrochloric acid, sodium chloride, sodium

hydroxide, Sodium bicarbonate and Magnessium chloride were of analytical grade. Cell culture reagents such as FBS (Fetal bovine serum), Ethylene Bromide, DEPC (Diethyl pyrocarbonate), DMEM (Dulbecco's Modified Eagle's Medium), 3-(4,5-dimethylthiazol-2-yl)-2,5-diphenyltetrazolium bromide (MTT), Trypsin - EDTA Solution and 4% Paraformaldehyde in Phosphate Buffered Saline were purchased from HiMedia laboratories, India.

B. Preparation and Characterization of Short Chain Aliphatic Lipids and ω-Amino Aliphatic acids Substituted PEI 10KDa Polymers

1. Synthesis and characterization of hexanoic acid and octanoic acid conjugated PEI

Hydrophobic modifications of PEI (10KDa) were performed using various lipids namely; hexanoic acid (HA) and octanoic acid (OA) as well as ω-amino-hexanoic acid (ω-amino-HA) and ω-amino-octanoic acid (ω-amino-OA).

For synthesis of HA and OA modified PEI, N-acylation of 10 kDa PEI with commercially available lipid chlorides (Figure 5.1) was performed. The synthesis procedure was adopted from a previously described procedure. Briefly, lipid chloride was dissolved in 2 mL of DCM and added drop wise to PEI in 2 ml of DCM. The lipid: PEI amine ratio was selected in a way that one primary amine group per PEI molecule gets systematically substituted by one acid chloride to yield one amide bond formation. The mixture was allowed to react for 24 h at room temperature under nitrogen. Excess ethyl ether was added to precipitate and wash (×3) the polymers. This final polymer was dissolved in purified water and dialysis was performed against 0.1 M NaOH for 4 hr followed by dialysis against purified water for 10hr using dialysis membrane (Spectra/Por MWCO 6KDa, SpectrumLabs). Purified lipid conjugated PEI thus obtained was freeze dried and analyzed by 1H NMR (Bruker 300 MHz; Billerica, MA) in D2O. The characteristic proton shift of the lipids (δ ~0.8 ppm; -C*H*3) and PEI (δ ~2.5-2.8 ppm; -NH-*C*H2-*C*H2-NH-) were integrated, normalized for the number of Hs in each peak, and used to obtain the extent of lipid substitutions on the modified polymers. The modified polymers were also analyzed by FTIR (Bruker; Billerica, MA) for characteristic amide bond peaks by KBr disc method.

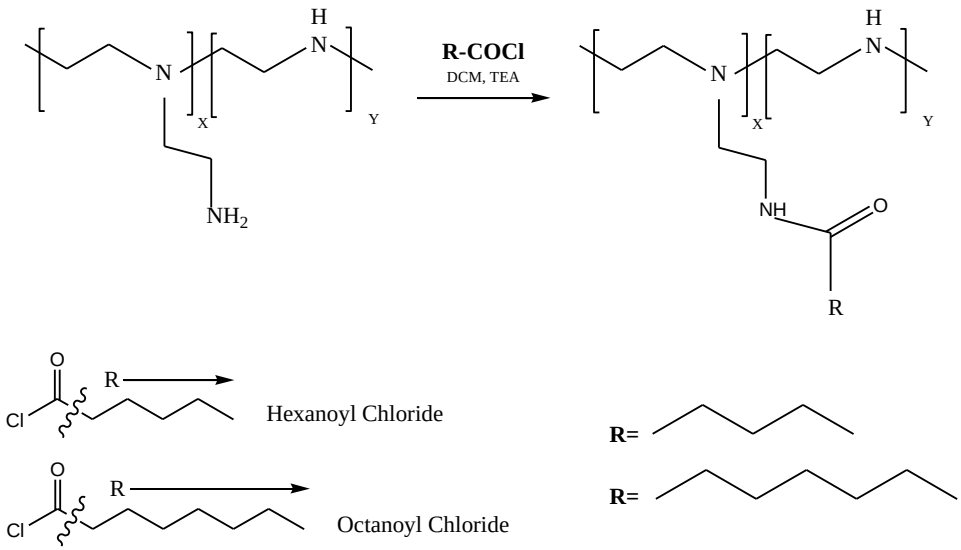

Figure 5.1 Synthesis scheme of HA-PEI and OA-PEI

2. Synthesis and characterization of ω-amino hexanoic acid and w-amino octanoic acid conjugated PEI

Synthesis was performed based on DCC-NHS coupling method (Figure 5.2). ω-amino hexanoic acid and w-amino octanoic acid were used as BOC protected acids. Briefly, acids were activated using equimolar DCC and NHS in DCM solution for 18hr. Activated acid solutions were added drop wise to the PEI solution in DCM. The lipid: PEI amine ratio was selected in a way that one primary amine group per PEI molecule gets systematically substituted by one carboxylic group of ω-amino aliphatic acid to yield amide bond formation. Reaction was allowed to occur for 24hr. Polymers thus modified were dissolved in water and DCU impurity was removed by centrifugation. Supernatant was dialyzed overnight to remove unreacted starting material. To this, at equal mole ratio, Tetrafluroacetic acid:Methylene Dichloride was added to remove BOC protection and allowed to react for 15-30 min. At the end of deprotection, DCM and TFA was vacuum evaporated. This final polymer was dissolved in purified water and dialysis was performed against 0.1 M NaOH for 4 hr followed by against purified water for 10hr using dialysis membrane (Spectra/Por MWCO 6KDa, SpectrumLabs).

Purified lipid conjugated PEI, thus obtained, was freeze dried and further analyzed using 1H NMR (Bruker 300 MHz; Billerica, MA) in D2O. The characteristic proton shift of PEI (δ ~2.5-2.8 ppm; -NH-*C*H2-*C*H2-NH-) were integrated, normalized for the number of Hs in each peak, and used to obtain the extent of lipid substitutions on

the modified polymers. The modified polymers were also analyzed by FTIR (Bruker; Billerica, MA) for characteristic peaks of amide bond by KBr disc method.

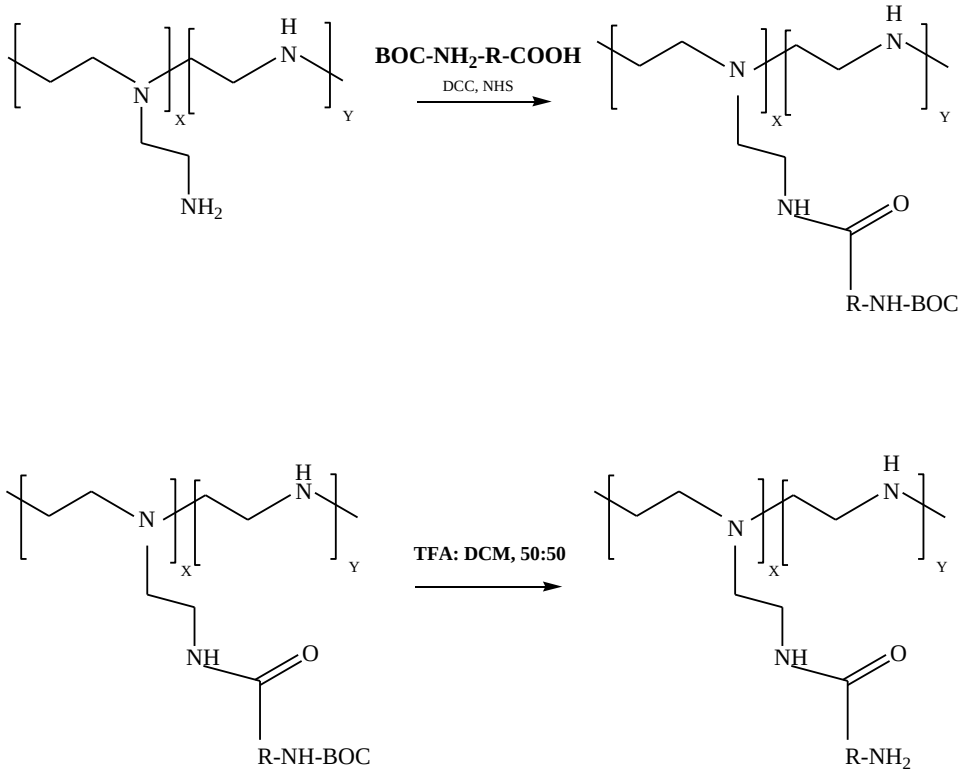

Figure 5.2 Synthesis scheme of ω-amino-HA-PEI and ω-amino-OA-PEI

3. TNBS assay

TNBS (2,4,6-Trinitrobenzenesulfonic acid) assay method is widely used method for quantitative determination and quantification of amine groups. Habeeb et al 1966 developed this method based on reaction of TNBS with amine groups of protein that take place at pH values near to 7 or above (34). Briefly, immediate before use 0.01%w/v TNBS was prepared using reaction buffer (0.1M sodium bicarbonate pH-8.5) as diluent. Polymers were directly dissolved in reaction buffer. Glutamic acid was dissolved in reaction buffer to achieve concentration of 2- 16 µg/ml. Then, 0.01% TNBS (0.25 ml) was added to 0.5ml of each sample and mixed well. All solutions were incubated at 37°C for 2hr. 0.25ml of 10% SDS and 0.125ml of 1N HCl was added to each sample and absorbance was measured at 335nm using UV Spectrophotometer (Shimadzu-1800, Japan).

4. Buffer capacity and pKa

PEI and modified PEI based polymers were dissolved in 10 ml of 150mM NaCl to yield 0.5 mg/ml final concentration. This solution was purged with N2 for 15 minutes under constant stirring to remove dissolved CO2 and then after pH of the solution was measured using pH meter (Labindia Instruments Pvt. Ltd., India) and pH was further adjusted to 11 using 0.1N NaOH. Titration was performed using 0.1N HCl under constant stirring. For titration 40µl of standardized 0.1N HCl was added gradually to the polymer solution and solution was allowed to equilibrate until pH reading was stable before next addition. Validity of the method was assessed using Ethanolamine as a standard.

Buffer capacity between two data points was calculated using following equation:

$$\beta = \frac{\Delta c(HCl)}{\Delta pH}$$

where,

$$\Delta c(HCl) = \frac{40\mu l * Normality\ of\ HCl}{Total\ volume\ of\ solution\ at\ pH(b) point}$$

$$\Delta c(HCl) = pH(a) - pH(b)$$

pH(a) indicates pH of the polymer solution before addition of HCl and pH(b) indicates pH of the polymer solution after addition of HCl.

5. Hemolysis assay

Hemolytic properties of PEI and modified polymers were evaluated using ASTM's Standard Practice for Assessment of Hemolytic Properties of Materials with slight modification (35, 36). Fresh blood from rat was obtained in EDTA coated vacutainers (BD Biosciences, Franklin Lakes, NJ). Blood was centrifuged at 700g at 4^{o}C for 10min. Supernatant was aspirated and cell pellet was mixed with 150mM NaCl and centrifuged at 700g at 4^{o}C for 5 min to wash RBCs. Subsequently, PBS (pH 7.4) wash was given until clear supernatant was obtained. 2.5%V/V of RBC suspension in PBS (pH 7.4) was prepared for further use. In a 96 well plate, 10µl of modified PEI polymer solution or 20% Triton X-100 as positive control or PBS as negative control was mixed with 190µl of RBC suspension. Plate was allowed to incubate at 37^{o}C for 1hr in orbital shaker incubator. After incubation, plate 8was centrifuged at 500g for 5min. Without disturbing pellet, 100µl of supernatant was transferred to another 96 well plate using multichannel pipette. If accidentally pellets get disturbed, plate was again centrifuged. Absorbance of supernatant was measured at 540nm in ELISA plate

reader. Similarly, experiment was also performed in whole blood, using same procedure, to assess the influence of plasma proteins on cationic polymer induced hemolysis. The experiment was performed in triplicate and % hemolysis was calculated using following equation:

$$\%\text{Hemolysis} = \frac{A_{540}\ \text{Sample} - A_{540}\text{PBS}}{A_{540}\ \text{Triton} - A_{540}\text{PBS}} * 100$$

C. Selection, Amplification and Purification of pDNA

pAL119-mCTLA4-IGHG1 was procured from Dr. Maria castro's lab (addgene # 194368). pEGFP-N1 was a kind gift from Prof. Gregory J. Gores (Mayo clinic, Minnesota 55905). Both the pDNAs were transformed and amplified in DH5-α cells. pDNA isolation was performed using Qiagen® maxi plasmid purification kit (Qiagen INC, USA) as per user instructions.

1. Preparation of competent cells

DH5-α cells were made competent using method described by chung et al (37). Briefly, 25ml of culture of E-coli DH5α was grown overnight and 200-400 µl of it was added in 5 ml of LB media until OD reaches 0.3-0.4. Cell culture was centrifuged and pellet was resuspended in to 500 µl of TSS buffer (transformation and storage solution, PEG 8000 10%W/V, 1M $MgCl_2$ 20-50mM mg^{+2} as $MgCl_2$ and DMSO 5% W/V) which yielded competent cells. Competent cells thus prepared was mixed with chilled 50% glycerol and stored at -80oC.

2. Transformation of competent cells

Heat shock technique was used for E. coli DH5α transformation. Briefly, Competent cells (E. coli DH5-α) were thawed from -80 °C deep freeze on ice. The thawed competent cells were gently mixed by flicking, and then 100 µl were transferred to pre-chilled micro centrifuge tubes tube (2 ml). To 100 µl competent cells, 50-100 ng of DNA was added and mixed properly by flicking without harming cells. The cells were placed on ice for 10 mins and then heat-shocked in a temperature controlled water bath at 42 °C for 45-50 sec. Cells were then immediately placed on ice for 2 mins. Cold (4 °C) 300 µl LB medium was added and then tubes were incubated at 37 °C and 200 rpm for 45 mins using a temperature-controlled shaker (Scigenics, India).

Cells were then centrifuged and pellet was resuspended in 200 µl of LB media. For each transformation, 100 µl of transformed cells as well as untransformed were plated

on LB agar plate containing antibiotic (100 μg/ml ampicillin for pAL119-mCTLA4-IGHG1 and 50 μg/ml kanamycin for pEGFP-N1) and LB agar plates without antibiotic. Plates spread with untransformed cells served as negative control. All plates were then incubated upside down for 18 hr in a shaker incubator (Scigenics, India) at 37 °C. All four plates were observed and a single colony picked from antibiotic positive plate spread with transformed cells was incubated in 2 ml of LB broth containing ampicillin (100 μg/ml final concentration) in a 50 ml tube and was allowed to grow for 10 h at 37 °C and 200rpm in shaker incubator (Scigenics, India). For long term storage, the culture (0.5 ml) that was grown for 10hr at 37°C was mixed with sterile 50% glycerol (0.5 ml) solution and transferred to microcentifuge tube (Tarson, India) and then stored at -80 °C.

3. pDNA isolation and purification

Transformed cell culture (200 μl) was added in 100ml of LB media (Flask should be of capacity 1L or larger) with ampicillin (100 μg/ml final concentration). The flask was then incubated for 18 h (overnight) at 37 °C and 200rpm in shaker incubator. The cell culture thus obtained was utilized for pAL119-mCTLA4-IGHG1 (Low copy plasmid hence 500ml) and pEGFP-N1 (high copy plasmid hence 100ml) respectively, and isolation was performed using Qiagen® maxi plasmid purification kit (Qiagen INC, USA) as per user instructions. This method operates on the basis of a modified method described by Sambrook et al. (38) and with the use of Qiagen anion exchange resin.

Briefly, for pEGFP-N1, the cells thus obtained after incubation were centrifuged at 6,000 rpm for 15 mins at 4 °C using sigma centrifuge (Sigma 3K30; Germany). Bacterial pellet was resuspended in 10 ml Buffer P1 (50 mM Tris·Cl, pH 8.0; 10 mM EDTA; 100 μg/ml RNase A). Equal volume of Buffer P2 (200 mM NaOH, 1% SDS w/v) was added to it and mixed by vigorously inverting the tube 4–6 times. Then the tube was incubated at room temperature (15–25°C) for 5 min. to this 10 ml of chilled Buffer P3 (3.0 M potassium acetate, pH 5.5) was added and mixed immediately by vigorously inverting 4–6 times and then was incubated on ice for 20 min. This sample was centrifuged at ≥20,000x g for 30min at 4°C. After centrifugation, supernatant containing plasmid DNA was promptly removed. This supernatant was again centrifuged at ≥20,000 x g for 15 min at 4°C and supernatant containing plasmid DNA was promptly removed. Meanwhile, a QIAGEN-tip 50 was allowed to

equilibriate by applying 10 ml Buffer QBT (750 mM NaCl; 50 mM MOPS, pH 7.0; 15% isopropanol v/v; 0.15% Triton® X-100 v/v), and was allowed to empty by gravity flow. The supernatant obtained after centrifugation was applied to the QIAGEN-tip and was allowed to enter the resin packed in column by gravity flow. Then QIAGEN-tip was washed twice with30 ml Buffer QC (1.0 M NaCl; 50 mM MOPS, pH 7.0; 15% isopropanol v/v). DNA was eluted from column with 15 ml Buffer QF (1.25 M NaCl; 50 mM Tris·Cl, pH 8.5; 15% isopropanol v/v) and was collected as elute. DNA was precipitated by adding 10.5 ml (0.7 volumes) room-temperature isopropanol to the eluted DNA. DNA was centrifuged immediately at ≥15,000 x g for 30 min at 4°C and supernatant was carefully decanted. DNA pellet was washed with 5 ml of room-temperature 70% ethanol, and was again centrifuged at ≥15,000 x g for 10 min. Supernatant was carefully decanted without disturbing the DNA pellet. DNA pellet thus obtained was allowed to air-dry the for 5–10min, and the DNA was dissolved in a suitable volume of TE buffer (Tris-EDTA butter, pH 8.0). Genomic and plasmid DNA were stored in TE Buffer at 4ºC (39.2ºF) for short-term use and at -20ºC (-4ºF) to -80ºC (-112ºF) for long-term storage. Repeated freeze-thaw cycles were avoided to prevent pDNA damage.

4. Determination of pDNA yield and purity

To determine the yield, pDNA concentration was determined by both UV spectrophotometry analysis (UV Spectrophotometer, UV-1800, Shimadzu, Japan) at 260 nm and quantitative analysis on an agarose gel. A260 readings that lied between 0.1 and 1.0 were considered reliable. Ratio of A260 to A280 between 1.75-1.90 was considered acceptable for DNA purity.

To determine purity and for quantitative analysis agarose gel electrophoresis was also performed. For purity and integrity analysis, after proper dilution, pDNA was run along with DNA marker ladder on 1.2% agarose gel using EtBr as an intercalating agent. In addition, pDNA was digested using single site digestion enzyme KpnI and double site digestion enzyme XbaI. Gel was analyzed on UV transilluminator (BioRAD Gel Doc XR System, USA). For quantification and minimum detection amount determination, isolated pDNA was serially diluted to yield 20 ng, 40 ng, 60 ng, 80 ng, 100 ng, 200 ng, 300 ng and 400 ng of pDNA and agarose gel electrophoresis was performed.

D. Preparation of polyplexes using HA-PEI, OA-PEI, ω-amino-HA-PEI AND ω -amino-OA-PEI

Polycation-nitrogen/ polyanion-phosphorous ratio (N/P ratio) was considered as an index of polyplex preparation or complex formation. Initial concentration of pAL119-mCTLA4-IGHG1 was 397.5ng/µl in TE buffer (pH 8.0), which was further diluted using 150mM NaCl to get 15.9ng/µl concentration. In some experiments, pEGFP-N1 has been used which was also diluted similarly. PEI solution was also prepared, separately, in 150mM NaCl to get desired concentration of 50ng/µl. Polyplexes were prepared by allowing modified PEI and pDNA to form complexes at required N/P ratio (for example 0, 0.5, 0.75, 1, 2, 4, 8 and 12). For this purpose required amount of modified PEI and pDNA were mixed in 150 mM NaCl solution and allowed to form polyplexes at 37^{o}C for 30 to 45 min.

E. Physicochemical characterization of polyplexes:

1. Dynamic Light Scattering (DLS)

Polyplex size measurements were carried out with Zetasizer Nano ZS from Malvern Instruments, Worcs., UK at 25 °C (10 mW HeNe laser, 633 nm). Scattered light was detected by optics arranged at positions 173° angle. The viscosity (0.8905 mPas) and refractive index (1.333) of pure water at 25 °C were used. Measurements of hydrodynamic diameters (Z-average) and polydispersity indices (PDI) were performed from average of 30 runs optimized by software.

2. Transmission Electron microscopy

The polyplex solution was applied onto a 150-mesh carbon-coated copper grid for 10sec. The excess solution was wicked off with filter paper. This coating procedure was repeated 5 times. Images were recorded using a transmission electron microscope (FEI, Netherland; performed at Sun Pharma Advanced Research centre, Vadodara) operated at a voltage of 75 kV with an original magnification of 30,000.

3. Laser Doppler Anemometry/ Electrophoresis/ velocimetry

ζ-potential (zeta-potential) measurements of the polyplexes were carried out in the Folded Capillary electrophoresis cell of the Zetasizer Nano ZS from Malvern Instruments, Worcs., UK at position 17° angle and 25 °C. Measurement was performed in automatic mode with 30 default runs. Average values of the ζ-potential were recorded with the data from 30 runs.

4. Agarose Gel Retardation Assay

Polyplexes were prepared by allowing modified PEI and pDNA to form polyplexes at various N/P ratios such as 0, 0.5, 0.75, 1, 2, 4, 8 and 12. For this purpose required amount of modified PEI and pDNA were mixed in 150mM NaCl solution and allowed to form polyplexes at 37^{o}C for 30 to 45 min. Each 18µl polyplex solution was made to final 20µl volume by adding 2µl of 6X gel loading buffer (HiMedia Lic) and was loaded on 1.2% agarose gel stained with EtBr (0.5µg/ml; ethidium bromide). Electrophoresis was carried out at a voltage of 100 V for 45 min in 1X TAE running buffer solution (0.04 M Tris – Acetate, 1 mM EDTA; pH-8.0). Agarose gel was visualized and images were captured using UV transilluminator supported with Image Lab software (Gel Doc™ XR, Bio-Rad, USA).

F. *In Vitro* characterization of polylplexes

1. MTT cytotoxicity assay

Human embryonic kidney 293 cells (HEK 293 cells) were obtained from Dr. Senthil Natesan's laboratory, Genomic research centre, Faculty of science, The M. S. University of Baroda. HEK 293 cells were grown and maintained in DMEM (Dulbecco's Modified Eagle's Medium) with 10% FBS (Fetal bovine serum) in 5% CO_2/ 95% air incubator at 37^{o}C (JouanIGO150 5% CO2 incubator, Thermo-Fischer, Germany). Routinely, cell passaging or subculturing was performed, in regulated Laminar air flow (HEPA filter) environment (Weiber Laminar Air Flow), to maintain and expand cells for subsequent *in vitro* cell culture experiments.

For evaluation of cytotoxicity of HA-PEI, OA-PEI, ω-amino-HA-PEI and ω-amino-OA-PEI, 3-(4,5-dimethylthiazol-2-yl)-2,5-diphenyltetrazolium bromide (MTT) based assay method was used. MTT based cytotoxicity assay is a colorimetric assay that is dependent on assessing cell metabolic activity of living cells. All living cells have NADPH dependent oxidoreductase enzymes that can reduce tetrazolium MTT dye to insoluble Formazan crystals, which has purple colour which can be dissolved using DMSO and further analyzed using U.V. Spectrophotometry.

Prior to MTT cytotoxicity experiments, Cells were grown at desired level of confluency in a T25 or T75 flask with DMEM and 10% FBS. Media was aspirated and cells were washed with PBS. Warm trypsin/EDTA solution (1 ml for 2-3 ml for T75 flask) was added without disturbing cells. Flask was returned to a 37°C incubator. After 5-10 minutes, flask was observed under optical microscope to ensure

complete cell lifting (trypsinization). Action of trypsin was stopped by adding 5–6 ml Complete Cell Culture Medium and cells were transfered to sterile conical tubes for centrifugation at 300 x g for 7 minutes. Supernatant was discarded and cells were suspended in DMEM medium. Cells were again centrifuged at 300 x g for 7 minutes for washing. Supernatant was decanted and cells were suspended in complete DMEM medium. Cell density was estimated by microscopic method using tryptan blue.

For MTT cytotoxicity assay, cells were seeded at a density of 3 X 10^4 cells/well in flat bottom 96-well plate (Tarsons, India) using DMEM with 10% FBS as cell culture media. Plate was incubated for 24 hr in 5% CO_2/ 95% air incubator before transfection to achieve ~ 80% confluency. Medium was replaced after 24 hr with DMEM without FBS. Cells were treated, in triplicate, with different concentrations of 10KDa PEI, 25KDa PEI, HA modified 10KDa PEI, OA modified 10KDa PEI, ω-amino HA modified 10KDa PEI, ω-amino OA modified 10KDa PEI or polyplexes at different N/P ratios containing a final volume of 100µl/well. Untreated cells (containing complete DMEM media) in triplicate were considered as negative control. Then, 96-well plate was incubated at 37°C in 5% CO_2/ 95% air incubator for 4 hr. cells were then washed with DMEM and further incubated overnight with complete DMEM media. At 24 hr, Media was replaced with 100 µL of fresh DMEM with 10% FBS media (phenol red free) and then 10 µL of MTT (12mM, 5mg/ml in PBS) was added per each well. Cells were incubated at 37°C for 4hr. After 4 hr, MTT containing media was carefully replaced with 100 µL of DMSO and cells were incubated for 30 minutes to completely dissolve purple formazan crystals. For cell toxicity study at 4hr (only for polymers at different concentrations not polyplexes), cells were not incubated for 24 hr whereas directly after 4hr of treatment cells were used for MTT assay. The absorbance was measured at 540 nm using a microplate reader (Bio-Rad, USA) Results were reported as mean ± SD and difference between observations was statistically analyzed using ANOVA test.

2. Fluorescence microscopy

HEK 293 cells were seeded in 6-well plate at 0.5 x 10^6 cells per well containing sterile coverslip at bottom of each well using 2ml of DMEM medium with 10% FBS. After 24 hours when cells reached 50-60% confluency, treatment of polyplexes prepared from pEGFP-N1 and PEI, HA-PEI, OA-PEI, ω-amino-HA-PEI and ω-amino-HA-PEI at N/P ratio 12 was given using incomplete DMEM medium. 100 µl

of polyplexes were made at a 12:1 N/P ratio containing 2.0 µg of pEGFP-N1 plasmid DNA. After 4hr of treatment, medium was replaced with fresh DMEM with 10% FBS and then cells were incubated at 37°C with 5.0% CO2 for 48hr. At the end of transfection, cells were fixed using 1ml of freshly prepared 3.7% paraformaldehyde in PBS per well for 10min at 25°C. Paraformaldehyde was aspirated and cells were washed thrice with PBS. After paraformaldehyde fixing cells were stained using 2ml of 1µg/ml DAPI solution for 10-15 min for nuclei staining. Cells were washed thrice using PBS. Coverslip with cells was mounted on slide and preceded for fluorescence microscope (Nikon 2000 inverted Fluorescence Microscope, Nikon, Japan).

3. Confocal microscopy

HEK 293 cells were seeded in 6-well plate at 0.5 x 10^6 cells per well containing sterile coverslip at bottom of each well using 2ml of DMEM medium with 10% FBS. After 24 hours when cells reached 50-60% confluency, treatment of polyplexes of pEGFP-N1 prepared with PEI, HA-PEI, OA-PEI, ω-amino-HA-PEI and ω-amino-HA-PEI at N/P ratio 12 was given using DMEM medium without 10% FBS. 100 µl of polyplexes were made at a 12:1 N/P ratio containing 2.0 µg of pEGFP-N1 plasmid DNA. After 4hr of treatment, medium was replaced with fresh DMEM with 10% FBS and then cells were incubated at 37°C with 5.0% CO_2 for 48hr. At the end of transfection, cells were fixed using 1ml of freshly prepared 3.7% paraformaldehyde in PBS per well for 10min at 25°C. Paraformaldehyde was aspirated and cells were washed thrice with PBS. After paraformaldehyde fixing cells were stained using 2ml of 1µg/ml DAPI solution for 10-15 min for nuclei staining. Cells were washed thrice using PBS. Coverslip with cells was mounted on slide and preceded for confocal microscopy using confocal laser scanning microscope (LSM 710, Carl-Zeiss Inc., USA) under 40 and 60X oil immersion objective with filters. The zeiss LSM710 confocal system consists of a Zeiss AXIO Observer Z1 inverted microscope with 405 nm Diode laser, Argon/2 (458, 488, 514 nm), HeNe1 (543/561 nm) and HeNe2 (633 nm) laser illumination sources and 34 channel confocal and transmitted light detectors. Microscope was equipped with ZEN 2011 software to control the microscope, scanning, laser module, tools and the image acquisition and processing.

Excitation of the EGFP protein was performed by using the 488 nm excitation line and the resulting fluorescence was observed by using a 515–540 nm emission band

pass filter. Similarly, excitation of DAPI stain was performed at 365nm excitation line and resultant fluorescence was observed at 450nm emission band pass filter.

4. Gene expression analysis by flow cytometry

HEK 293 cells were seeded in 6-well plate at 0.5 x 10^6 cells per well using 2ml of DMEM medium with 10% FBS. After 24 hours when cells reached 50-60% confluency, treatment of polyplexes prepared of pEGFP-N1 with PEI, HA-PEI, OA-PEI, ω-amino-HA-PEI and ω-amino-HA-PEI at N/P ratio 12 was given using incomplete DMEM medium. 100 µl of polyplexes were made at a 12:1 N/P ratio containing 2.0 µg of pEGFP-N1 plasmid DNA. After 4hr of treatment, medium was replaced with fresh DMEM with 10% FBS and then cells were incubated at 37°C with 5.0% CO_2 for 48hr. After incubation for 36hr, the cells were harvested by trypsinization and washed thrice with cold PBS (pH 7.4) by centrifugation. Cells were suspended in FACS buffer (0.5% BSA, 0.5%FBS in sterile PBS pH7.4) and then strained using cell strainer (Himedia, India) to get single cell suspension. From suspension 10,000 cells were then analyzed for mean fluorescence activity of EGFP protein using fluorescence activated cell sorter (FACS-BD-Aria-III, BD, USA). Cells treated with naked plasmid were used as negative control.

5. Determination of *mCTLA4-IGHG1* mRNA expression

Quantification of *mCTLA4-IGHG1* mRNA was performed to predict and correlate mCTLA4-IGHG1 protein expression that can be induced using pAL119-mCTLA4-IGHG1plasmid transformation as mRNA expression occurs prior to protein synthesis and hence may give better correlation. Previous experiments such as confocal microscopy, fluorescence microscopy and FACS analysis for evaluation of transfection efficiency were performed using marker plasmid p-EGFP-N1; expression efficiency of pAL119-mCTLA4-IGHG1 plasmid was confirmed by m-RNA expression analysis by using a sophisticated technique called Real Time Polymerase Chain Reaction (RT-PCR).

HEK 293 cells were seeded in 24-well plate at 0.05 x 10^6 cells per well using 2ml of DMEM medium with 10% FBS. After 24 hours when cells reached 50-60% confluency, treatment of polyplexes prepared for pAL119-mCTLA4-IGHG1 with PEI, HA-PEI, OA-PEI, ω-amino-HA-PEI and ω-amino-HA-PEI at N/P ratio 12 was given using incomplete DMEM medium. 100 µl of polyplexes were made at a 12:1 N/P ratio containing 1.0 µg of pAL119-mCTLA4-IGHG1 plasmid DNA. After 4hr of

treatment, medium was replaced with fresh DMEM with 10% FBS and then cells were incubated at 37°C with 5.0% CO_2 for 48hr. After incubation for 36hr, the cells were harvested by trypsinization and washed thrice with cold PBS (pH 7.4) by centrifugation.

Total RNA from harvested cells was isolated and purified using protocol described here. Cells were taken in a 1ml of autoclaved eppendorf (DEPC treated, RNase free microfuge tubes) and centrifuged at 6000 rpm for 5 min. Supernatant was moved and remaining pellet was washed with PBS. 500µl of Trizol reagent was added to cell pellet, mixed vigorously and kept it for 5 min at 15 to 30^{0}C. 200µl of chloroform was added to it and mixed vigorously by hand for 15 sec and incubated at 15 to 30^{0}C for 2-3 min. During this time centrifuge machine was maintained at 4^{0}C. Sample was then centrifuged at 12000g for 15 min at 2-8^{0}C. 50% of aqueous phase was transferred to fresh tubes. Because both DNA & RNA are in aqueous phase but RNA being smaller fragments remain in uppermost aqueous phase. To this aqueous phase add 0.5ml of isopropyl alcohol and incubated at 15-30^{0}C for 10min. Sample was then incubated to allow precipitation of RNA at -20^{0}C for 20min for RNA and centrifuged at 12000g for 10min at 2-8^{0}C. Supernatant was removed and the pellet was washed with 1ml of 75% ethanol. Pellet was mixed by vortexing and centrifuged at 7500g for 5min at 2-8^{0}C. Supernatant was removed and the RNA pellet was allowed to semi air dry. 50µl of DEPC treated water was added to dissolve the pellet and allowed to incubate at 55-60^{0}C for 10min. RNA integrity was verified by agarose gel electrophoresis/ ethidium bromide staining and O.D. 260/280 absorbance ratio >1.95. RNA was treated with DNase I (Ambion inc. Texas, USA) before cDNA synthesis to avoid DNA contamination. RNA quantification was done using U.V. spectrophotometer (Shimadzu-1800, Japan). One microgram of total RNA was used to prepare cDNA. cDNA synthesis was performed using the Verso cDNA Synthesis Kit (Thermo scientific, Lithuania, EU) according to the manufacturer's instructions using cDNA synthesis program of Step One real time PCR (Applied Biosciences, USA)

The levels of *mCTLA4-IGHG1* transcripts were measured by real-time PCR using gene specific primers (Table 5.1) (Eurofins, Bangalore, India). Expression of GAPDH gene was used as a reference. Real-time PCR was performed in duplicates in 15 µl volume (cDNA 1.5 µl, forward primer 0.7 µl, reverse primer 0.7 µl, SYBR Green I

Master mix 7.5 µl, Nuclease free water 4.6 µl) using LightCycler®480 SYBR Green I Master (Roche Diagnostics GmbH, Mannheim, Germany) following the manufacturer's instructions and carried out in the StepOne™ real time PCR (Applied Biosciences; Boston, MA, USA). The thermal cycling conditions included an initial activation step at 95°C for 10 min, followed by 45 cycles of denaturation, annealing (Temperature in Table 5.1) and amplification. The fluorescent data collection was performed during the extension step. At the end of the amplification phase a melt curve analysis was carried out on the product formed. The value of Cp was determined by the first cycle number at which fluorescence was greater than the set threshold value. All analysis of data was performed in triplicate using Student's t-test using Graph pad prism 6 (Graphpad software Inc; San Diego CA, USA, 2007). P-values less than 0.05 were considered statistically significant.

Table 5.1 Primers used for genotyping of pAL119-mCTLA4-IGHG1 expression analysis.

Plasmid/ Gene	**Primers**	**Amplicon size (bp)**	**Annealing Temp (^{o}C)**
pAL119-mCTLA4-IGHG1	F: 5'- TTCATCCCAGTCTTCTCTGA-3' R: 5'-TTCACATGGAAAGCTGGCGA-3'	90bp	60 ^{o}C
GAPDH	F: 5'-ATCCCATCACCATCTTCCAGGA-3' R: 5'-CAAATGAGCCCCAGCCTTCT-3'	122bp	63 ^{o}C

F: Forward Primer

R: Reverse Primer

G. *In vivo* efficacy studies

All mice were taken care and maintained in accordance with Regulations of Animal Welfare Act. Protocol for study was approved by the Institutional Animal Ethics Committee (IAEC) of Pharmacy department, Shri G.H. Patel pharmacy building, The M.S. University of Baroda (CPCSEA - Committee for the Purpose of Control And Supervision of Experiments on Animals - Reg. Number 404/01/a/CPCSEA dt. 25th

April 2001) as per Animal Study Proposal no. MSU/IAEC/2014-15/1439 approved by Institutional Animal Ethics Committee (IAEC) on dt. 26th Nov 2014.

One week prior to starting experiment, female BALB-c mice were maintained on acidified chlorinated water to reduce intestinal flora and enable them to withstand experimental conditions. After one week 100µl of 0.8mg/ml MTg in nonpyrogenic PBS pH 7.2 was emulsified with equal volume of CFA (complete Freund's adjuvant). 100µl of freshly prepared MTg-CFA emulsion (i.e. 40 µg mTg) was injected into the inner thigh by subcutaneously. On next week, in each animal, second dose of 100µl of freshly prepared MTg-CFA emulsion (i.e. 40 µg mTg) was injected into the alternate inner thigh by subcutaneously.

Thyroid glands from six mice that were not used for induction of experimental autoimmune thyroidits (EAT) served as negative control **Table 5.2.** One week after injection of second dose of MTg-CFA emulsion, thyroid glands of six mice were used for histological examination and these mice served as positive control **Table 5.2**. One week after injection of second dose of MTg-CFA emulsion, Group–III and IV were given treatment as shown in **Table 5.2**. One week after treatment thyroid glands of six mice of each group were removed and histopathological examination was performed. Group-V and VI served as groups for assessing efficacy of prepared polyplexes in prevention of EAT disease. Hence, treatment to Group-V and VI was given two days prior to injection of first and second dose of MTg-CFA emulsion as shown in **Table 5.2**. One week after injection of second dose of MTg-CFA emulsion, thyroid glands of six in each group were removed for histopathological examination. Thyroid glands were stored in Neutral buffered formaldehyde until thinly sectioned. Pathology Department, Faculty of medicine, S.S.G. Hospital, Vadodara, helped in sectioning as well as Haemotoxylin and Eosin staining of thyroid glands. Histopathology slides thus prepared were examined using Optical Microscope with polarizer (Olympus Co. Pvt. Ltd., Japan).

Table 5.2 Experimental design for evaluating efficacy of ω-amino-OA-PEI and pAL119-mCTLA4-IGHG1 polyplexes in treatment and prevention of autoimmune thyroiditis.

Groups		Administered samples	No. of animals
I	Negative Control	Non-EAT induced mice, Nonpyrogenic PBS pH 7.2.	6
II	Positive control	EAT-induced mice, Nonpyrogenic PBS pH 7.2.	6
III	Treatment Group-1	PEI 10 KDa and pAL119-mCTLA4-IGHG1 polyplexes (N/P ratio-12; 2.5µg/gm equi. plasmid, i.v.)	6
IV	Treatment Group-2	ω-amino-OA-PEI and pAL119-mCTLA4-IGHG1 polyplexes (N/P ratio-12; 2.5µg/gm equi. plasmid, i.v.)	6
V	Prevention Group-1	PEI 10 KDa and pAL119-mCTLA4-IGHG1 polyplexes (N/P ratio-12; 2.5µg/gm equi. plasmid, i.v.)	6
VI	Prevention Group-2	ω-amino-OA-PEI and pAL119-mCTLA4-IGHG1 polyplexes (N/P ratio-12; 2.5µg/gm equi. plasmid, i.v.)	6
	Total		36

Half lob of thyroid from each group was used for total mRNA isolation. Thyroid was immersed in TriZol and frozen using liquid nitrogen and then ground/minced. Total mRNA was isolated and converted to cDNA by reverse transcription PCR as per protocol described in previous sections. mCTLA4-IGHG1 mRNA expression was quantified using RT-PCR method using primers and conditions described in previous sections. Expression fold change was calculated from mean CT values of mCTLA4-IGHG1 using GAPDH as reference standard. Expression fold change was compared between groups using student's t test.

III. RESULTS AND DISCUSSION

A. Preparation and characterization of short chain aliphatic lipids substituted PEI 10KDa polymers

Low molecular weight PEIs (LMW PEI) possess low transfection efficiency as well as toxicity compared to HMW PEIs. Hence, in present investigation, branched LMW PEI 10KDa is modified so as to increase its transfection efficiency but at the same time maintaining its low cytotoxicity using HA, OA, ω-amino-HA and ω-amino-OA. In a previous study by Neamnark et al, LMW PEI was modified using aliphatic acids such as using caprylic acid, myristic acid, palmitic acid, stearic acid, oleic acid and linoleic acid (21). Modification by long chain aliphatic acids causes reduction in solubility of PEI and hence preparation of their formulation in aqueous phase becomes difficult. So as to avoid this difficulty and maintain high aqueous solubility of PEI 10KDa modifications using short chain aliphatic acids was performed. Additionally, PEI 10KDa was also modified using ω-amino group containing same aliphatic acid for comparison with short aliphatic acid modified PEI. Newly prepared polymers HA-PEI, OA-PEI, ω-amino-HA-PEI and ω-amino-OA-PEI as well as PEI were characterized using FTIR spectroscopy, NMR spectroscopy and TNBS assay.

Figure 5.3 shows the FTIR spectrum of PEI, HA-PEI, OA-PEI, ω-amino-HA-PEI and ω-amino-OA-PEI. The FTIR spectrum of PEI 10KDa (Figure 5.3A) shows bands at 3367.91 cm−1 and 2942.29 cm−1, which are attributed to the stretching and bending vibrations of the N–H and –NH2 groups, respectively. These stretching and bending vibrations of the N–H and –NH2 groups are also present in FTIR spectra of HA-PEI, OA-PEI, ω-amino-HA-PEI and ω-amino-OA-PEI (Figure 5.3B to Figure 5.3E). In addition to this, HA-PEI, OA-PEI, ω-amino-HA-PEI and ω-amino-OA-PEI (Figure 5.3B to Figure 5.3E), most notably, also show strong band at 1640-1690 which is attributed to stretching vibrations of C=O group of newly formed amide group (H2N-C=O). Band at 1640-1690 which is attributed to stretching vibrations of C=O group confirmed that PEI, HA-PEI, OA-PEI, ω-amino-HA-PEI and ω-amino-OA-PEI are successfully synthesized. Also intensity of amine N-H stretch band at 3500 – 3000 cm−1 was slightly reduced. Results indicate successful conjugation of HA, OA, ω-amino-HA and ω-amino-OA on PEI by way of amide bond formation.

A

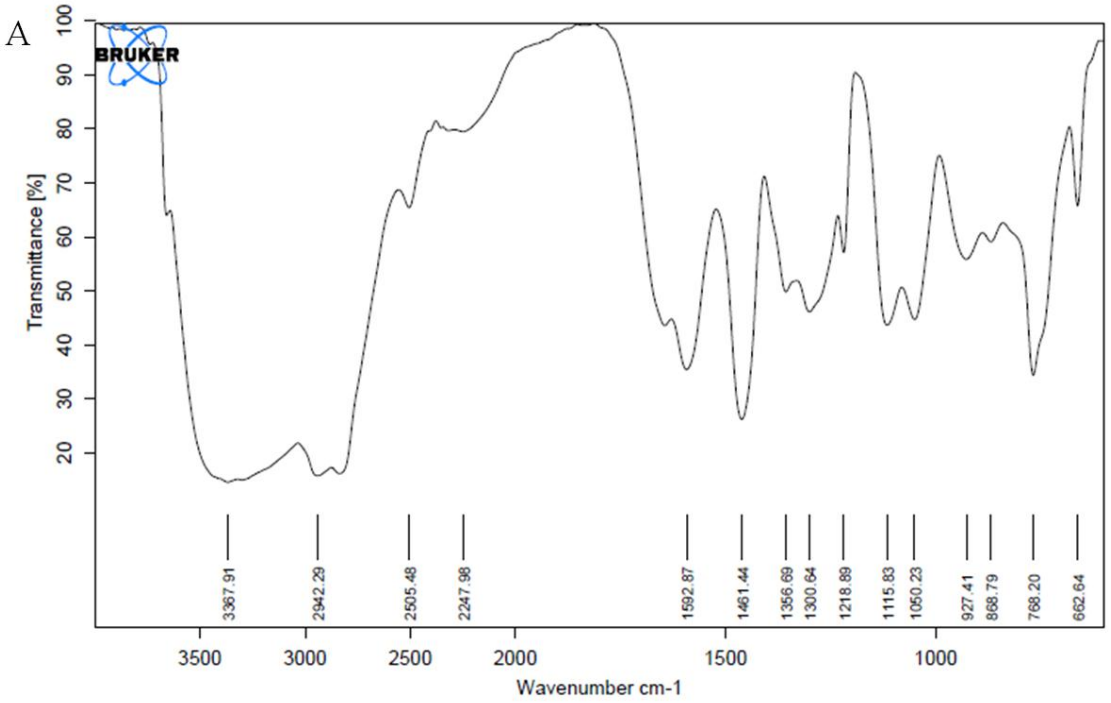
BRUKER
Transmittance [%]
100
90
80
70
60
50
40
30
20
3367.91
2942.29
2505.48
2247.98
1592.87
1461.44
1356.69
1300.64
1218.89
1115.83
1050.23
927.41
868.79
768.20
662.64
3500
3000
2500
2000
1500
1000
Wavenumber cm-1

B

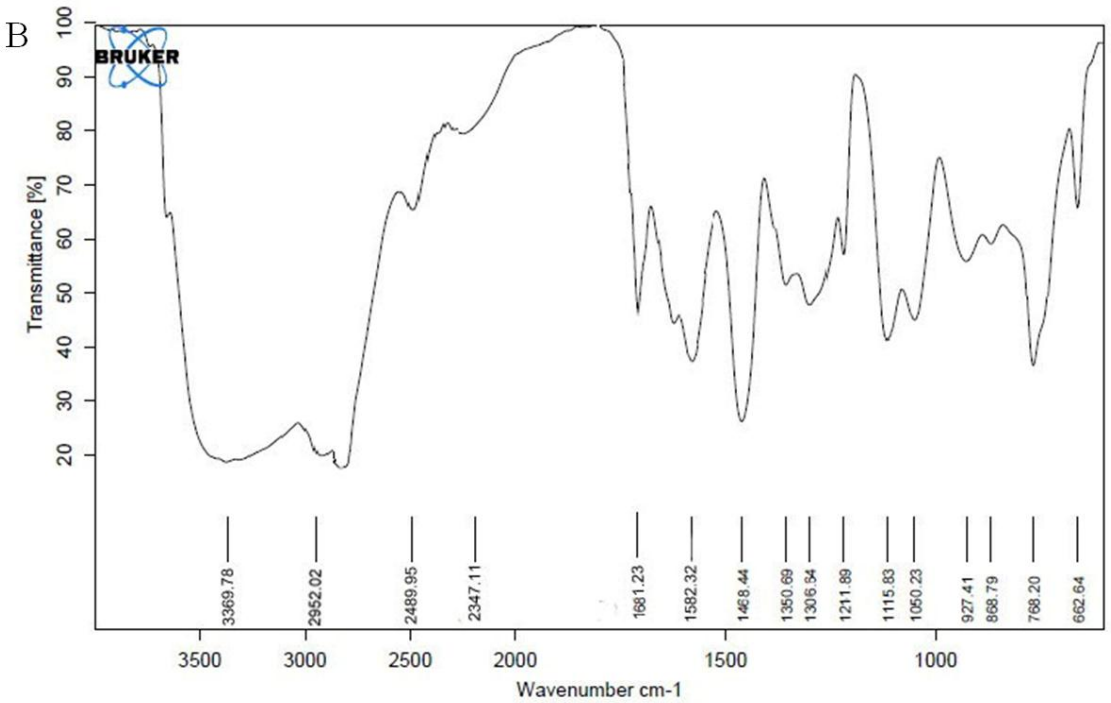
BRUKER
Transmittance [%]
100
90
80
70
60
50
40
30
20
3369.78
2952.02
2489.95
2347.11
1681.23
1582.32
1468.44
1350.69
1306.84
1211.89
1115.83
1050.23
927.41
868.79
768.20
662.64
3500
3000
2500
2000
1500
1000
Wavenumber cm-1

C

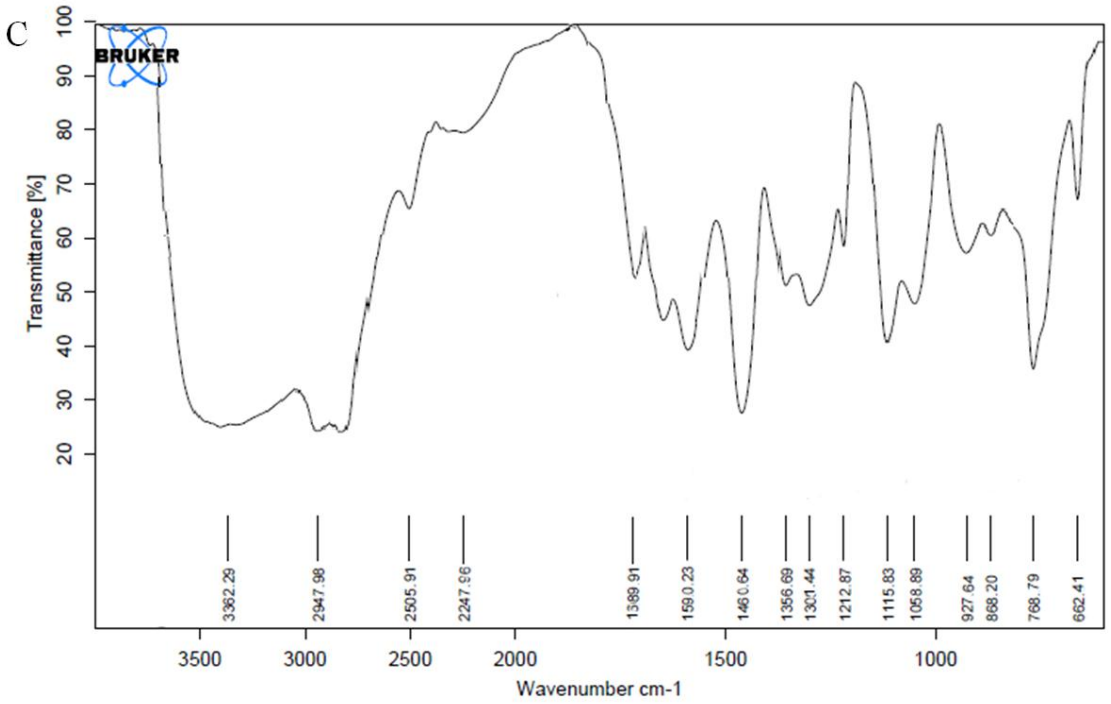
BRUKER
Transmittance [%]
100
90
80
70
60
50
40
30
20
3362.29
2947.98
2505.91
2247.66
1389.91
1590.23
1460.64
1356.69
1301.44
1212.87
1115.83
1058.89
927.64
868.20
768.79
662.41
3500
3000
2500
2000
1500
1000
Wavenumber cm-1

D

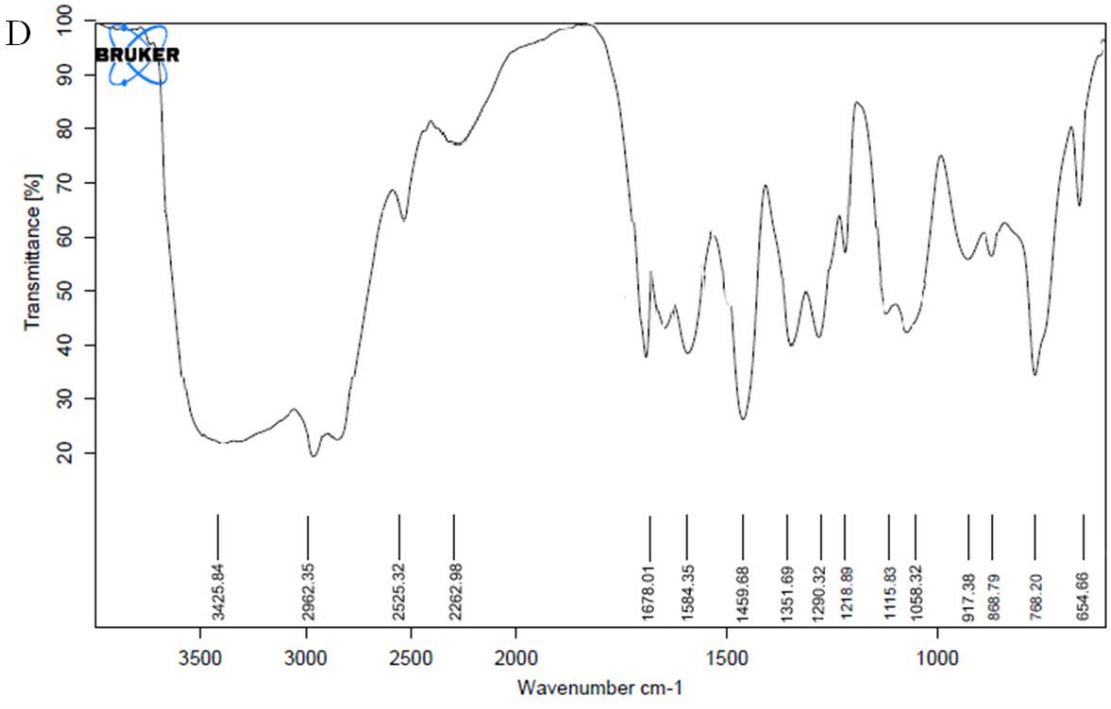
BRUKER
Transmittance [%]
100
90
80
70
60
50
40
30
20
3425.84
2962.35
2525.32
2262.98
1678.01
1584.35
1459.68
1351.69
1290.32
1218.89
1115.83
1058.32
917.38
868.79
768.20
654.66
3500
3000
2500
2000
1500
1000
Wavenumber cm-1

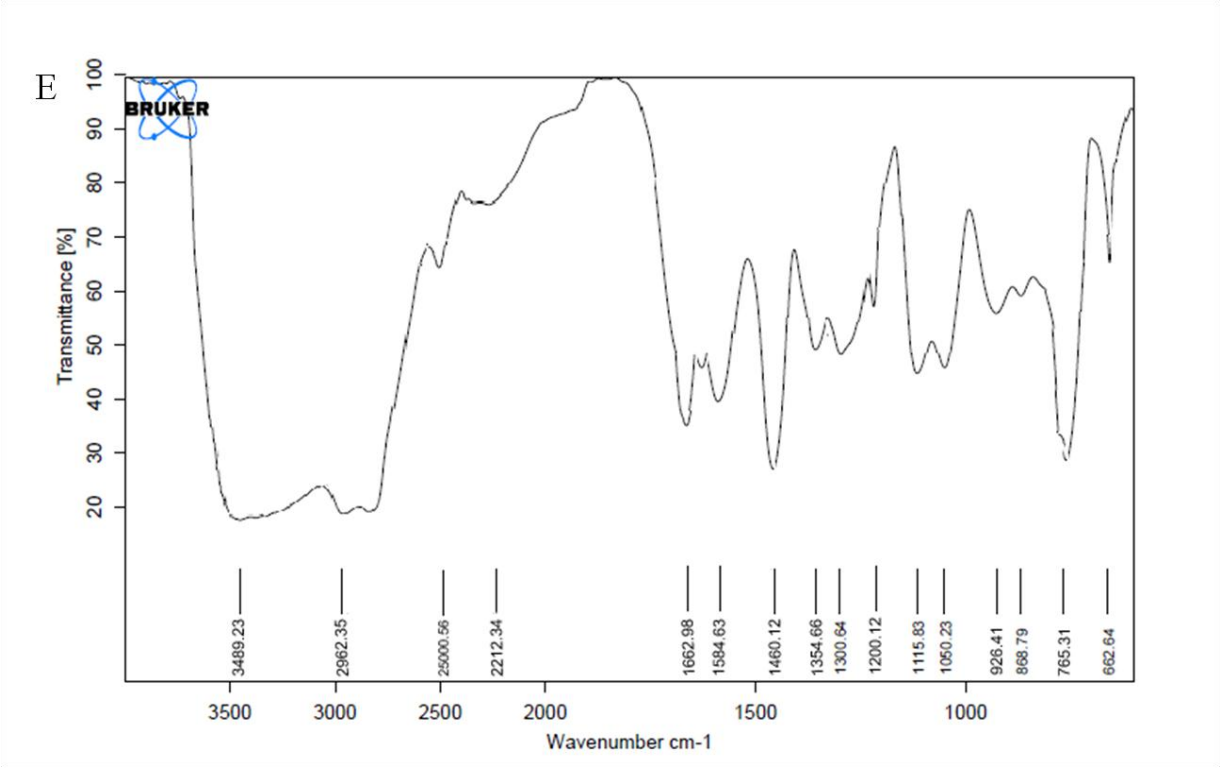

Figure 5.3 FTIR spectra of A) PEI 10 KDa, B) HA-PEI, C) OA-PEI, D) ω-amino-HA-PEI and E) ω-amino-OA-PEI.

Analysis of FTIR spectra suggests formation of new amide bond in HA-PEI, OA-PEI, ω-amino-HA-PEI and ω-amino-OA-PEI which is absent in spectra on PEI 10KDa. Further, to confirm results obtained in FTIR analysis and to obtain the extent of aliphatic lipid substitutions on PEI 10KDa NMR spectroscopy was also performed. The ^{1}H NMR spectra of PEI 10KDa (Figure 5.4A) showed peak from 2.4 to 2.8 ppm, which is attributed to the –N-CH2-CH2– groups. More detailed assignment of chemical shift to functional groups of PEI is made in Table 5.3.

Table 5.3 Assignments of chemical shift to functional group protons in 1H NMR spectra for PEI 10KDa. (39)

Sr. No.	Structural Unit	ppm
1	NH_2-CH_2-CH_2-NH-	2.76/2.75
2	NH_2-CH_2-CH_2-N-	2.70
3	-NH-CH_2-CH_2-NH-	2.69/2.68
4	-NH-CH_2-CH_2-N-	2.63
5	-NH-CH_2-CH_2-NH_2	2.62/2.61
6	-N-CH_2-CH_2-NH-	2.55
7	-N-CH_2-CH_2-N-	2.51
8	-N-CH_2-CH_2-NH_2	2.48

The ^{1}H NMR spectra of HA-PEI and OA-PEI (Figure 5.4B and Figure 5.4C) showed peak at 0.9 ppm as well as at 2.15 in addition to peak at 2.4 to 2.8 ppm. Chemical shift at 0.9 ppm is attributed to –CH3 group of HA and OA. Chemical shift at 2.15 ppm is attributed to –CO-CH2 group of HA and OA.

The ^{1}H NMR spectra of ω-amino-HA-PEI and ω-amino-OA-PEI (Figure 5.4C and Figure 5.4D) did not show peak at 0.9 ppm due to absence of –CH3 group but chemical shift at 2.15 in addition to peak at 2.4 to 2.8 ppm was present. Chemical shift at 2.15 ppm is attributed to –CO-CH2 group of ω-amino-HA-PEI and ω-amino-OA-PEI.

The characteristic peaks of –N-CH2-CH2– and –CH3 at chemical shift 2.4 to 2.8 ppm and 0.9 ppm respectively was integrated, normalized for number of Hs in each peak and was used to obtain the extent of HA and OA substitution on PEI 10KDa. Similarly, the characteristic peak of –N-CH2-CH2– and –CO-CH2 at chemical shift 2.4 to 2.8 ppm and 2.15 ppm respectively was integrated, normalized for number of Hs in each peak and used to obtain the extent of HA and OA substitution on PEI 10KDa. Additionally, Peaks at chemical shifts 1.6 ppm was also obtained for H in –CH2– group adjacent to –CO-CH2 and at 1.3 ppm for H in $–(CH2)_n–$ groups in HA, OA, ω-amino-HA-PEI and ω-amino-OA-PEI (where, n=3 for HA and ω-amino-HA-PEI and n=4 for OA and ω-amino-OA-PE).

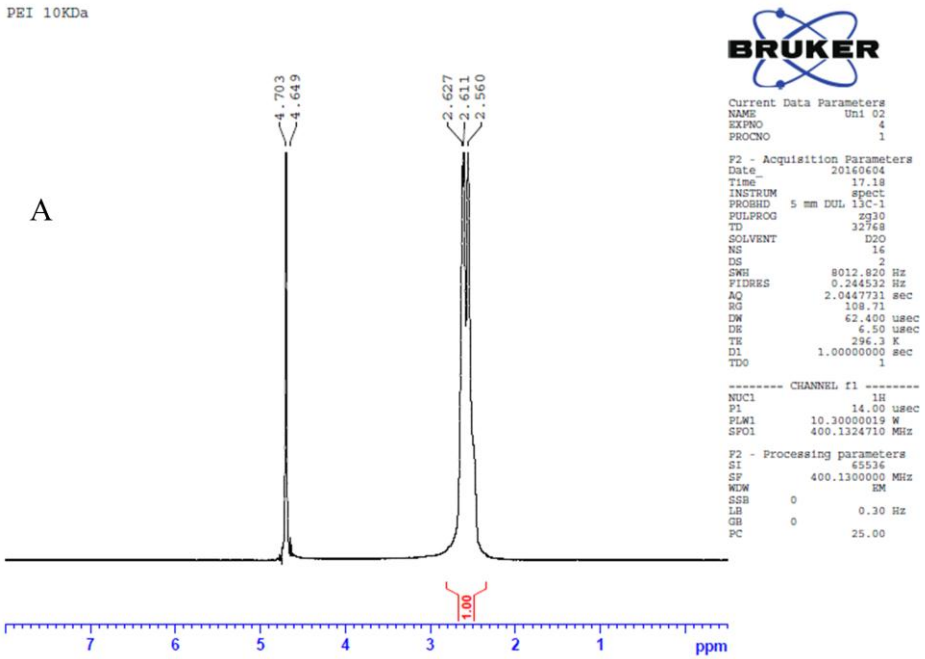
PEI 10KDa
A
4.703
4.649
2.627
2.611
2.560
1.00
7
6
5
4
3
2
1
ppm
BRUKER
Current Data Parameters
NAME Uni 02
EXPNO 4
PROCNO 1
F2 - Acquisition Parameters
Date_ 20160604
Time 17.18
INSTRUM spect
PROBHD 5 mm DUL 13C-1
PULPROG zg30
TD 32768
SOLVENT D2O
NS 16
DS 2
SWH 8012.820 Hz
FIDRES 0.244532 Hz
AQ 2.0447731 sec
RG 108.71
DW 62.400 usec
DE 6.50 usec
TE 296.3 K
D1 1.00000000 sec
TD0 1
-------- CHANNEL f1 --------
NUC1 1H
P1 14.00 usec
PLW1 10.30000019 W
SFO1 400.1324710 MHz
F2 - Processing parameters
SI 65536
SF 400.1300000 MHz
WDW EM
SSB 0
LB 0.30 Hz
GB 0
PC 25.00

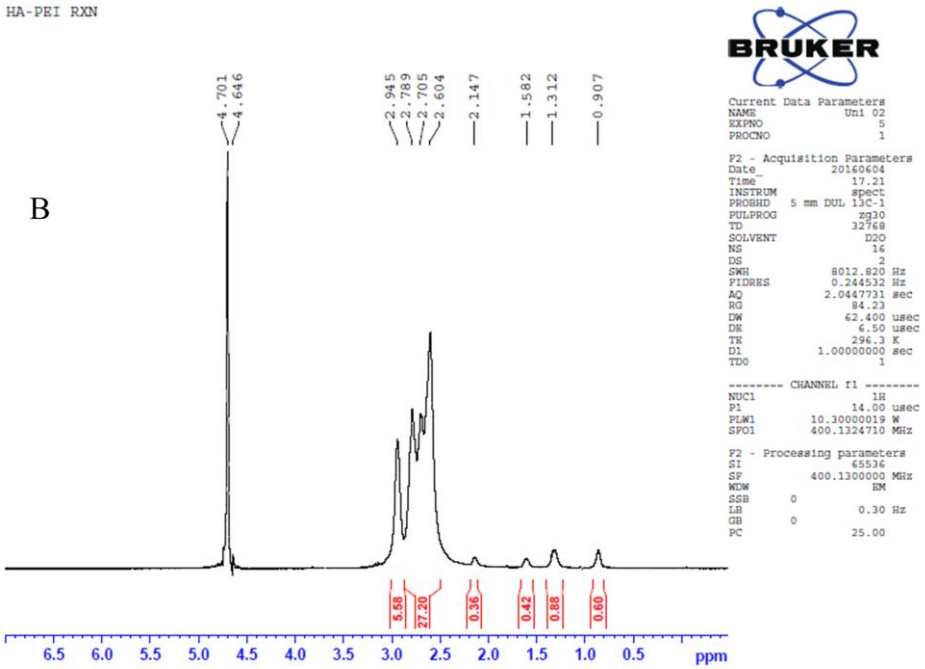
HA-PEI RXN
B
4.701
4.646
2.945
2.789
2.705
2.604
2.147
1.582
1.312
0.907
5.58
27.20
0.36
0.42
0.88
0.60
6.5
6.0
5.5
5.0
4.5
4.0
3.5
3.0
2.5
2.0
1.5
1.0
0.5
ppm
BRUKER
Current Data Parameters
NAME Uni 02
EXPNO 5
PROCNO 1
F2 - Acquisition Parameters
Date_ 20160604
Time 17.21
INSTRUM spect
PROBHD 5 mm DUL 13C-1
PULPROG zg30
TD 32768
SOLVENT D2O
NS 16
DS 2
SWH 8012.820 Hz
FIDRES 0.244532 Hz
AQ 2.0447731 sec
RG 84.23
DW 62.400 usec
DE 6.50 usec
TE 296.3 K
D1 1.00000000 sec
TD0 1
-------- CHANNEL f1 --------
NUC1 1H
P1 14.00 usec
PLW1 10.30000019 W
SFO1 400.1324710 MHz
F2 - Processing parameters
SI 65536
SF 400.1300000 MHz
WDW EM
SSB 0
LB 0.30 Hz
GB 0
PC 25.00

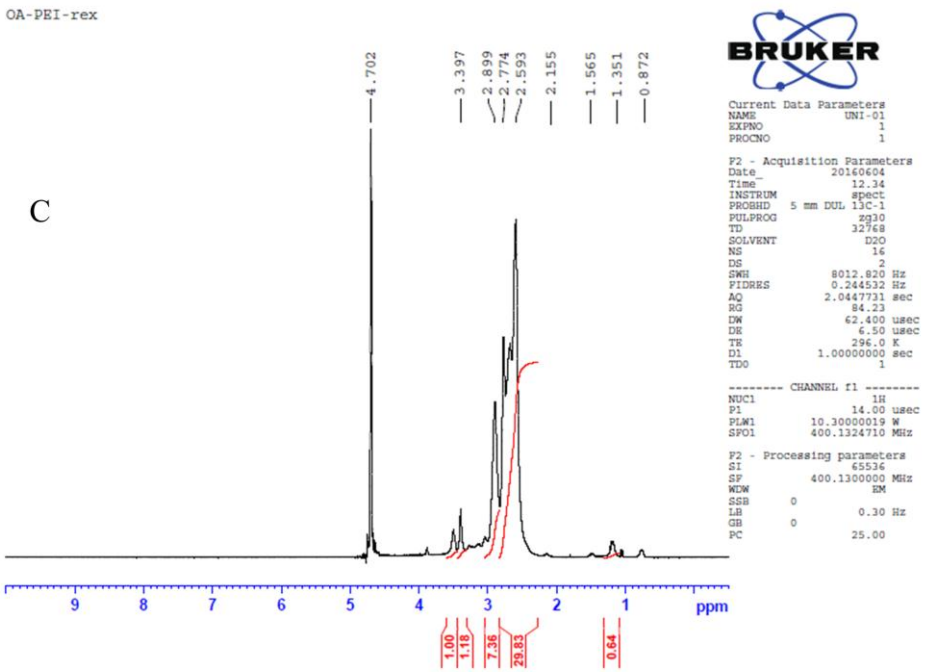
OA-PEI-rex
C
4.702
3.397
2.899
2.774
2.593
2.155
1.565
1.351
0.872
9
8
7
6
5
4
3
2
1
ppm
1.00
1.18
7.36
29.83
0.64
BRUKER
Current Data Parameters
NAME UNI-01
EXPNO 1
PROCNO 1
F2 - Acquisition Parameters
Date_ 20160604
Time 12.34
INSTRUM spect
PROBHD 5 mm DUL 13C-1
PULPROG zg30
TD 32768
SOLVENT D2O
NS 16
DS 2
SWH 8012.820 Hz
FIDRES 0.244532 Hz
AQ 2.0447731 sec
RG 84.23
DW 62.400 usec
DE 6.50 usec
TE 296.0 K
D1 1.00000000 sec
TD0 1
-------- CHANNEL f1 --------
NUC1 1H
P1 14.00 usec
PLW1 10.30000019 W
SFO1 400.1324710 MHz
F2 - Processing parameters
SI 65536
SF 400.1300000 MHz
WDW EM
SSB 0
LB 0.30 Hz
GB 0
PC 25.00

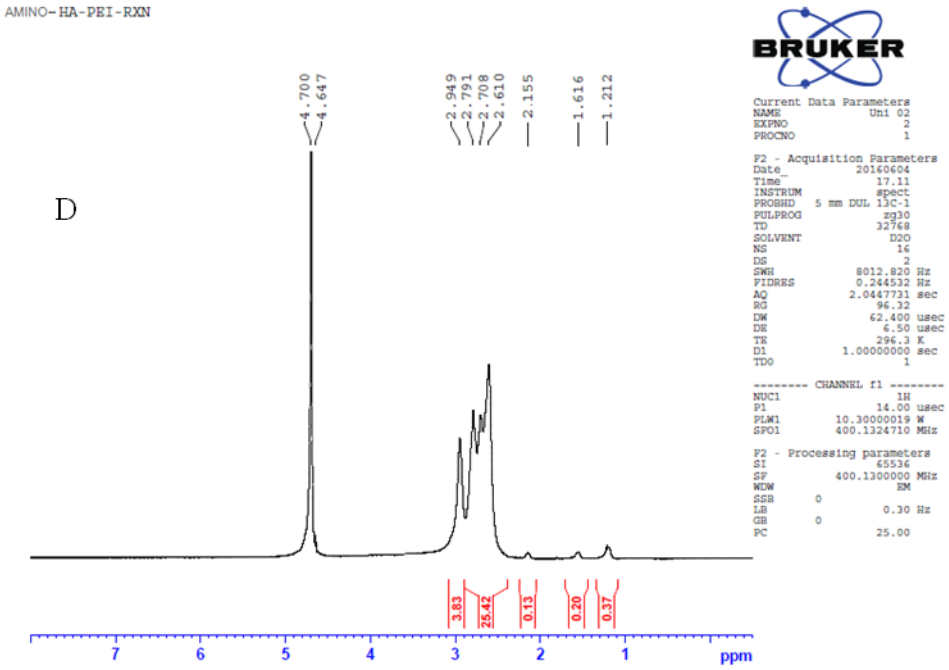
AMINO-HA-PEI-RXN
D
4.700
4.647
2.949
2.791
2.708
2.610
2.155
1.616
1.212
7
6
5
4
3
2
1
ppm
3.83
25.42
0.13
0.20
0.37
BRUKER
Current Data Parameters
NAME Uni 02
EXPNO 2
PROCNO 1
F2 - Acquisition Parameters
Date_ 20160604
Time 17.11
INSTRUM spect
PROBHD 5 mm DUL 13C-1
PULPROG zg30
TD 32768
SOLVENT D2O
NS 16
DS 2
SWH 8012.820 Hz
FIDRES 0.244532 Hz
AQ 2.0447731 sec
RG 96.32
DW 62.400 usec
DE 6.50 usec
TE 296.3 K
D1 1.00000000 sec
TD0 1
-------- CHANNEL f1 --------
NUC1 1H
P1 14.00 usec
PLW1 10.30000019 W
SFO1 400.1324710 MHz
F2 - Processing parameters
SI 65536
SF 400.1300000 MHz
WDW EM
SSB 0
LB 0.30 Hz
GB 0
PC 25.00

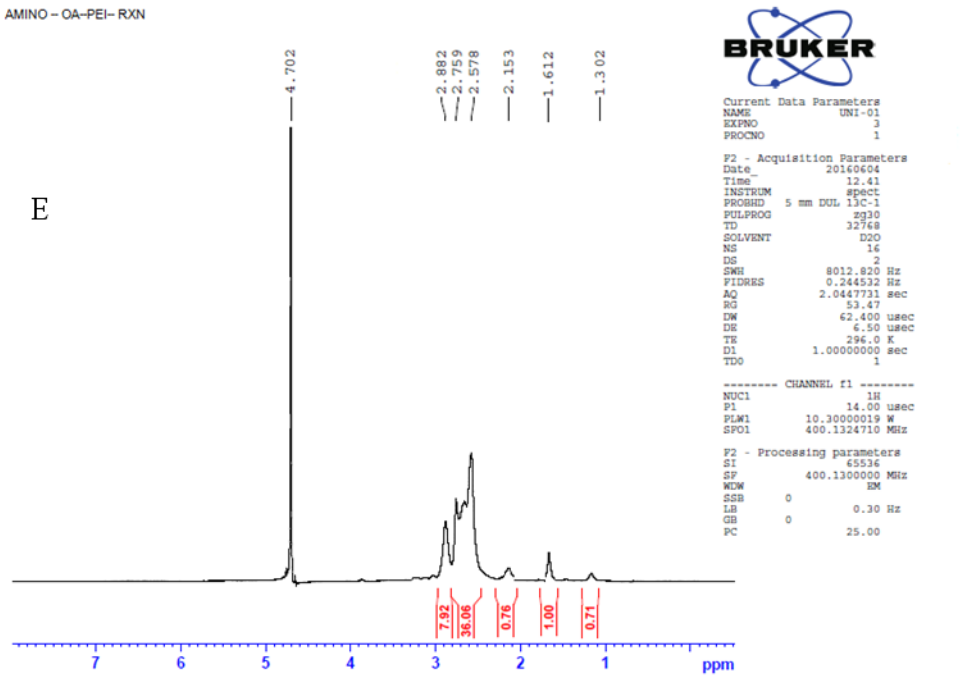

Figure 5.4 ^{1}H NMR spectra of A) PEI, B) HA-PEI, C) OA-PEI, D) ω-amino-HA-PEI and E) ω-amino-OA-PEI.

Molar ratio of substitution of HA, OA, ω-amino-HA and ω-amino-OA on PEI was calculated from ^{1}H NMR spectra and results are represented in Table 5.4.

Table 5.4 Extent of HA, OA, ω-amino-HA and ω-amino-OA substitution on PEI represented as % substitution based on 1H-NMR analysis.

Polymer	Weight ratio of PEI: lipid substituent taken	Number of PEI: Number of Lipid substituent ratio (Theo)	Mole ratio of PEI: lipid substituent fromNMR	Number of PEI: Number of Lipid substituent ratio	% Substitution of primary amino groups per one PEI
HA-PEI	74.29	1:1	0.9928	0.9928:1.0000	0.7148
OA-PEI	61.48	1:1	1.0561	1.0561:1.0000	0.7603
ω-amino-HA-PEI	43.23	1:1	0.9876	0.9876:1.0000	0.7110
ω-amino-OA-PEI	38.56	1:1	0.9978	0.9978:1.0000	0.7184

Results indicate that approximately one molecule of each substituent is conjugated to one molecule of PEI which indicates that only one primary amine group per PEI is substituted by each lipid substituent such as of HA, OA, ω-amino-HA and ω-amino-OA.

Number of primary amine groups in PEI, HA-PEI, OA-PEI, ω-amino-HA-PEI and ω-amino-HA-PEI were also quantified suing TNBS assay. PEI 10KDa was found to have 138 primary amine groups per one PEI molecule. Degree of substitution calculated for HA-PEI and OA-PEI showed 0.96 and 1.07 molecule substituted per one molecule of PEI respectively. Similarly, Degree of substitution calculated for ω-amino-HA-PEI and ω-amino-OA-PEI showed 1.12 and 1.17 molecules substituted per one molecule of PEI respectively. Results obtained in TNBS assay are in accordance with NMR analysis.

Ionization behavior of PEI and modified polymers was determined using acid titration method by determining pKa value and buffer capacity. Buffer capacity was obtained from equation stated above. Inverse of slope of titration curve between two

adjacent pH points can also give buffer capacity for those two pH points (Figure 5.5). The pKa value obtained for ethanolamine (pKa = 9.26) using same method was found to be in close agreement with reported literature value (pKa = 9.50) (40) which represents accuracy of used method. Furthermore, our data are in close agreement with other studies reporting pKa value of PEI 10KDa (41) (42).

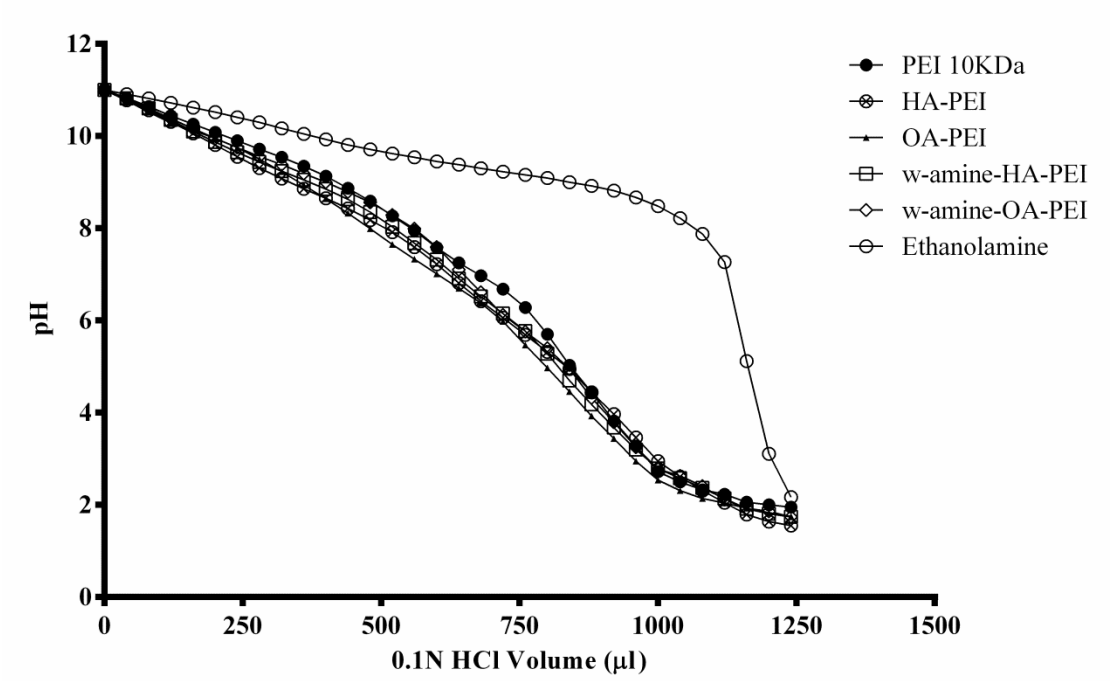

Figure 5.5 Acid-base titration of PEI, HA-PEI, OA-PEI, ω-amino-HA-PEI and ω-amino-OA-PEI. Each data point represents the average of three experiments ± standard deviation.

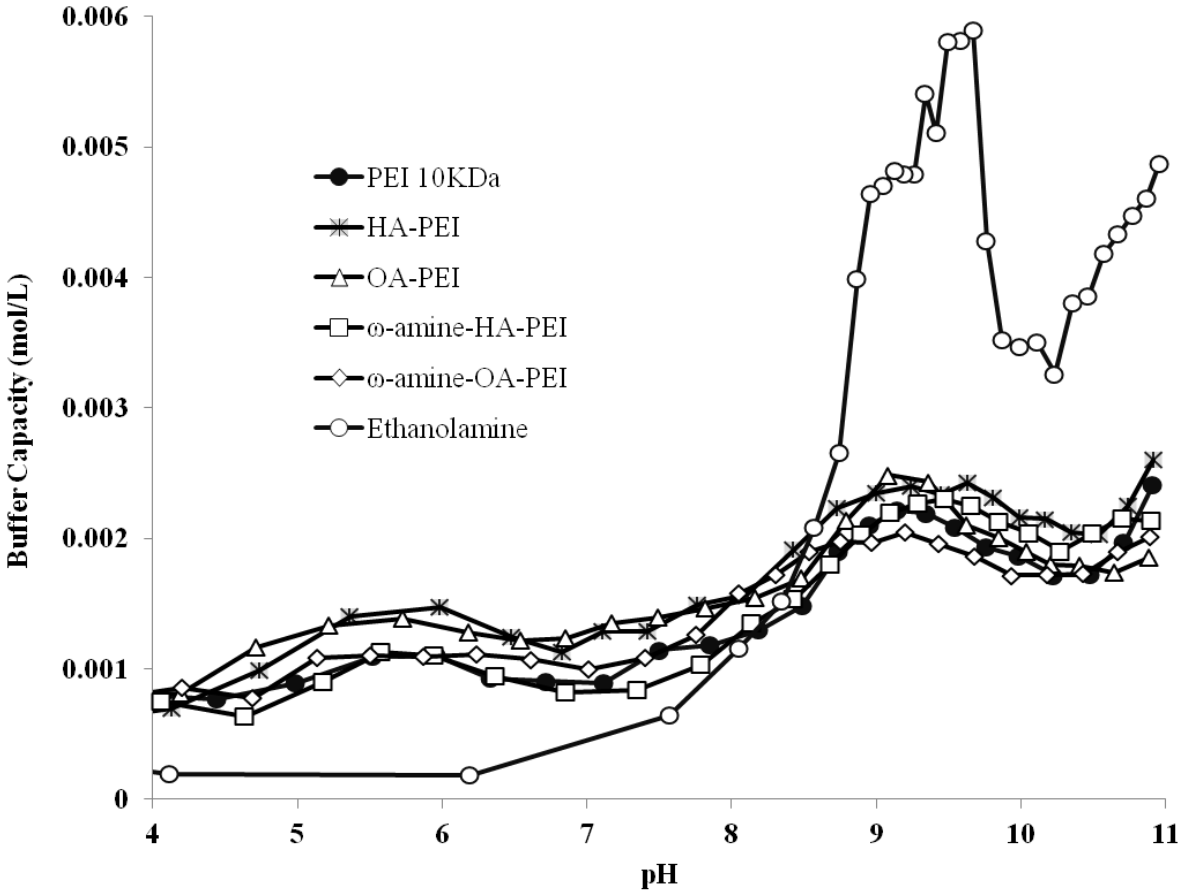

Figure 5.6 Buffer capacity of PEI, HA-PEI, OA-PEI, ω-amino-HA-PEI and ω-amino-OA-PEI in pH range 4 to 11. Each data point represents the average of three experiments ± standard deviation.

Buffer capacity of PEI is considered to be responsible for escape of PEI based polyplexes from endosome before entering in to lysosomes, the process is known as endosome escape. The mechanism by which PEI does so is called "Proton Sponge Effect" (10) (43). Buffer capacity of modified polymers was compared to unmodified PEI. Buffer capacity was not found to significantly (p>0.05) change due to HA and OA modifications on PEI as well as due to ω-amino-HA and ω-amino-OA modifications on PEI.

For three types of amine groups (primary, secondary and tertiary) present in polymers, two peaks were obtained in buffer capacity Vs pH curve, one at pH around ~6-7 and another at pH ~9-10 (Figure 5.6). The first peak at around 6-7 is due to tertiary amines and the more prominent second peak at pH around 9-10 is due to primary and secondary amines (42, 44).

The pH value corresponding to buffer capacity at highest point on peak represents pKa value for polymers under study and hence PEI and modified PEI based polymers have two pKa values. pKa values corresponding to primary and secondary amines is greater than 9 (denoted as pKa_1) and hence at physiological and lysosomal pH conditions, primary and secondary amines remain protonated. Whereas, pKa value corresponding to tertiary amine is around 5 - 6.4 (denoted as pKa_2) and hence tertiary amines will not be protonated at physiological pH.

Buffer capacity at pKa_1 value for PEI, HA-PEI, OA-PEI, ω-amino-HA-PEI and ω-amino-OA-PEI were found to be 0.0219, 0.00242, 0.00248, 0.00227 and 0.00205 mol/L respectively. Furthermore, Buffer capacity at pKa_2 value for PEI, HA-PEI, OA-PEI, ω-amino-HA-PEI and ω-amino-OA-PEI were found to be 0.00111, 0.00147, 0.00139, 0.00113 and 0.00111 mol/L respectively. These results indicate that HA, OA, ω-amino-HA and ω-amino-OA modifications on PEI 10 KDa do not significantly affect buffer capacity of PEI.

Furthermore, it is preferable to achieve endosomal escape earlier due to the cytotoxicity of late endosomal/lysosomal proteases. In addition, lower pKa values may reduce the ability of polymer to achieve endosomal escape in a timely manner. Hence, designing polymers that can buffer in the higher endosomal pH range (pH ∼6−7.4) can help easily escape endosome and enhance gene transfection efficiencies while reducing cytotoxicity. pKa value of polymers in this investigation suggest that all the polymers are capable of buffering pH range from 4.7 to 7, which includes early and late stage pH of endosome. Hence capable of buffering entire endosomal pH range.

B. Selection of therapeutic gene for autoimmune hypothyroidism, its amplification and purification

1. pAL119-mCTLA4-IGHG1

pAL119-mCTLA4-IGHG1 is selected as therapeutic gene for analyzing its utility in prevention and treatment of autoimmune hypothyroidism. Details of plasmid are provided in Table 5.5, Figure 5.7 and Figure 5.8. pAL119-mCTLA4-IGHG1 is constructed from pAL119 vector inserted with mCTLA4-IGHG1 gene in to multiple cloning site (MCS) of the plasmid. This vector operates under promoter of cytomegalovirus (CMV) and contains no transfection marker protein tag. pAL119-mCTLA4-IGHG1 encodes CTLA-4 IG protein with 92KDa molecular weight, a

fusion protein of extracellular domain of Mouse cytotoxic T-murine Lymphocyte Antigen 4 and Human IgG1-FC region (45, 46).

Table 5.5 pAL119-mCTLA4-IGHG1 plasmid Description.

Plasmid Name	pAL119-mCTLA4-IGHG1
Vector Name	pAL119
Insert Gene Name	mCTLA4-IGHG1
Plasmid Size	9432bp
Vector Type	Mammalian Expression Vector
Expression Method	Constitutive
Promoter	CMV
Antibiotic Resistance	Ampicillin
Protein Tag	None

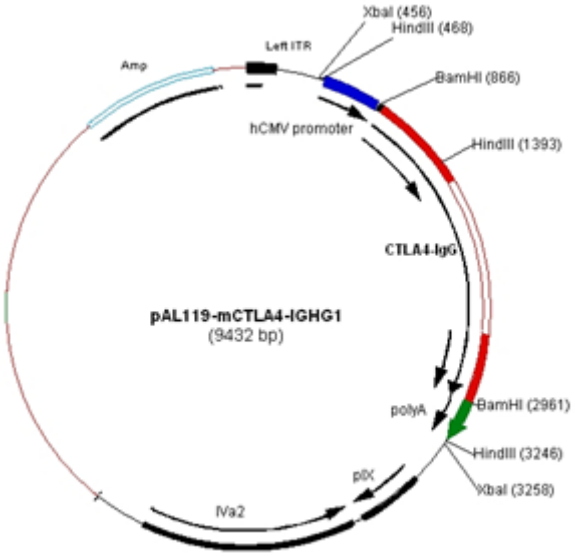

Figure 5.7 pAL119-mCTLA4-IGHG1 plasmid circular map.

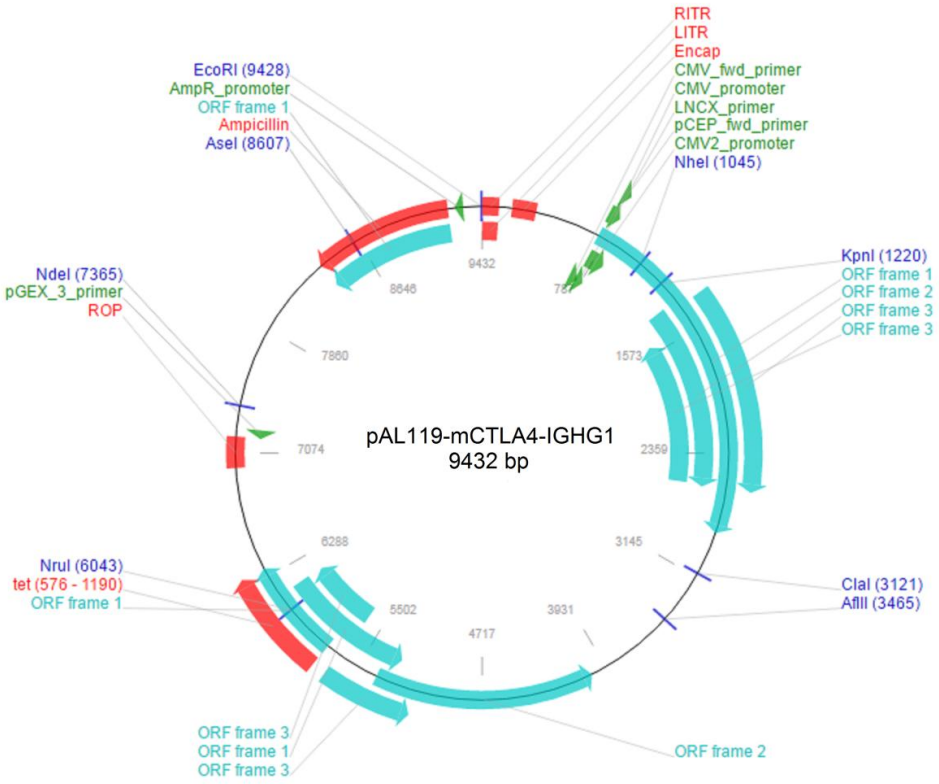

Figure 5.8 pAL119-mCTLA4-IGHG1 plasmid circular detailed map.

CTLA4, also known as CD152, is a protein receptor present on the surface of T cells that down regulates the immune system (47). On the other hand CD28 receptor on the T cells stimulates the immune system. Down regulation or stimulation of immune system occurs through respective binding of CTLA4 or CD28 to CD80 (B7-1)/CD86 (B7-2) receptors present on activated Antigen Presenting Cells (APC). CTLA4 has twenty times more binding affinity for B7 receptors than C28. Pairing with either a CD28 or CTLA4 present on a T cell can produce, respectively, "co-stimulatory signal to enhance" or "inhibitory signal to decrease" the activity of the Major Histocompatibility Complex-T Cell Receptor signal between the APC and the T cell. Apart from, being present on activated APCs, CD80 receptor is also found on T-cells themselves. Binding of CD28 or CTLA4 present on a T cell to another T cell's CD80 can send stimulatory or inhibitory T-cell signal respectively (47) (48).

In general, full activation of T cell occurs in two steps: 1) binding of the TCR to the antigen-MHC complex on the APC, and 2) generation of a co-stimulatory signal due to the binding of CD28 to the B7 protein on the APC (48). CTLA-4 IG contains a high binding affinity for B7 and hence prevents them from delivering the co-

stimulatory signal to T cells, thus by preventing second step of T cell activation and thus prevents the full activation of T cells (49). Due to CTLA4 extracellular domain, CTLA-4 IG is a capable of binding with more avidity to CD80 (B7-1) rather than to CD86 (B7-2) and like CTLA-4 can down regulate immune system by inhibiting this signals (50). Due to IgG moiety, CTLA4 IG has prolonged *in vivo* half life which further contributes to prolonged duration of action. In summary, CTLA-4 IG is a selective co-stimulation modulator as it inhibits the co-stimulation of T cells (51) (52). Furthermore, in extensive studies, it is also found to reduce cell-mediated immunity and T cells dependent antibody production. It also contribute to induction of immune tolerance. Illustration of mechanism of action of CTLA-4 IG is also provided in Figure 5.9. CTLA-4 IG is clinically approved by various regulatory agencies for clinical management of moderate to severe Rheumatoid Arthritis (53).

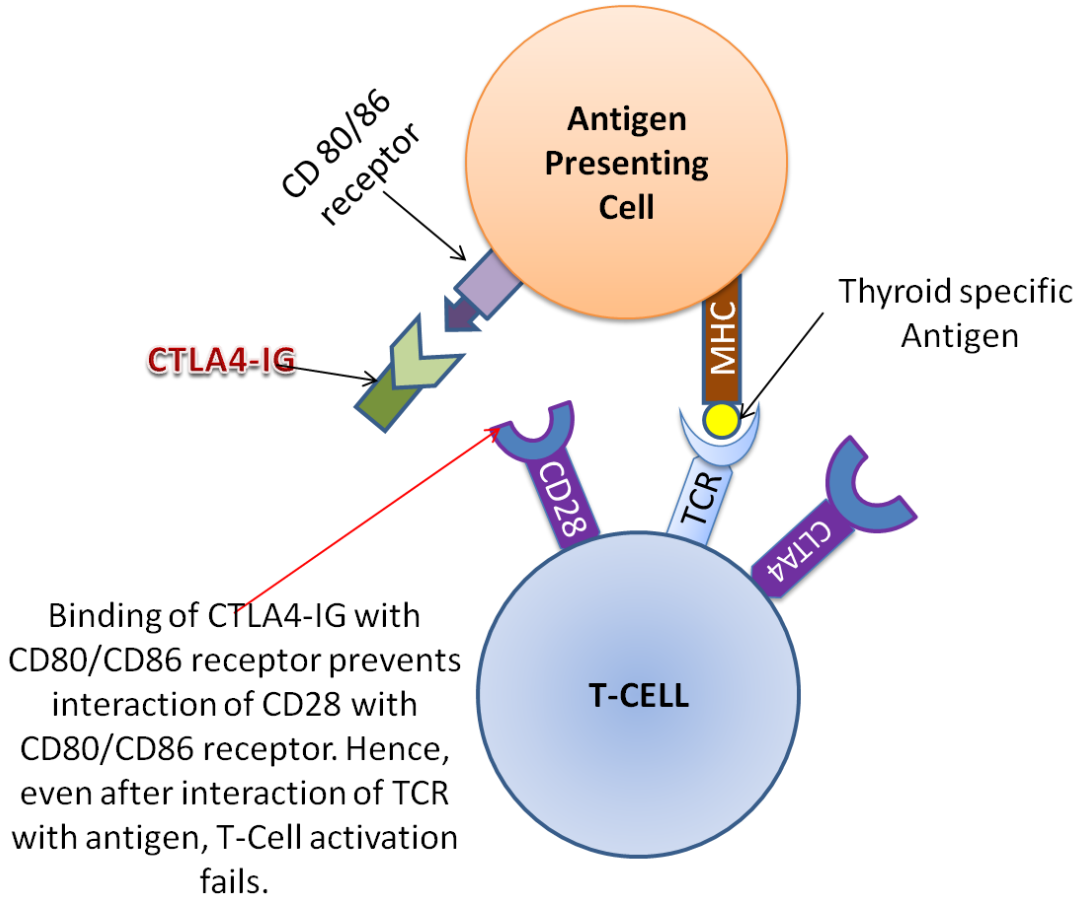

Figure 5.9 Mechanism of action of CTLA4-IG protein translated from pAL119-mCTLA4-IGHG1 plasmid.

2. pEGFP-N1

pEGFP-N1 operates under promoter of CMV and encodes a red-shifted variant of wild-type Green Fluorescent Protein (GFP) known as Enhanced Green Fluorescent Protein (EGFP) (54) (55). Details of plasmid are provided in Table 5.6 and Figure 5.10.

pEGFP-N1 has been developed as transfection marker by optimization of brighter fluorescence than GFP and higher expression in mammalian cells. (Excitation maximum = 488 nm; emission maximum = 507 nm) (55). The target gene such as mCTLA4-IGHG1can also be cloned into pEGFP-N1 by Fusions to the N terminus of EGFP which retains the fluorescent properties of the native protein allowing the localization of the fusion protein *in vivo*. As stated earlier, pAL119-mCTLA4-IGHG1 does not contain transfection marker protein tag and hence in certain studies of present investigation, such as fluorescence microscopy, confocal microscopy and flow cytometry, pEGFP-N1 is used as marker plasmid.

Table 5.6 pEGFP-N1 Plasmid vector Description.

Vector Name	**pEGFP-N1**
Insert Gene Name	**EGFP** (Enhanced Green Fluorescent Protein)
Total Vector Size	4733 bp
Vector Type	Mammalian Expression Vector
Expression Method	Constitutive
Promoter	CMV
Antibiotic Resistance	Kanamycin

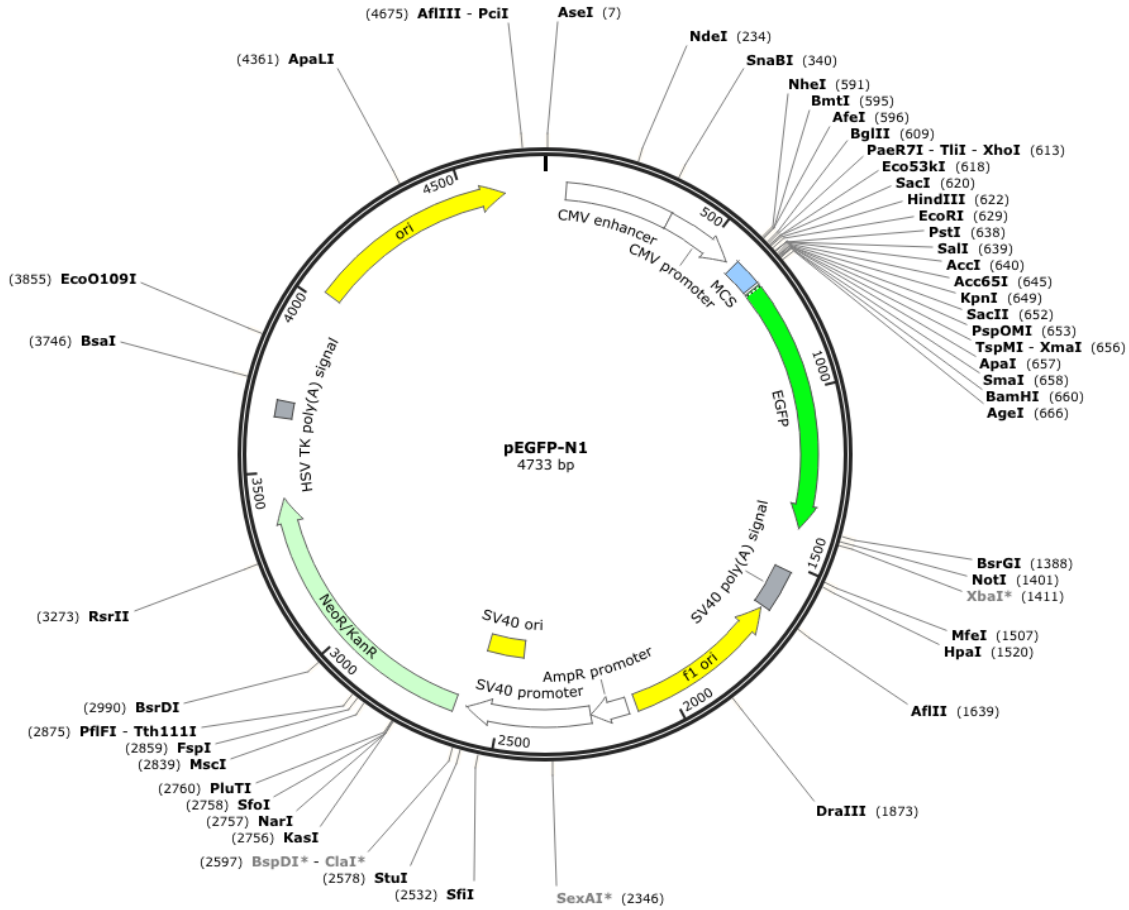

Figure 5.10 pEGFP-N1 plasmid detailed circular map.

pAL119-mCTLA4-IGHG1 isolated by Qiagen™ plasmid Maxi kit was of good purity and integrity. Size of isolated pAL119-mCTLA4-IGHG1 was in agreement with the data provided by depositor from where pDNA was procured (Figure 5.11).

In addition, pAL119-mCTLA4-IGHG1 digested using single site digestion enzyme KpnI yielded single linear original pDNA (9432bp) and double site digestion enzyme XbaI yielded two fragments of original pDNA (6630bp and 2802bp). Further, size of these digested products was in agreement with the data provided by depositor from where pAL119-mCTLA4-IGHG1 was procured (Figure 5.11).

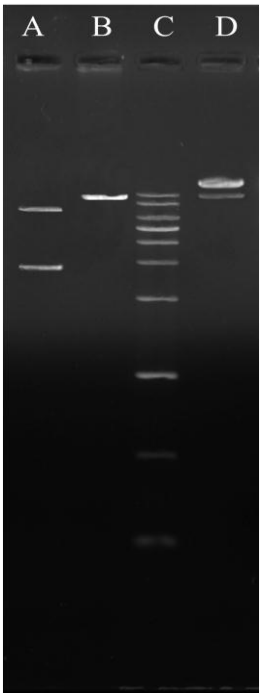

Figure 5.11 Gel electrophoresis analysis of A) pAL119-mCTLA4-IGHG1 digested by XbaI B) pAL119-mCTLA4-IGHG1 digested by KpnI C) DNA marker (HiMedia) D) pAL119-mCTLA4-IGHG1 undigested.

pDNA was detectable at all amounts by UV transilluminator after quantitative analysis. Hence, a midpoint amount, 100 ng of pAL119-mCTLA4-IGHG1 was used for all further experiments (Figure 5.12).

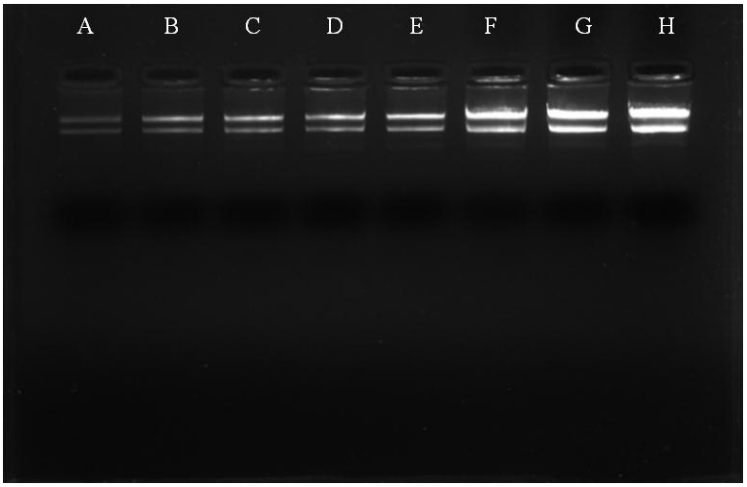

Figure 5.12 Gel electrophoresis analysis of pAL119-mCTLA4-IGHG1 for minimum detectable amount determination. Lane A) 20 ng, B) 40 ng, C) 60 ng, D) 80 ng, E) 100 ng, F) 200 ng, G) 300 ng and H) 400 ng respectively.

C. Physicochemical characterization of polyplexes

1. Size and morphology of polyplexes

TEM and DLS analysis was performed to study the influence of lipid modifications on size and shape of the polylexes formed with plasmid DNA (56) (57) (58). In this study, physiological salt concentration (150mM NaCl, pH 7.4) was used. Polyplexes prepared at all the N/P ratio 0.5, 0.75, 1.0, 2.0, 4.0, 8.0 and 12.0 were used for size analysis by DLS technique to understand effect of change in N/P ratio on size of polyplexes. These results show that size of polyplexes reduced at each N/P ratio when prepared using HA-PEI, OA-PEI, ω-amino-HA-PEI and ω-amino-OA-PEI in the order of HA-PEI > OA-PEI > ω-amino-HA-PEI > ω-amino-OA-PEI compared to polyplexes prepared using PEI 10KDa. Furthermore, increase in N/P ratio decreased size of polyplexes. Hydrodynamic diameters representing size for all the types of polyplexes is reported in Figure 5.13.

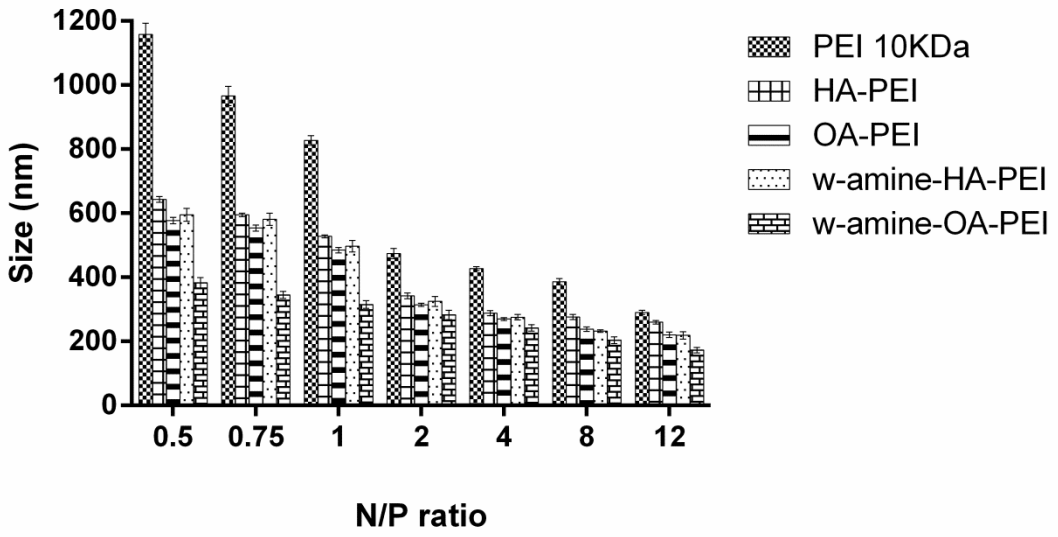

Figure 5.13 Size of polyplexes prepared from PEI 10KDa, HA-PEI, OA-PEI, ω-amino-HA-PEI and ω-amino-OA-PEI in 150mM NaCl, pH 7.4. Each data point represents the average of three experiments ± standard deviation.

Polyplexes prepared at the N/P ratio 12 were used for TEM study because at this ratio acceptable size was achieved. All polyplexes were found to be spherical and compact. Polyplexes prepared from HA-PEI and OA-PEI were found to have 200 ± 32nm and 180 ± 24nm size respectively. Whereas, polyplexes prepared from ω-amino-HA-PEI and ω-amino-OA-PEI were significantly smaller with 130 ± 26nm and 80 ± 20nm size respectively. PEI 10kDa also formed spherical polyplexes with 290 ± 46nm size (Figure 5.14).

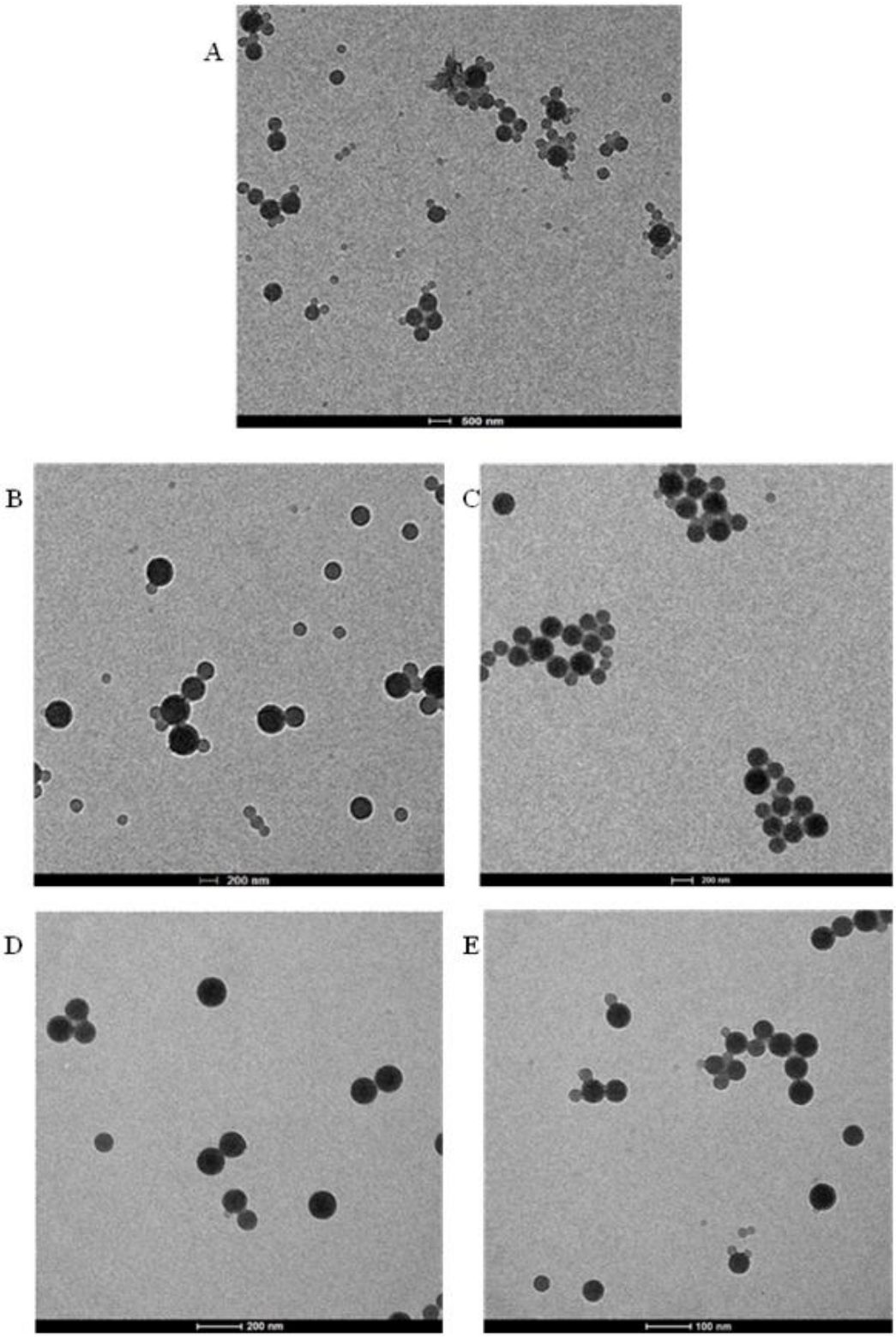

Figure 5.14 TEM images of polyplexes prepared from A) PEI 10KDa, B) HA-PEI, C) OA-PEI, D) ω-amino-HA-PEI and E) ω-amino-OA-PEI in 150mM NaCl, pH 7.4 at N/P ratio 12.

The results of TEM experiments and the DLS measurements demonstrated that all modified polymers yielded spherical polyplexes and as N/P ratio increases from 0.5 to 12, polyplexes become more compact as observed from decrease in size. Therefore, here we demonstrated that lipid based modifications of PEI using HA, OA, w-amine-HA and w-amine-OA do not necessarily interfere with the condensation process of pDNA during polyplex formation. Comparison of size of polyplexes prepared from modified PEI with unmodified 10KDa PEI shows that they form polyplexes significantly smaller in size compared to PEI 10KDa in the order of HA-PEI > OA-PEI > ω-amino-HA-PEI > ω-amino-OA-PEI.

Results suggest that hydrophobic interaction of lipid chain of HA and OA in polyplexes prepared from HA-PEI and OA-PEI may be responsible for more compact polyplex in comparison to PEI 10KDa. Furthermore, in the contrast to polyplexes prepared from HA-PEI and OA-PEI, hydrophobic HA and OA moieties of ω-amino-HA-PEI and ω-amino-OA-PEI do not completely stand out of polyplexes prepared from ω-amino-HA-PEI and ω-amino-OA-PEI. In addition to hydrophobic interaction that occurs between lipid chain and pDNA there also occurs significant electrostatic interactions between ω-amino group (positively charged at physiological pH) and phosphate group of pDNA (negatively charged at physiological pH), these two interactions collectively lead to partial folding of hydrophobic HA and OA chains inwards toward core of polyplexes which may be responsible for formation of smallest size polyplexes in case of ω-amino-HA-PEI and ω-amino-OA-PEI. Hydrophobic interaction being relatively stronger in case of ω-amino-OA-PEI than ω-amino-HA-PEI, due to longer OA lipid chain than HA, polyplexes prepared from ω-amino-OA-PEI has least complex size.

However, size from TEM are not completely in well agreement (as same as size obtained from DLS) with DLS because latter is an intensity-based technique; whereas, TEM is a number-based technique (59) which make them fundamentally different. In addition, in DLS, sample under analysis is always hydrated; whereas, TEM operates under very high vacuum conditions and hence sample under analysis is always dry (60). Hence, size obtained from TEM analysis is often smaller than that obtained from DLS (Figure 5.15).

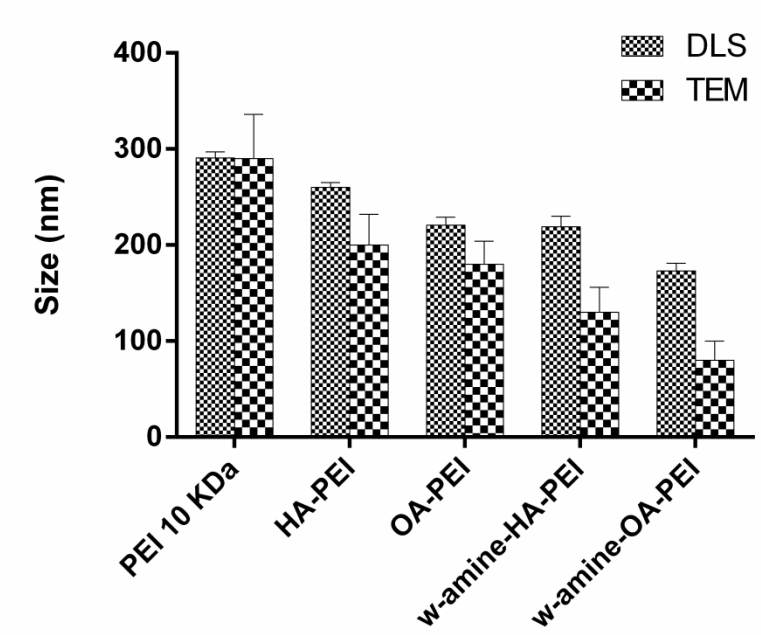

Figure 5.15 Size of polyplexes prepared from A) PEI 10KDa, B) HA-PEI, C) OA-PEI, D) ω-amino-HA-PEI and E) ω-amino-OA-PEI in150mM NaCl, pH 7.4 at N/P ratio 12 using DLS and TEM analysis (Comparative analysis). Each data point represents the average of three experiments ± standard deviation.

2. Laser Doppler Anemometry/ Electrophoresis/ velocimetry

To estimate the surface charge of the polyplexes prepared at different N/P ratio we measured the ζ-potential by laser Doppler anemometry technique. The results are shown in figure 5.16.

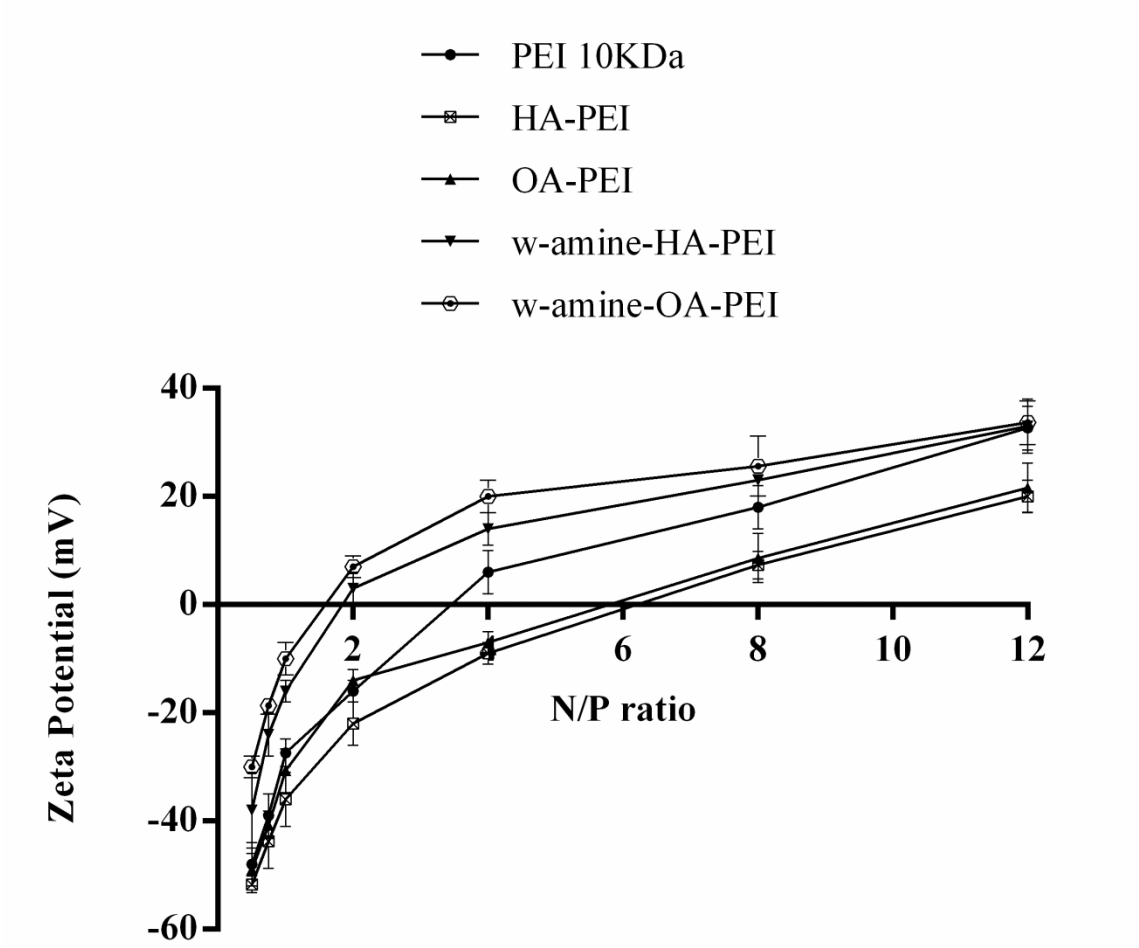

Figure 5.16 Zeta potential of polyplexes prepared from A) PEI 10KDa, B) HA-PEI, C) OA-PEI, D) ω-amino-HA-PEI and E) ω-amino-OA-PEI in 150mM NaCl, pH 7.4. Each data point represents the average of three experiments ± standard deviation.

Zeta was found to decrease in case of polyplexes prepared from HA-PEI and OA-PEI in comparison to polyplexes prepared from 10KDa PEI for different N/P ratios. From these observations it seems hydrophobic HA and OA moieties that stand out of polyplexes due to hydrophobic interaction and protect the cationic polyplexes, also cover the counter ion at shear plane of the cationic polyplexes and act as a screen to partially disrupt electric double layer formation and hence reduces potential at shear plane i.e. zeta potential. At N/P ratio 12, there was no significant difference between zeta potential of polyplexes prepared from HA-PEI and OA-PEI ($p=0.6262$),

however, in comparison to polyplexes prepared from 10KDa PEI (p= 0.0144 and p= 0.0352 respectively) significant difference was observed.

In addition, Zeta was found to increase in case of polyplexes prepared from ω-amino-HA-PEI and ω-amino-OA-PEI in comparison to polyplexes prepared from 10KDa PEI at different N/P ratios except at N/P ratio 12. At N/P ratio 12, there was no significant difference between zeta potential of polyplexes prepared from ω-amino-HA-PEI and ω-amino-OA-PEI (p= 0.8666), as well as, in comparison to polyplexes prepared from 10KDa PEI (p= 0.9391 and p= 0.8023) respectively. From these observations it seems that, in the contrast to polyplexes prepared from HA-PEI and OA-PEI, hydrophobic HA and OA moieties do not completely stand out of polyplexes prepared from ω-amino-HA-PEI and ω-amino-OA-PEI. In addition to hydrophobic interaction that occurs between lipid chain and pDNA there also occurs significant electrostatic interactions between ω-amino group (positively charged at physiological pH) and phosphate group of pDNA (negatively charged at physiological pH) which collectively leads to partial folding of hydrophobic HA and OA chains inwards toward core of polyplexes. Due to this folding of hydrophobic chain, distance of tightly bound layer and diffuse layer of electric double layer may increase from original surface of polyplex and hence counter ions are loosely bound to surface leading to more positive zeta potential compared to polyplexes prepared from PEI 10KDa.

3. Agarose Gel Retardation Assay

Agarose gel retardation was performed to study complexation and complete condensation of pDNA by cationic polymers as a function of N/P ratio. Polyplexes were prepared by allowing modified PEI and pDNA to interact at various N/P ratios such as 0, 0.5, 0.75, 1, 2, 4, 8 and 12. Complexation of pDNA with PEI, ω-amino-HA-PEI and ω-amino-OA-PE was observed at N/P ratio 2; whereas, with HA-PEI and OA-PEI was observed at N/P ratio 4. Complete EtBr exclusion or complete condensation of pDNA was observed at N/P ratio > 8. From this observation it is clear that lipid modifications on PEI do not interfere with pDNA condensation process. However slight change in N/P ratio for HA-PEI and OA-PEI suggest that HA and OA slightly hinder interaction and condensation of pDNA with PEI (Figure 5.17).

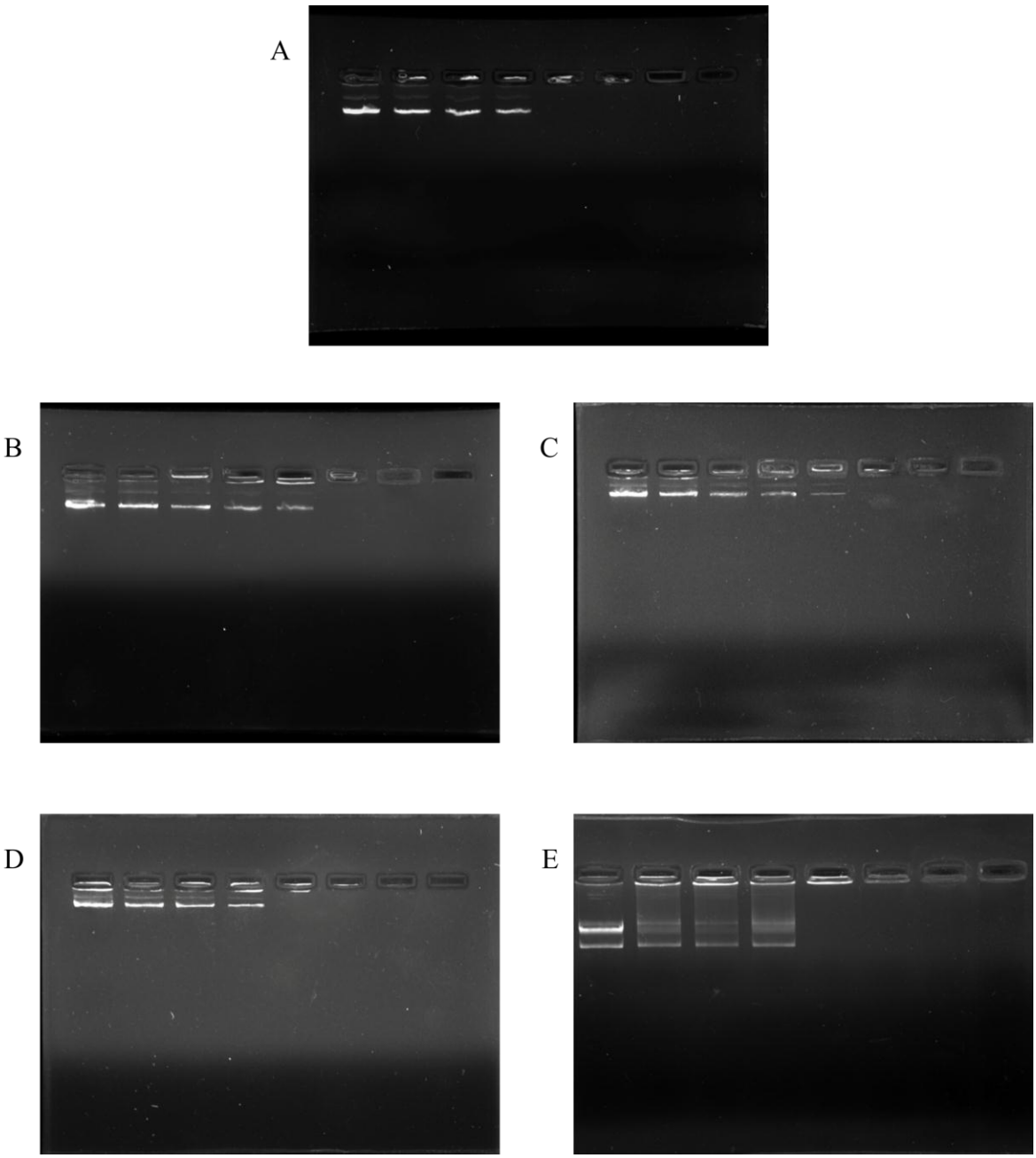

Figure 5.17 Gel retardation assay of polyplexes prepared from A) PEI 10KDa, B) HA-PEI, C) OA-PEI, D) ω-amino-HA-PEI and E) ω-amino-OA-PEI at N/P ratios 0, 0.5, 0.75, 1, 2, 4, 8 and 12.

4. Hemolysis assay

Hemolytic properties of PEI 10KDa and modified polymers were evaluated using ASTM's Standard Practice for Assessment of Hemolytic Properties of Materials (36). As per this test, biomaterials can be classified on hemolysis scale based on % haemoglobin released. Based on % Hemolysis 0%–2%, 2%–5, or >5%, biomaterials can be classified as non-hemolytic, slightly hemolytic, or haemolytic respectively. In

present study, hemolysis study was performed using washed RBC in normal saline and whole blood. Results obtained from both the experiments were not identical. Hemolysis study performed using washed RBC in saline suggest that PEI 10KDa, HA-PEI, OA-PEI, ω-amino- HA-PEI and ω-amino- OA-PEI are haemolytic at concentration above 20.0 µg/ml and slightly haemolytic at concentrations 1.0 and 10.0 µg/ml. Whereas, study performed using washed whole blood suggest that PEI 10KDa, HA-PEI, OA-PEI, ω-amino- HA-PEI and ω-amino- OA-PEI are non-haemolytic at all the concentrations.

The difference in results might be due to the protection provided by the plasma proteins that bind cationic polymers and form complexes which reduces affinity of cationic polymers towards RBCs due to cationic charge neutralization (61, 62). The results also demonstrate that cationic polymers induced approximately five to six times more percentage hemolysis on washed RBCs than on whole blood. Furthermore, Figure 5.18 and Figure 5.19 show that all the cationic polymers i.e. PEI 10KDa, HA-PEI, OA-PEI, ω-amino- HA-PEI, and ω-amino- OA-PEI induced hemolysis in a concentration dependent manner.

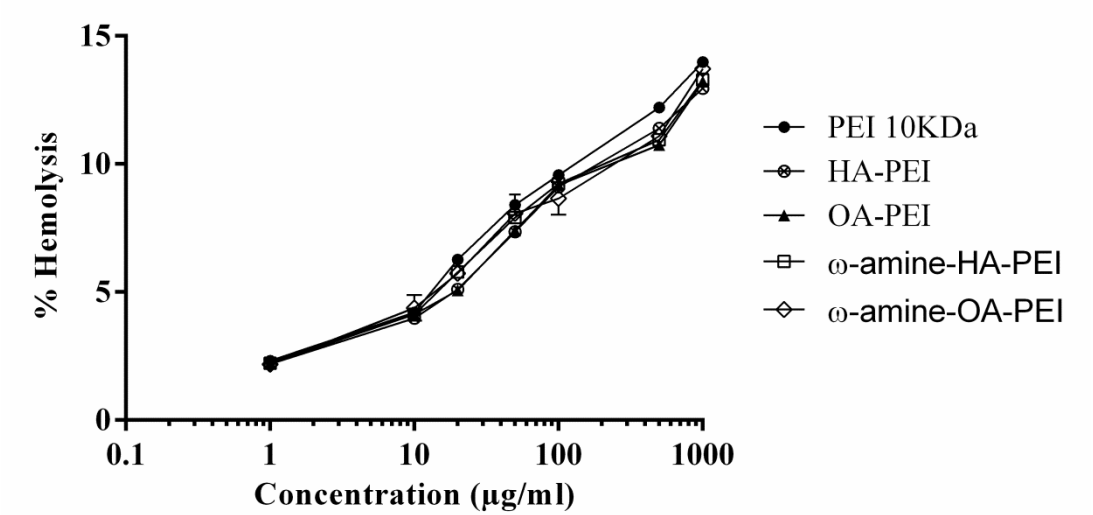

Figure 5.18 Hemolysis analysis of PEI 10KDa, HA-PEI, OA-PEI, ω-amino- HA-PEI and ω-amino-OA-PEI at various concentrations using Washed RBCs. Each data point represents the average of three experiments ± standard deviation.

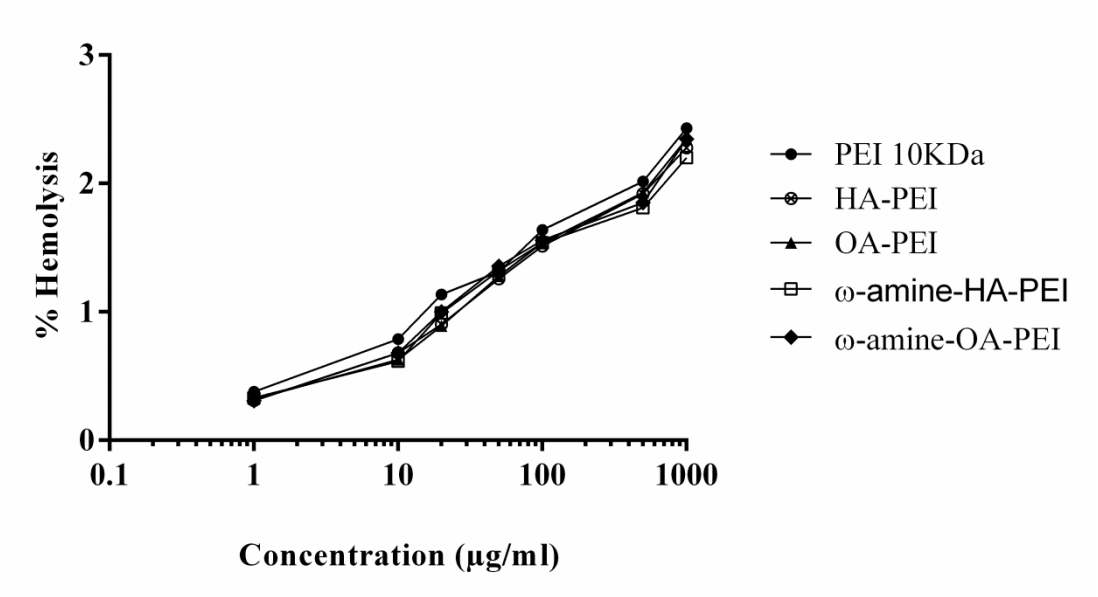

Figure 5.19 Hemolysis analysis of PEI 10KDa, HA-PEI, OA-PEI, ω-amino-HA-PEI, and ω-amino- OA-PEI at various concentrations using Whole Blood. Each data point represents the average of three independent experiments ± standard deviation.

Fischer et al. were first to observe and report this behaviour of PEI (63). These authors considered interaction and further binding of polycations with membrane proteoglycans responsible for cytotoxicity associated with polycations such as PEI (63). Study performed to indentify cytotoxicity mechanism, not perfomed particularly on RBC though, revealed that binding of polycations with membrane proteoglycans may induce redistribution of phosphotidylserine from inner plasma membrane to outer cell surface leading to membrane destabilization (64).

D. *In vitro* characterization of polylplexes

1. *In vitro* cytotoxicity and viability

The *in vitro* cytotoxicity of HA-PEI, OA-PEI, ω-amino-HA-PEI and ω-amino-OA-PEI was compared to PEI using MTT assay. PEI and newly synthesized PEI based cationic polymers were added to culture medium in different concentrations and MTT assay was performed to evaluate degree of cellular damage. MTT assay performed at 4hr and 24 hr after cells treatment reveal that viability of cells treated with HA-PEI and OA-PEI was not significantly different than cells treated with PEI. However, viability of cells treated with ω-amino-HA-PEI and ω-amino-OA-PEI was higher than cells treated with PEI. Furthermore, it was found that cell survival was concentration dependent. However, cell viability was significantly higher at 4hr than after 24hr after

treatment with cationic polymers indicating time dependent toxicity of PEI and other synthesized polymers. IC50 of HA-PEI, OA-PEI, ω-amino-HA-PEI and ω-amino-OA-PEI as well as PEI after 4 hr of treatment was found to be more than 1.0mg/ml as 80% of cells were viable at 1.0mg/ml concentration. IC50 of HA-PEI, OA-PEI, ω-amino-HA-PEI and ω-amino-OA-PEI as well as PEI after 24 hr of treatment was found ~80µg/ml. IC50 of HA-PEI, OA-PEI, ω-amino-HA-PEI, ω-amino-OA-PEI and PEI after 24 hr of treatment was found to be 81.17, 80.76, 79.79, 79.15, 79.21 µg/ml respectively (Figure 5.20).

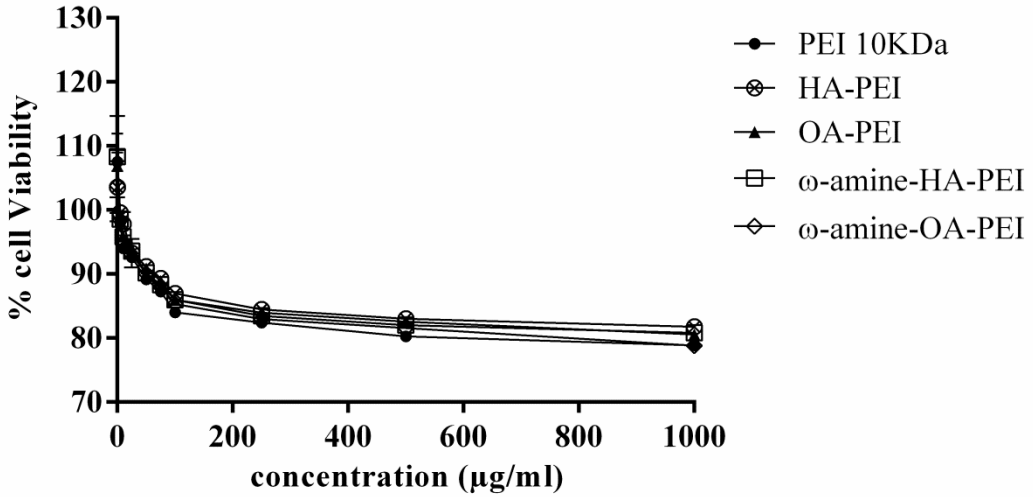

Figure 5.20 Viability of HEK 293 cells, 4 hr after treatment of PEI 10KDa, HA-PEI, OA-PEI, ω-amino-HA-PEI and ω-amino-OA-PEI at various concentrations. Each data point represents the average of three independent experiments ± standard deviation.

We also performed cell viability study with polyplexes prepared from HA-PEI, OA-PEI, ω-amino-HA-PEI and ω-amino-OA-PEI in comparison with PEI at N/P ratio 0, 0.5, 0.75, 1, 2, 4, 8 and 12. Results indicate that, at higher N/P ratio 12, viability of cells treated with of polyplexes prepared from HA-PEI, OA-PEI, ω-amino-HA-PEI and ω-amino-OA-PEI was more than 80% (89.600 ± 0.046, 87.100 ± 0.046, 83.473 ± 0.206 and 81.230 ± 0.101) and is comparable to PEI (85.033 ± 0.076) (Figure 5.21).

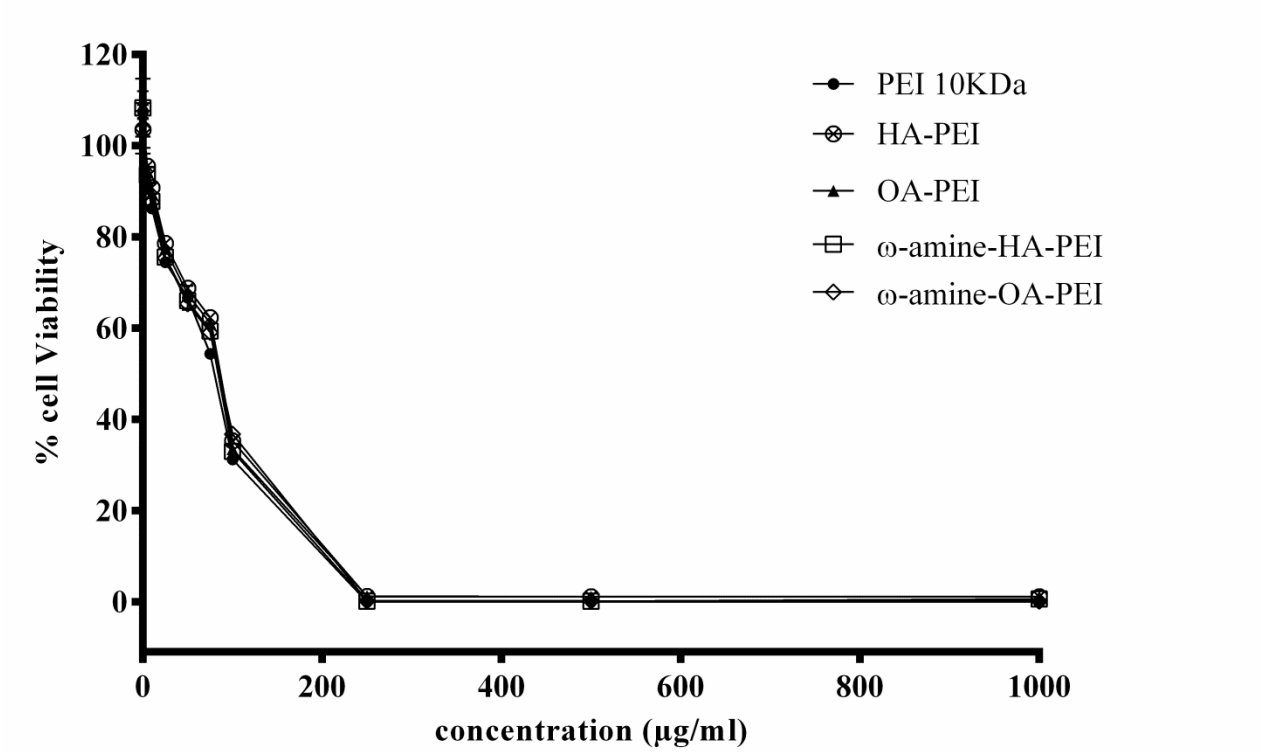

Figure 5.21 Viability of HEK 293 cells, 24 hr after treatment of PEI 10KDa, HA-PEI, OA-PEI, ω-amino-HA-PEI and ω-amino-OA-PEI at various concentrations. Each data point represents the average of three independent experiments ± standard deviation.

Viability of cells treated with polyplexes prepared from ω-amino-HA-PEI and ω-amino-OA-PEI was lowest among all treatment groups; this may be attributed to their higher zeta potential and smaller size in comparison to polyplexes from PEI 10KDa, HA-PEI and OA-PEI (Figure 5.15 and Figure 5.16). Interaction and further binding of polycations with membrane proteoglycans is responsible for cytotoxicity associated with polycations such as PEI, which is attributed to their cationic charge (63). Cell viability study performed after 4hr revealed cytotoxicity due to binding of polycations with membrane proteoglycans that induce redistribution of phosphotidylserine from inner plasma membrane to outer cell surface leading to membrane destabilization and cell death. Furthermore, results obtained after 24hr revealed cytotoxicity due to mitochondrial potential change followed by mitochondria mediated programmed cell death (64).

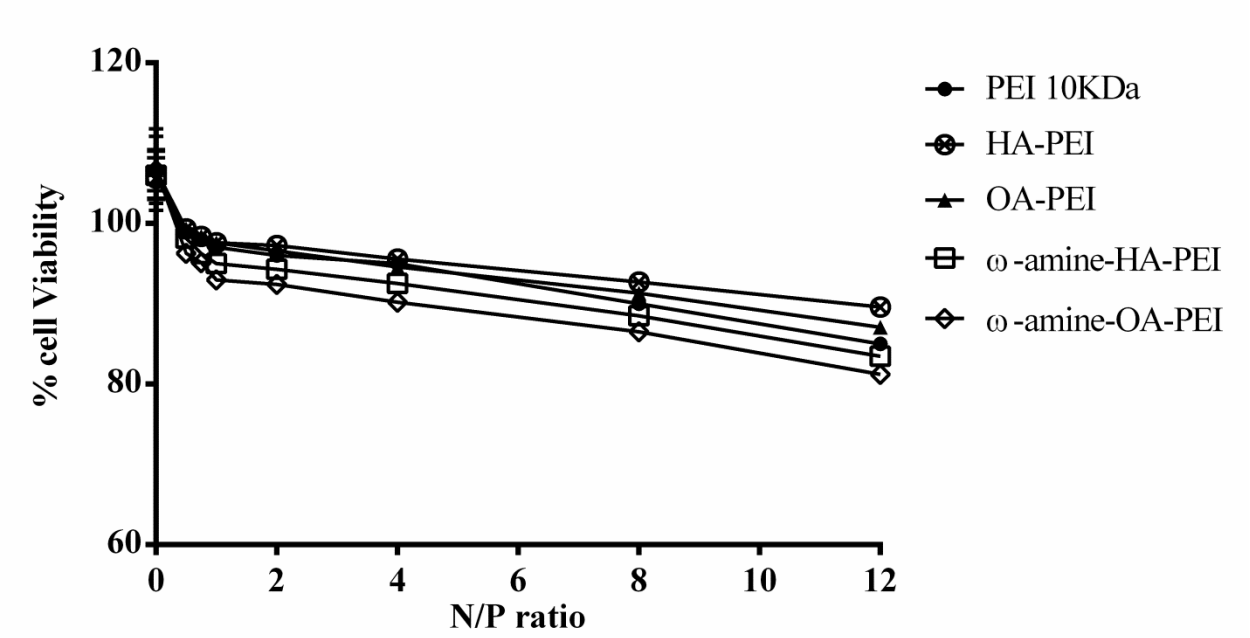

Figure 5.22 Viability of HEK 293 cells after treatment of polyplexes prepared from PEI 10KDa, HA-PEI, OA-PEI, ω-amino-HA-PEI and ω-amino-OA-PEI at N/P ratio 12. Each data point represents the average of three independent experiments ± standard deviation.

Cytotoxicity determination carried out for polymers without complexation with pDNA provides worst case estimation of cytotoxicity of polymers by allowing direct intercation with cells. To allow direct comparison of cytotoxicty of polymers only, cyctotoxicy determination for polymers alone was carried out. As results indicate, generally, this cytotoxicy of cationic polymers is decreased after complexation with pDNA due to charge neutralization. Polyplexes prepared from PEI 10KDa, HA-PEI, OA-PEI, ω-amino-HA-PEI and ω-amino-OA-PEI at N/P ratio 12 showed around more than 80% cell viability indicating an acceptable cytotoxicity profile under *in vitro* conditions (Figure 5.22).

2. *In vitro c*ellular uptake and transfection efficiency

Polyplexes formed between pDNA and the cationic polymers were assessed for their *in vitro* cellular uptake using fluorescence and confocal microscopy.

Fluorescence microscopy was performed to analyze cellular uptake of polyplexes, in a way to assess the ability of synthesized polymer to aid in intracellular entry of pDNA. Results obtained were not used for quantitative determination of percentage cellular uptake. HEK 293 Cells transected with naked pDNA did not show any green fluorescence of EGFP, this indicates that naked pDNA without vector support cannot

efficiently enter cell (Figure 5.23). HEK 293Cells transfected with polyplexes of pEGFP-N1 prepared from cationic polymers such as PEI 10KDa, HA-PEI, OA-PEI, ω-amino-HA-PEI and ω-amino-OA-PEI showed green fluorescence in cytoplasm of cells which indicates that all synthesized polymers, similarly to PEI, were capable of intracellular delivery of pDNA (Figure 5.23).

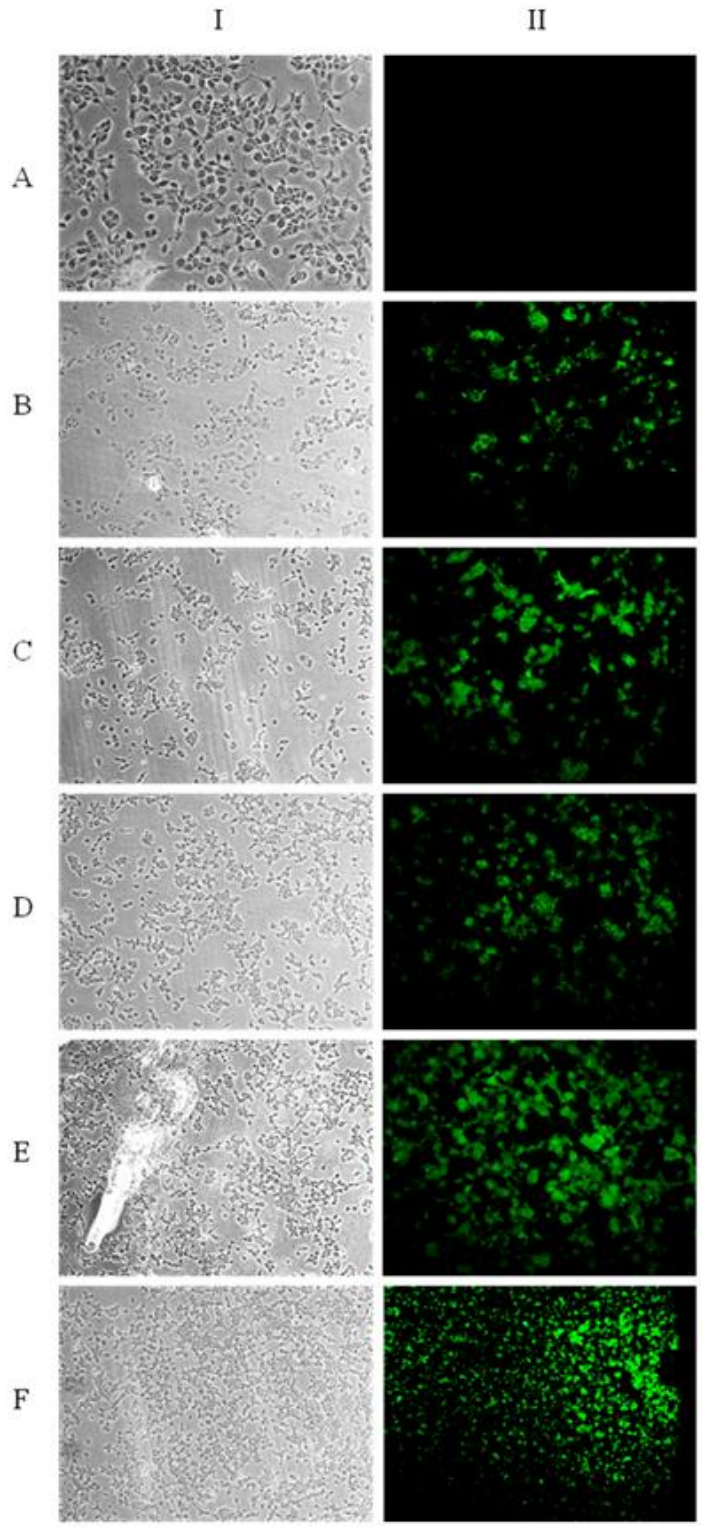

Figure 5.23 Fluorescence microscopy images of HEK 293 cells treated with A) Naked pEGFP-N1, and polyplexes prepared at N/P ratio-12 using B) 10 KDa PEI, C) HA-PEI, D) OA-PEI, E) ω-amino-HA-PEI and F) ω-amino-OA-PEI. The first column (I) represents images captured without fluorescent filter, the second quadrant (II) represents images captured under fluorescent filter. All images are obtained at 20X magnification except for A) Naked pEGFP-N1, obtained at 40X magnification.

Confocal microscopy based cell uptake analysis was performed to qualitatively assess the ability of synthesized polymer to aid in intracellular entry of pDNA and also to confirm results of Fluorescence microscopy. Results obtained were not used for quantitative determination of percentage cellular uptake. Transfection of HEK293 cells was observed using confocal microscopy. Cells transected with naked pDNA did not show any green fluorescence due to EGFP this indicates that naked pDNA without vector support cannot efficiently enter cell (Figure 5.24). Cells transfected with polyplexes prepared from cationic polymers such as PEI, HA-PEI, OA-PEI, ω-amino-HA-PEI and ω-amino-OA-PEI showed green fluorescence inside cells in cytoplasm which indicates that all synthesized polymers, like PEI, were capable of intracellular delivery of pDNA (Figure 5.24).

Fine balance between association and dissociation of cationic polymers with pDNA is very much important. To efficiently protect pDNA in presence of blood during *in vivo* use, it is very much important for cationic polymers to remain associated to pDNA so as to protect pDNA from serum nucleases. These results prove that polyplex from cationic polymers, such as HA-PEI, OA-PEI, ω-amino-HA-PEI and ω-amino-OA-PEI, are capable of protecting pDNA in culture medium. Hence, these results indicate that prepared polymers remain associated with pDNA in culture medium and hence are capable of protecting pDNA, results are in line with other studies performed for PEI and its modifications (11). However, from confocal microscopy, we were unable to confirm whether polyplexes are capable of protecting pDNA in presence serum nucleases because polyplexes treatment was given in DMEM without containing 10% FBS.

At the same time, once inside the cell, dissociation of cationic polymers from pDNA should occur in timely manner. HA-PEI, OA-PEI, ω-amino-HA-PEI and ω-amino-OA-PEI are modifications of PEI 10 KDa and hence would work in similar fashion as that of unmodified PEI. All PEIs, irrespective of linear or branched; high molecular weight or low molecular weight, escape the harsh environment of late stage endosome and lysosome by a mechanism known as “Proton Sponge effect” (10). During Proton Sponge process, it is necessary that pDNA remains associated to PEI so as to prevent its degradation. But once polyplexes are in cytoplasm, after escape from late stage endosome and lysosome, it is necessary that polyplexes or dissociated pDNA enter nucleus. It is still unclear, exactly where pDNA dissociates from PEI; in

cytoplasm immediately after proton sponge or inside nuclease. If pDNA dissociates from PEI immediately after proton sponge then pDNA has to enter inside nucleus on its own. If pDNA enters the nucleus associated with PEI, it is necessary that it dissociates from pDNA so that transcription to mRNA occurs and further mRNA enter cytoplasm and undergo translation for protein expression (65).

Therefore results obtained in cellular uptake analysis by conofocal microscopy also confirm that all polymers were able to dissociate from pDNA so that pDNA can be available for protein expression.

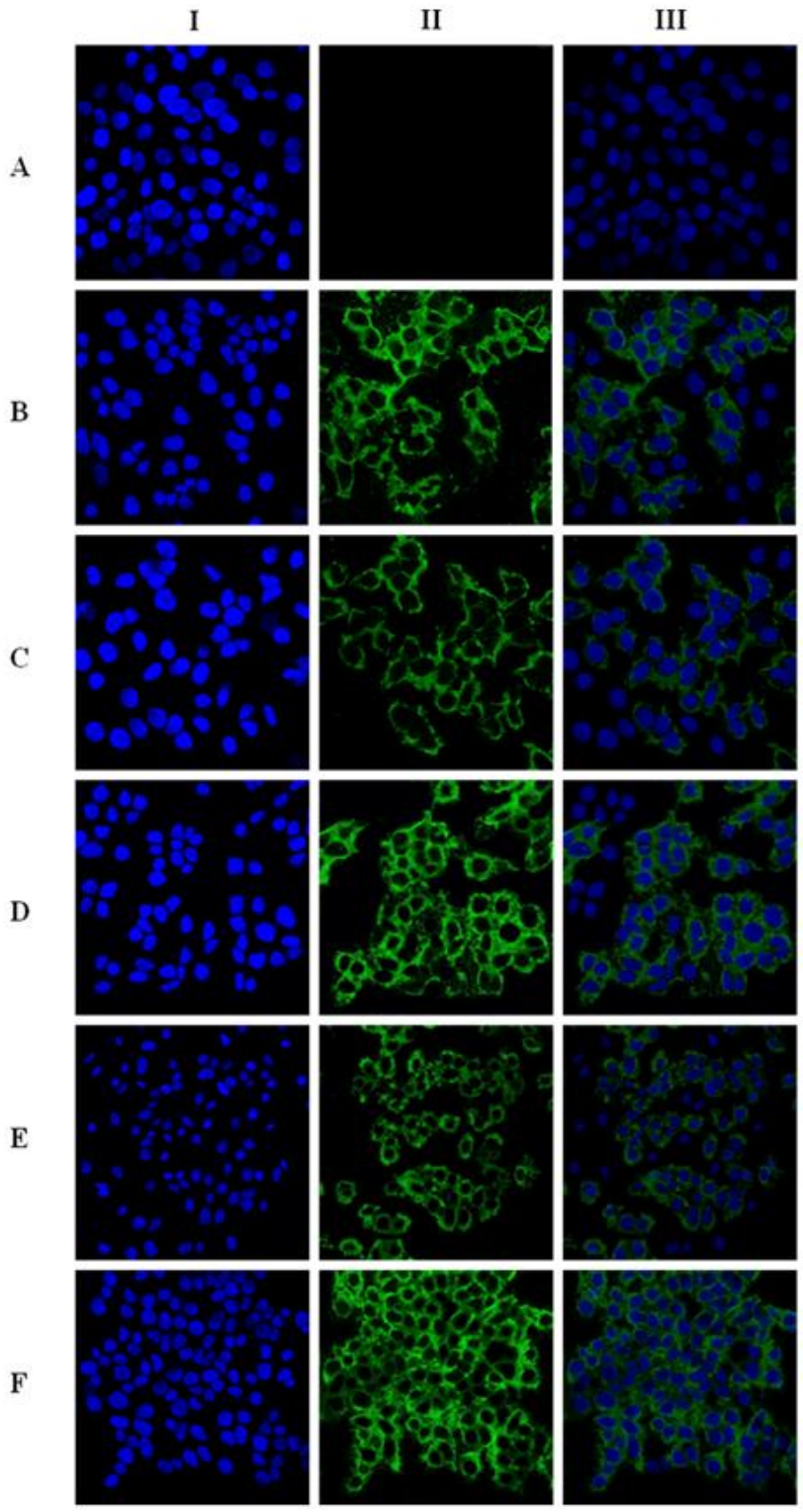

Figure 5.24 Confocal microscopy images of HEK 293 cells treated with A) Naked pEGFP-N1, and with polyplexes prepared at N/P ratio-12 using B) 10 KDa PEI, C) HA-PEI, D) OA-PEI, E) ω-amino-HA-PEI and F) ω-amino-OA-PEI. The first column (I) represents images captured under DAPI filter, the second quadrant (II) represents images captured under fluorescent filter and the third quadrant (III) shows the merged images.

As mRNA expression occurs prior to protein synthesis, quantification of *mCTLA4-IGHG1* mRNA was performed to predict and correlate mCTLA4-IGHG1 protein expression that can be induced using pAL119-mCTLA4-IGHG1 plasmid. Previous experiments such as confocal microscopy and fluorescence microscopy, and FACS analysis for evaluation of transfection efficiency are performed using marker plasmid p-EGFP-N1; expression efficiency of pAL119-mCTLA4-IGHG1 plasmid was confirmed by m-RNA expression analysis by using a sophisticated technique called RT-PCR. Mean ΔCp values obtained for every treatment were compared with one another. $2^{-\Delta\Delta Cp}$ analysis was performed to obtain fold change in expression of *mCTLA4-IGHG1* transcript due to treatment. Melt curve analysis was performed which indicated melting temperature for mCTLA4-IGHG1 and GAPDH amplicon at 84°C and 86°C respectively.

Comparison of the mean ΔCp showed that there was significantly increased expression of *mCTLA4-IGHG1* transcripts in cells treated with HA-PEI, OA-PEI, ω-amine-HA-PEI and ω-amine-OA-PEI in comparison to cells treated with PEI 10KDa after normalization with *GAPDH* expression (p=0.0009, p= 0.0004, p= 0.0003 and p= 0.0001 respectively) (Figure 5.25).

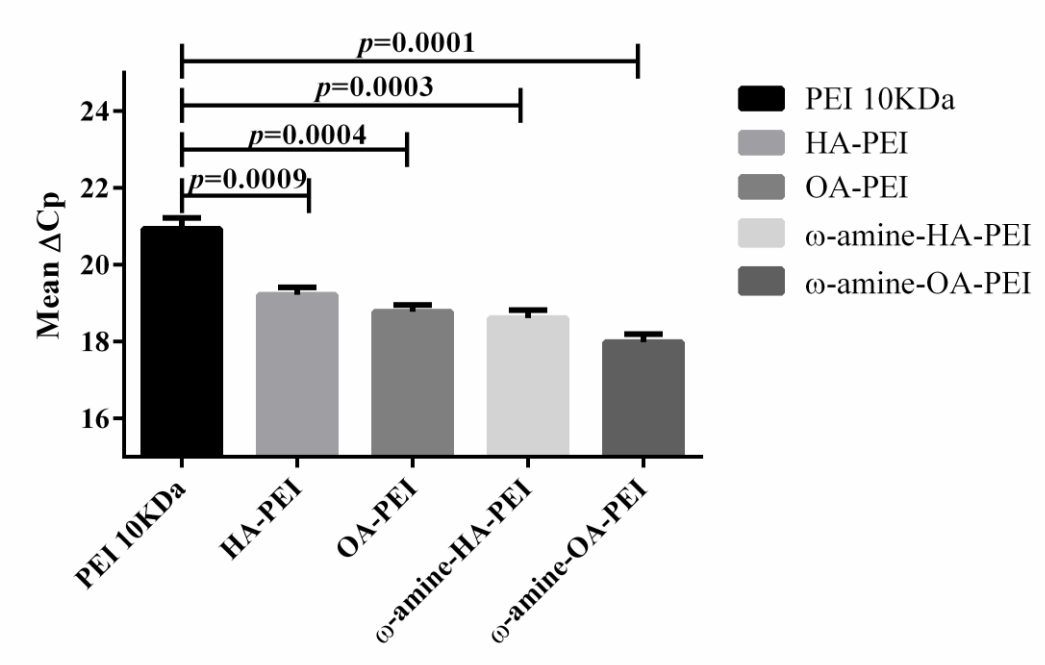

Figure 5.25 Relative expression of mCTLA4-IGHG1 mRNA after treatment with polyplexes of pAL119-mCTLA4-IGHG1 prepared with A) PEI-10 KDa; B) HA-PEI; C) OA-PEI; D) ω-amine-HA-PEI and E) ω-amine-OA-PEI at N/P ratio 12. Each data point represents the average of three experiments ± standard deviation.

Comparison of the mean ΔCp also showed that there was statistically significant increase in expression of *mCTLA4-IGHG1* transcripts in cells treated with OA-PEI in comparison to HA-PEI (p=0.0404), ω-amine-HA-PEI in comparison to HA-PEI (p=0.0203), ω-amine-OA-PEI in comparison to OA-PEI (p=0.0072) and ω-amine-OA-PEI in comparison to ω-amine-HA-PEI (p=0.0224). however, no significant difference for *mCTLA4-IGHG1* transcripts was observed between ω-amine-HA-PEI and OA-PEI (p=0.3371) (Figure 5.26).

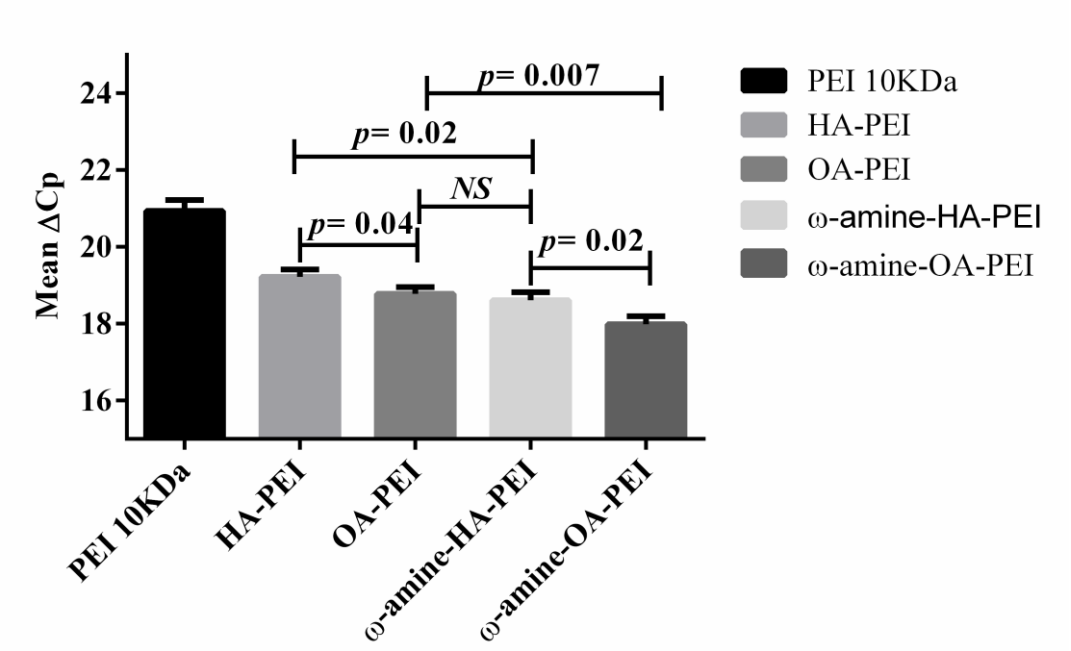

Figure 5.26 Relative expression of mCTLA4-IGHG1 mRNA in polyplexes of pAL119-mCTLA4-IGHG1 prepared with A) PEI-10 KDa; B) HA-PEI; C) OA-PEI; D) ω-amine-HA-PEI and E) ω-amine-OA-PEI at N/P ratio 12 as suggested by Mean ΔCp. Each data point represents the average of three experiments ± standard deviation.

The $2^{-\Delta\Delta Cp}$ analysis showed 3.29, 4.47, 5.03 and 7.73 fold increase in the expression levels of *mCTLA4-IGHG1* in cells treated with HA-PEI, OA-PEI, ω-amine-HA-PEI and ω-amine-OA-PEI respectively, in comparison to cells treated with PEI 10KDa after normalization with *GAPDH* expression (Figure 5.27).

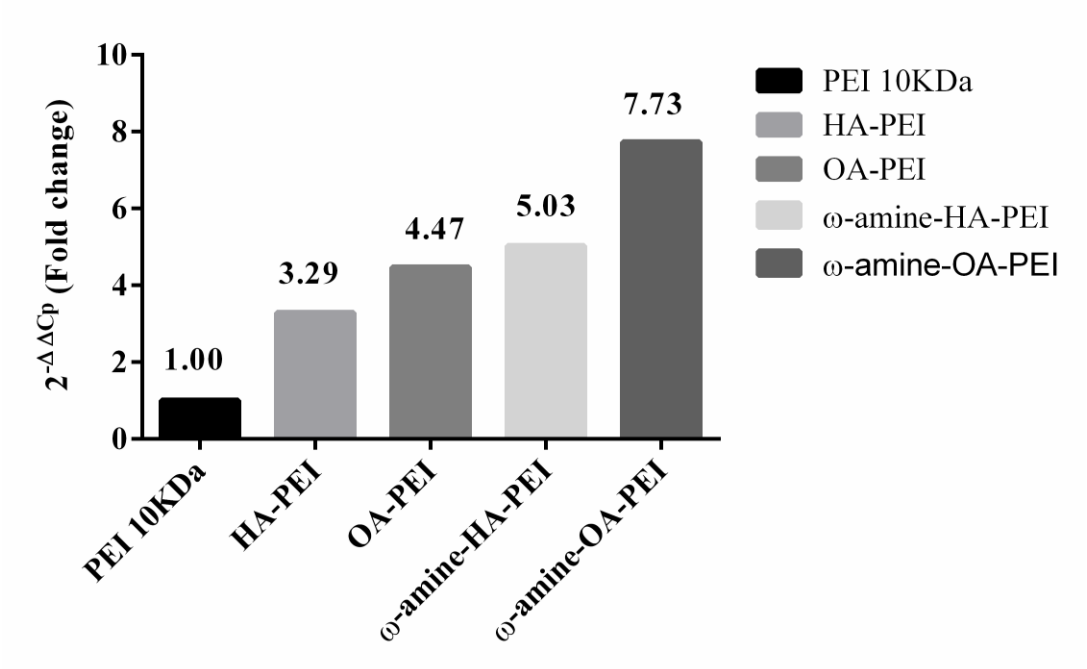

Figure 5.27 Expression fold change of mCTLA4-IGHG1 mRNA after treatment with polyplexes of pAL119-mCTLA4-IGHG1 prepared with A) PEI-10 KDa; B) HA-PEI; C) OA-PEI; D) ω-amine-HA-PEI and E) ω-amine-OA-PEI at N/P ratio 12 as suggested by $2^{-\Delta\Delta Cp}$ value.

To support qualitative results obtained for cellular uptake studies performed using confocal microscopy and fluorescence microscopy as well as to support quantitative m-RNA expression results obtained from RT-PCR analysis, cellular uptake of pEGFP-N1 was quantified using Flow cytometry. Percentage of cells transfected performed in presence and in absence of serum (10% FBS) was obtained from histograms to quantify EGFP expressing cells. (Figure 5.28 and 5.29).

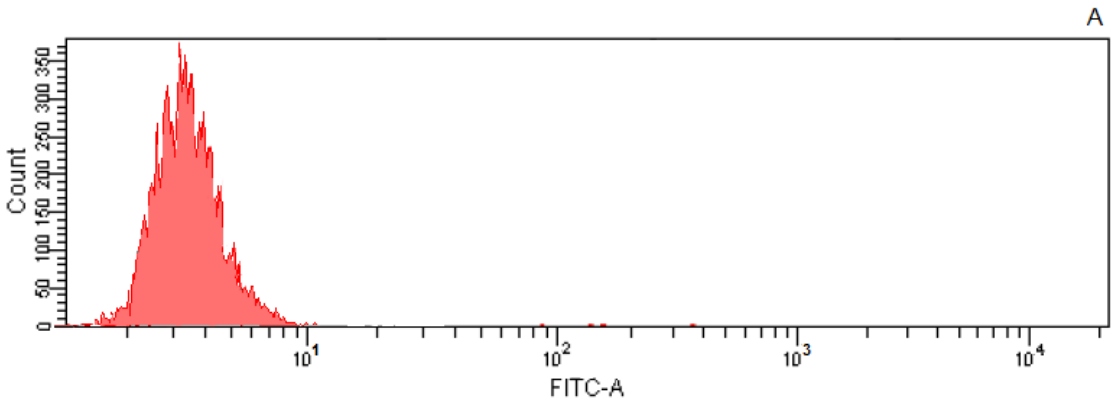

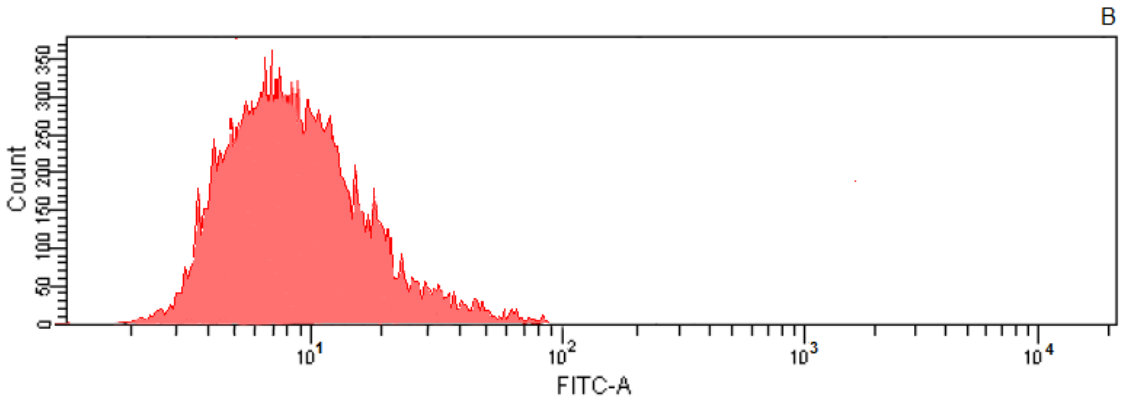
B
Count
0
50
100
150
200
250
300
350
10^1
10^2
10^3
10^4
FITC-A

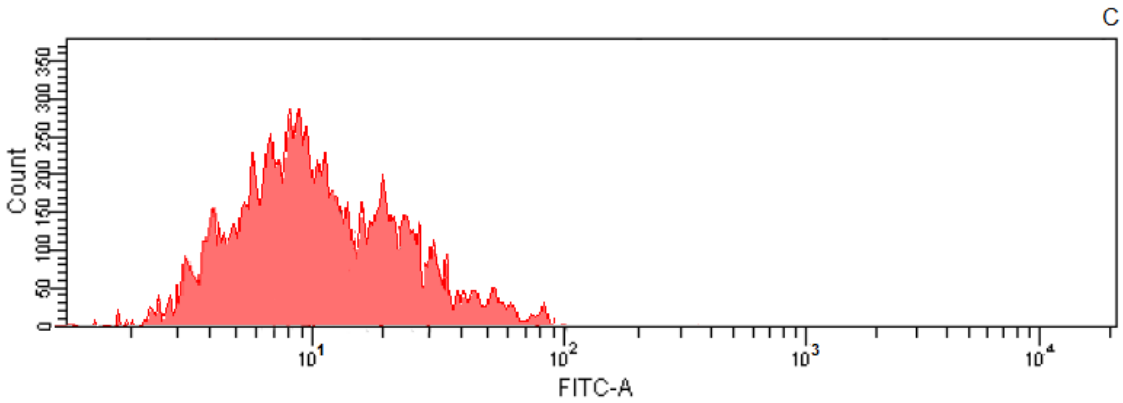
C
Count
0
50
100
150
200
250
300
350
10^1
10^2
10^3
10^4
FITC-A

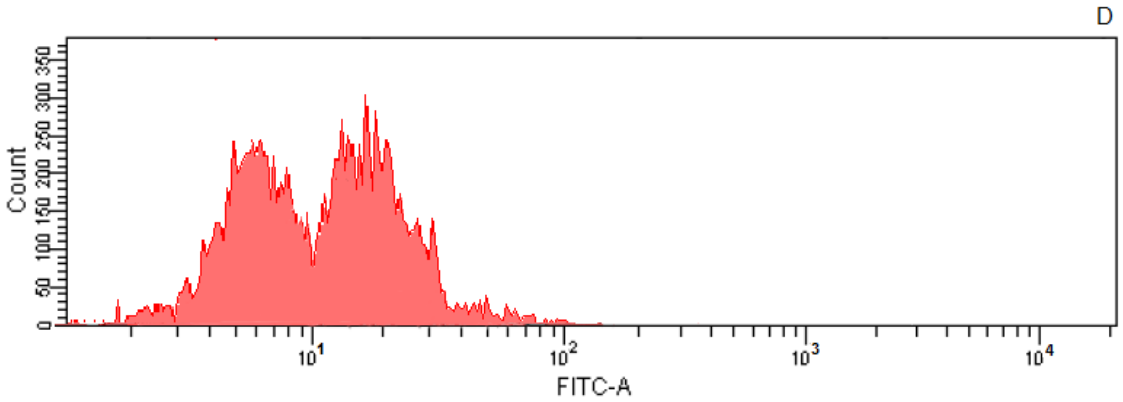
D
Count
0
50
100
150
200
250
300
350
10^1
10^2
10^3
10^4
FITC-A

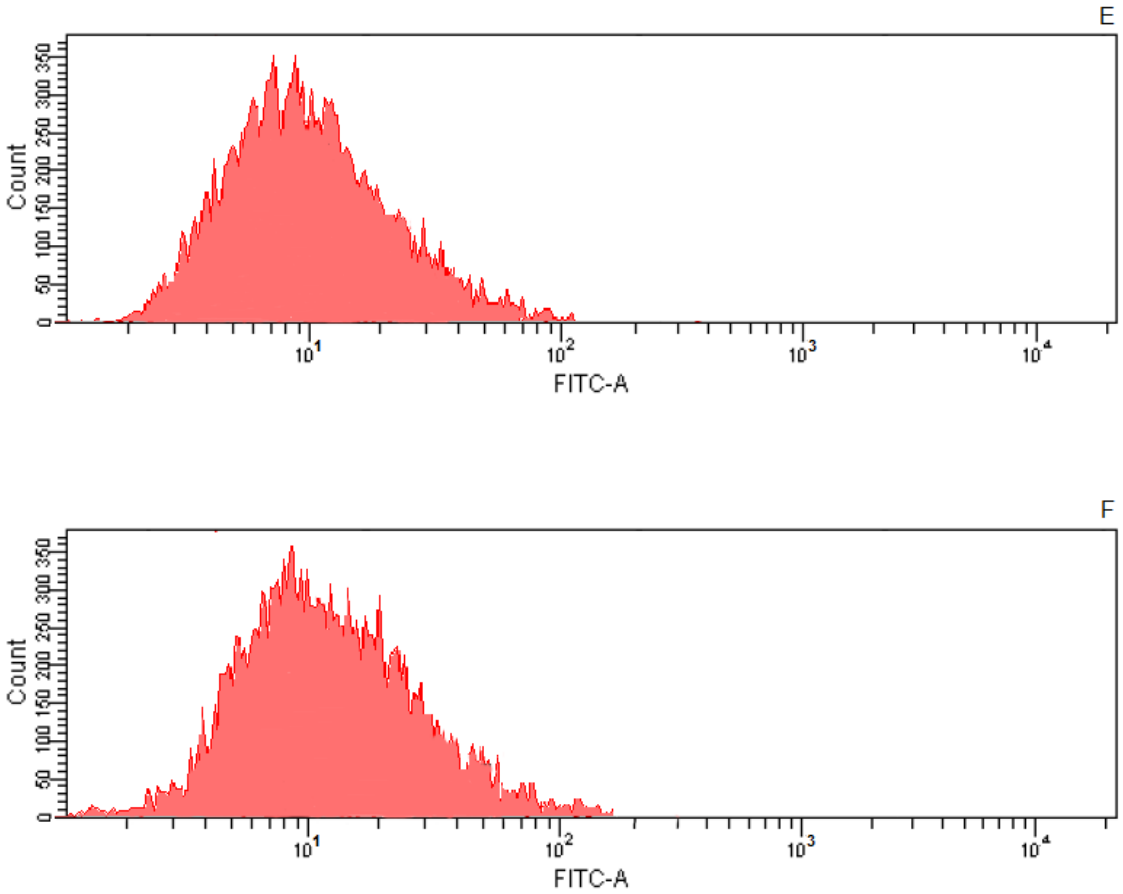

Figure 5.28 FACS analysis quantifying EGFP expression in HEK-293 cells in presence of serum (10% FBS). Images display results of fluorescence measurement of 10,000 cells transformed with A) Naked pDNA, and polyplexes prepared at N/P ratio-12 using B) PEI 10KDa, C) HA-PEI, D) OA-PEI, E) ω-amino-HA-PEI and F) ω-amino-OA-PEI.

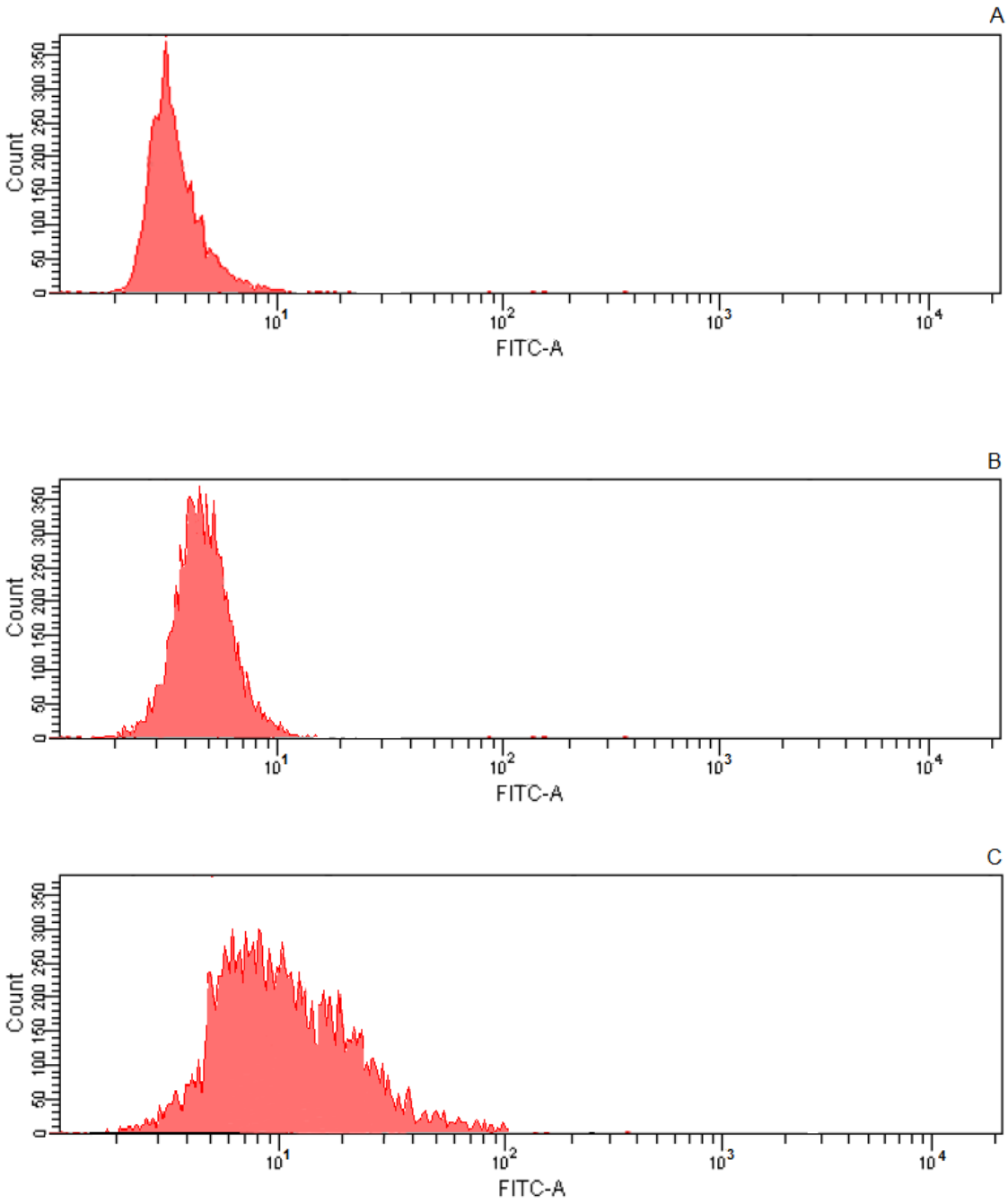
A
Count
0
50
100
150
200
250
300
350
10^1
10^2
10^3
10^4
FITC-A
B
Count
0
50
100
150
200
250
300
350
10^1
10^2
10^3
10^4
FITC-A
C
Count
0
50
100
150
200
250
300
350
10^1
10^2
10^3
10^4
FITC-A

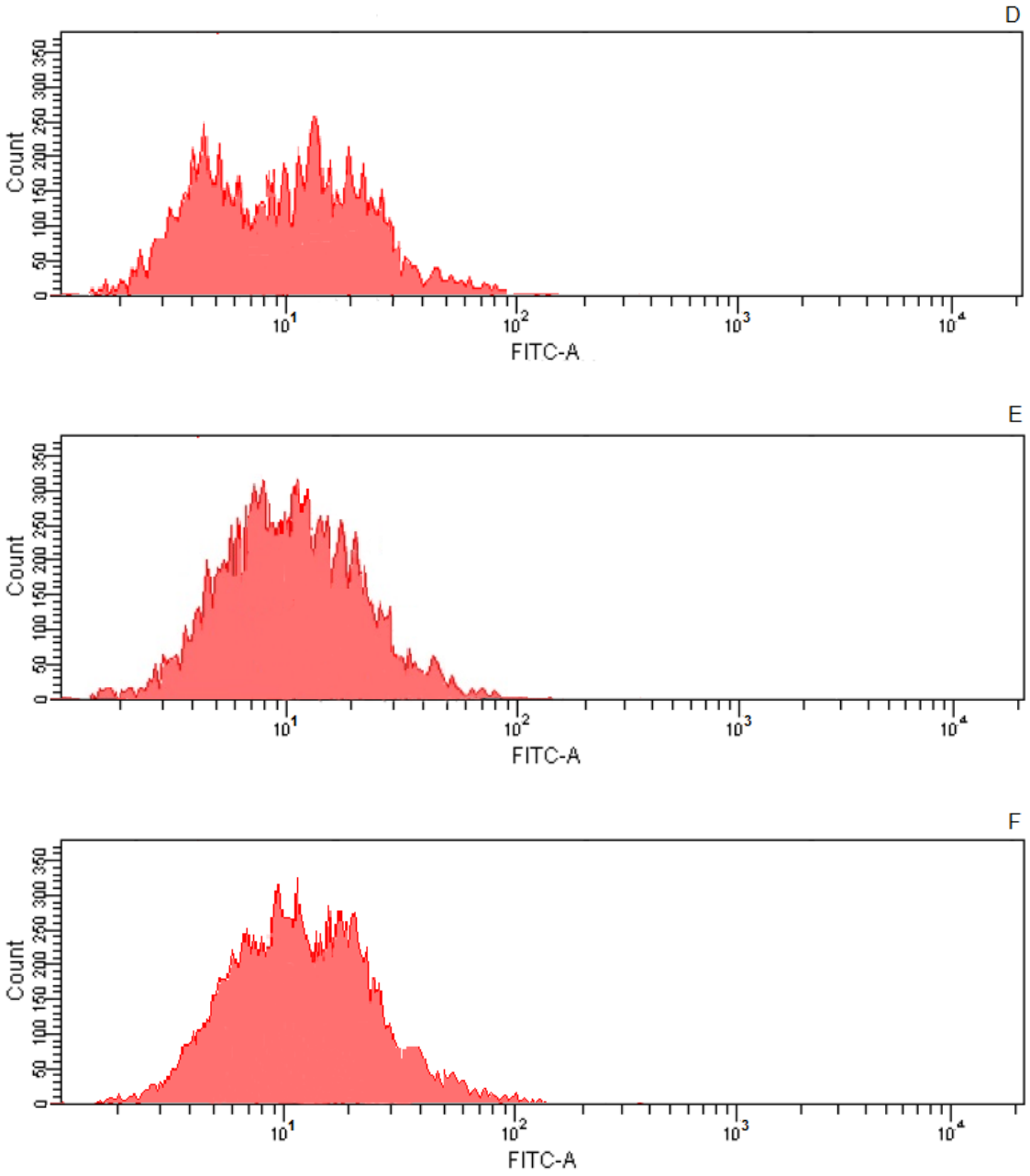
D
Count
0 50 100 150 200 250 300 350
10^1 10^2 10^3 10^4
FITC-A
E
Count
0 50 100 150 200 250 300 350
10^1 10^2 10^3 10^4
FITC-A
F
Count
0 50 100 150 200 250 300 350
10^1 10^2 10^3 10^4
FITC-A

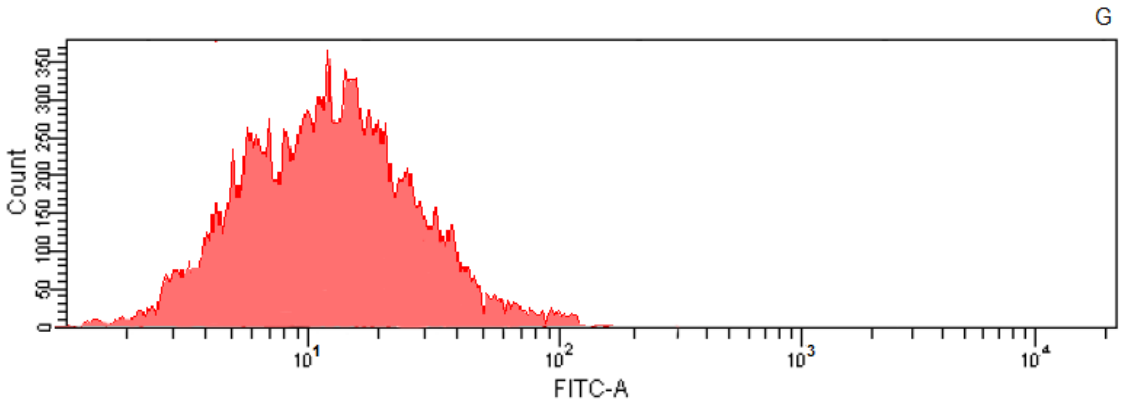

Figure 5.29 FACS analysis quantifying EGFP expression in HEK-293 cells in absence of serum (10% FBS). Images display results of fluorescence measurement of 10,000 cells transformed with A) Naked pDNA, and polyplexes prepared at N/P ratio-12 using B) PEI 10KDa, C) HA-PEI, D) OA-PEI, E) ω-amino-HA-PEI and F) ω-amino-OA-PEI.

When compared to untreated cells, naked pDNA showed 2.72 ± 0.94 % and 0.02 ± 0.12 % of cell transfection in absence and in presence of serum respectively. Irrespective of presence or absence of serum, ω-amino-HA-PEI showed highest percentage cell transfection in comparison to all other polymers. Highest transfection efficiency of ω-amino-OA-PEI can be compared to results obtained in previous studies such as particle size analysis and cell toxicity analysis using MTT assay. Lower particle size and higher zeta of ω-amino-OA-PEI polyplexes in comparison to all other polymers under investigation may have facilitated internalization. Comparable toxicity of ω-amino-OA-PEI polyplexes as that of PEI 10KDa may also have additional advantage. Furthermore, in absence of serum, HA-PEI, OA-PEI, ω-amino-HA-PEI and ω-amino-OA-PEI showed significantly increased cell transfection in comparison to PEI 10KDa (p=0.0489, p=0.0032, p=0.0027, p=0.0003 respectively). Similarly, in presence of serum HA-PEI, OA-PEI, ω-amino-HA-PEI and ω-amino-OA-PEI showed significantly increased cell transfection in comparison to PEI 10KDa (p=0.0439, p=0.0024, p=0.0022, p=0.0003 respectively). Results indicate that all modifications of PEI 10KDa were capable of increasing transfection efficiency of pDNA in comparison to PEI 10KDa. However, there was no significant difference in transfection efficiency of OA-PEI in comparison to w-amine-HA-PEI (p>0.05) in presence as well as in absence of serum (Figure 5.30). Furthermore, transfection efficiency of pEGFP-N1 was found to be significantly reduced in presence of serum

for HA-PEI, OA-PEI, ω-amino-HA-PEI and ω-amino-OA-PEI as well as PEI 10KDa (p<0.05) (Figure 5.30).

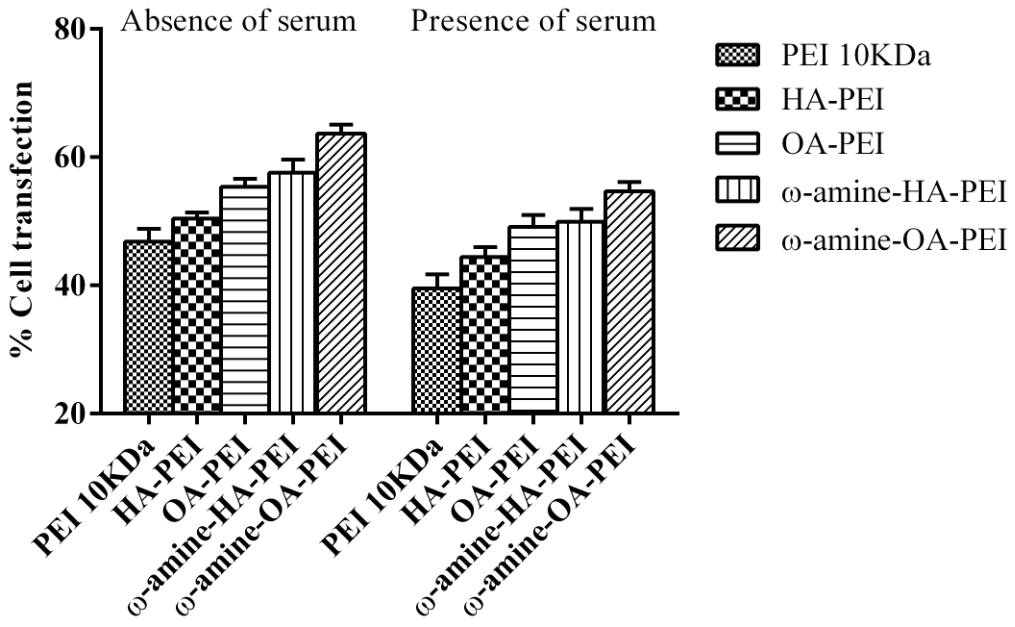

Figure 5.30 Transfection efficiency of pEGFP-N1 polyplexes prepared using A) PEI 10KDa, B) HA-PEI, C) OA-PEI, D) ω-amino-HA-PEI and E) ω-amino-OA-PEI at N/P ratio-12. (Results are represented as average of three independent experiments ± standard deviation).

This can be due to positive charge on the surfaces of polyplexes prepared using these polymers, as was evident from zeta potential measurement study. Cationic charge on surface of polyplexes could possibly increase size of polyplexes in presence of serum which in turn hinders internalization and hence transfection is reduced. However, cationic charge in absence of serum will allow sufficient interaction with negatively charged cell membrane and facilitate internalization of polyplexes.

Transfection efficiency of pEGFP-N1 polyplexes prepared at N/P ratio-12 was found to be increasing in order of PEI 10KDa < HA-PEI < OA-PEI ~ ω-amino-HA-PEI < ω-amino-OA-PEI. Results obtained for flow cytometry are in agreement with RT-PCR analysis. However, cytotoxicity analysis showed cell viability in order of PEI 10KDa > HA-PEI > OA-PEI ~ ω-amino-HA-PEI > ω-amino-OA-PEI. These results can be collectively explained in conjugation with results obtained in size and zeta analysis of prepared polymers. Higher zeta of polyplexes may cause aggregation

of polyplexes with blood components and may lead to exclusion of larger aggregates from cell entry. Higher zeta along with smaller polyplex size may be more favorable due to formation of micro-aggregates capable of being internalization by endocyctosis than slightly lower zeta along with higher polyplex size forming macro-aggregates incapable of cell entry. Hence transfection efficiency of polyplexes prepared from PEI 10KDa, HA-PEI, OA-PEI, ω-amino-HA-PEI and ω-amino-OA-PEI depends on size, branching and surface charge density.

E. *In vivo* efficacy

Hashimoto's thyroiditis (HT) in humans and mouse thyroglobulin (MTg)–induced EAT in mice share the common characteristics such as, autoantibody production against thyroid autoantigens, thyroid follicular destruction, mononuclear cell (lymphocytic cell) infiltration and T cell proliferative response against thyroglobulin (Tg) (66). Hence EAT model in mice was utilized for assessing *in vivo* efficacy of prepared polyplexes in autoimmune hypothyroidism. After induction of EAT using mouse thyroglobulin (MTg) size of thyroid gland from EAT mice was compared to normal healthy mice in which EAT was not induced (negative control). EAT positive mice served as positive control and normal healthy mice served as negative control for other groups.

Size of thyroid in positive control group is comparatively larger than other groups and Size of thyroid in negative control group is comparatively smaller than other groups. Size of thyroids in both the treatment groups and both the prevention groups is smaller than positive control group which suggests that pAL119-mCTLA4-IGHG1 has potential to treat as well as prevent EAT in mice model (Figure 5.31).

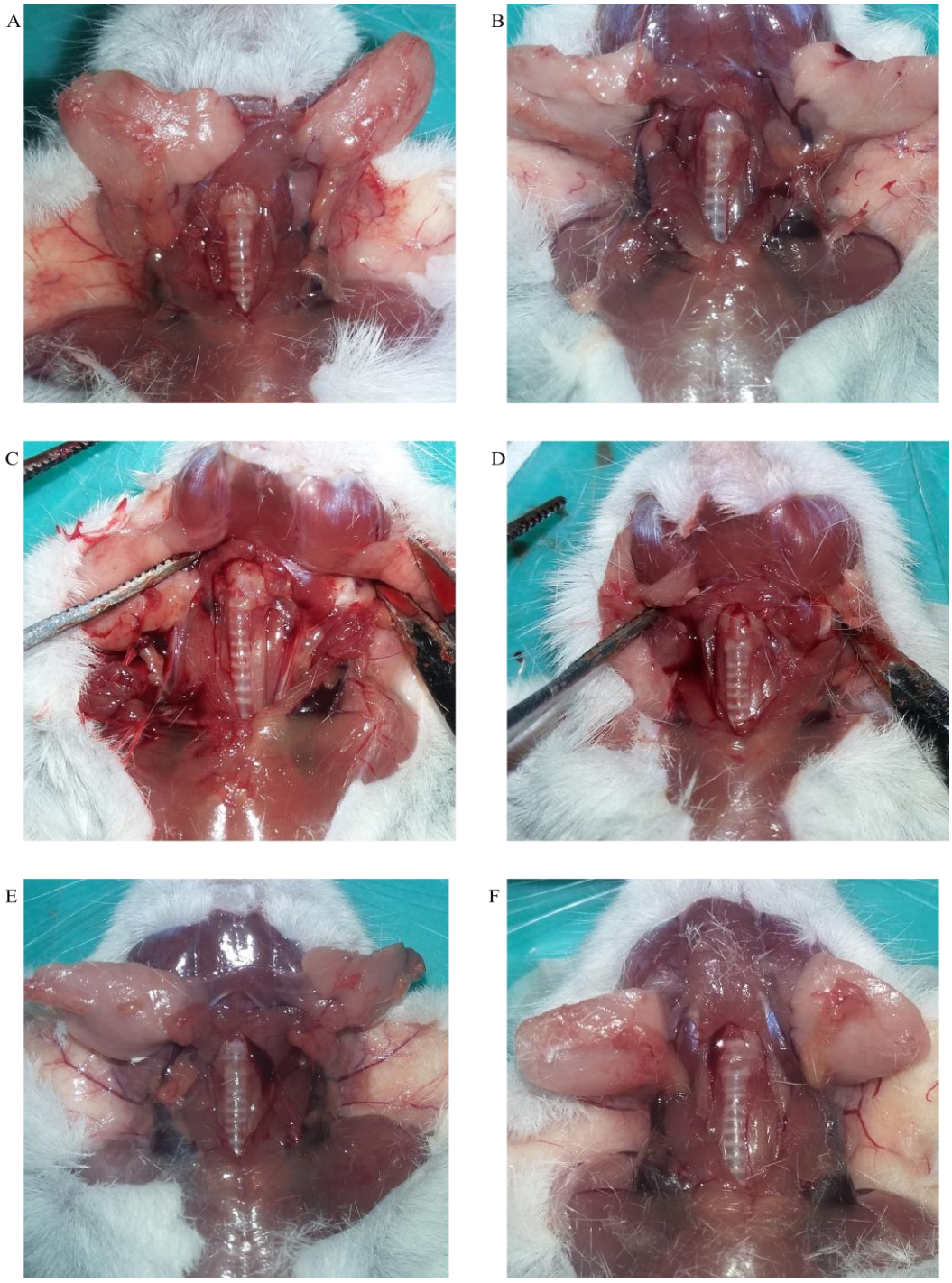

Figure 5.31 Size analysis of thyroid glands. Thyriod glands of A) Negative control group B) Positive control group C) Treatment group-1, PEI 10 KDa and pAL119-mCTLA4-IGHG1 polyplexes D) Treatment group-2, ω-amino-OA-PEI and pAL119-mCTLA4-IGHG1 polyplexes E) Prevention group-1, PEI 10 KDa and pAL119-mCTLA4-IGHG1 polyplexes F) Prevention group-2, ω-amino-OA-PEI and pAL119-mCTLA4-IGHG1 polyplexes.

In thyroid histopathology images, the mononuclear cell infiltration of the thyroid gland was graded as per previously described method, to evaluate severity EAT (67).

Grade 1: interstitial accumulation of inflammatory cells between two or more follicles;

Grade 2: one and two foci of inflammatory cells reaching at least the size of one follicle;

Grade 3: 10 % to 40 % of the thyroid gland replaced by inflammatory cells;

Grade 4: >40 % of the thyroid gland replaced by inflammatory cells.

Hematoxylin and eosin-stained paraffin sections of thyroid histopathology study, figure 5.32, showed that negative control group (represents normal thyroid state) has roughly circular thyroid follicles, epithelial cells around follicle wall and lumen containing thyroglobulin colloid is present (Colloid present inside thyroid follicles is stained pink. Cuboidal epithelial cells are stained as violet color around pink thyroid follicles). On the other hand positive control group showed thyroid follicle damage and irregular thyroid epithelial cells. Destruction of thyroid follicles and infiltration of mononuclear cells are also clearly seen (Grade-4). In comparison to positive control group (Grade-4), treatment group-1 and treatment group-2 showed lower lymphocytic infiltration. Furthermore, mice in treatment group-2 (Grade-2) showed significantly low lymphocytic infiltration and follicular damage in comparison to treatment group-1 (Grade-3) ($p<0.05$, change in grade was considered as significant difference with p-value < 0.05).

Similarly, In comparison to positive control group (Grade-4), mice in prevention group-1 (Grade-2) as well as prevention group-2 showed lower lymphocytic infiltration (Grade-1) ($p<0.05$).

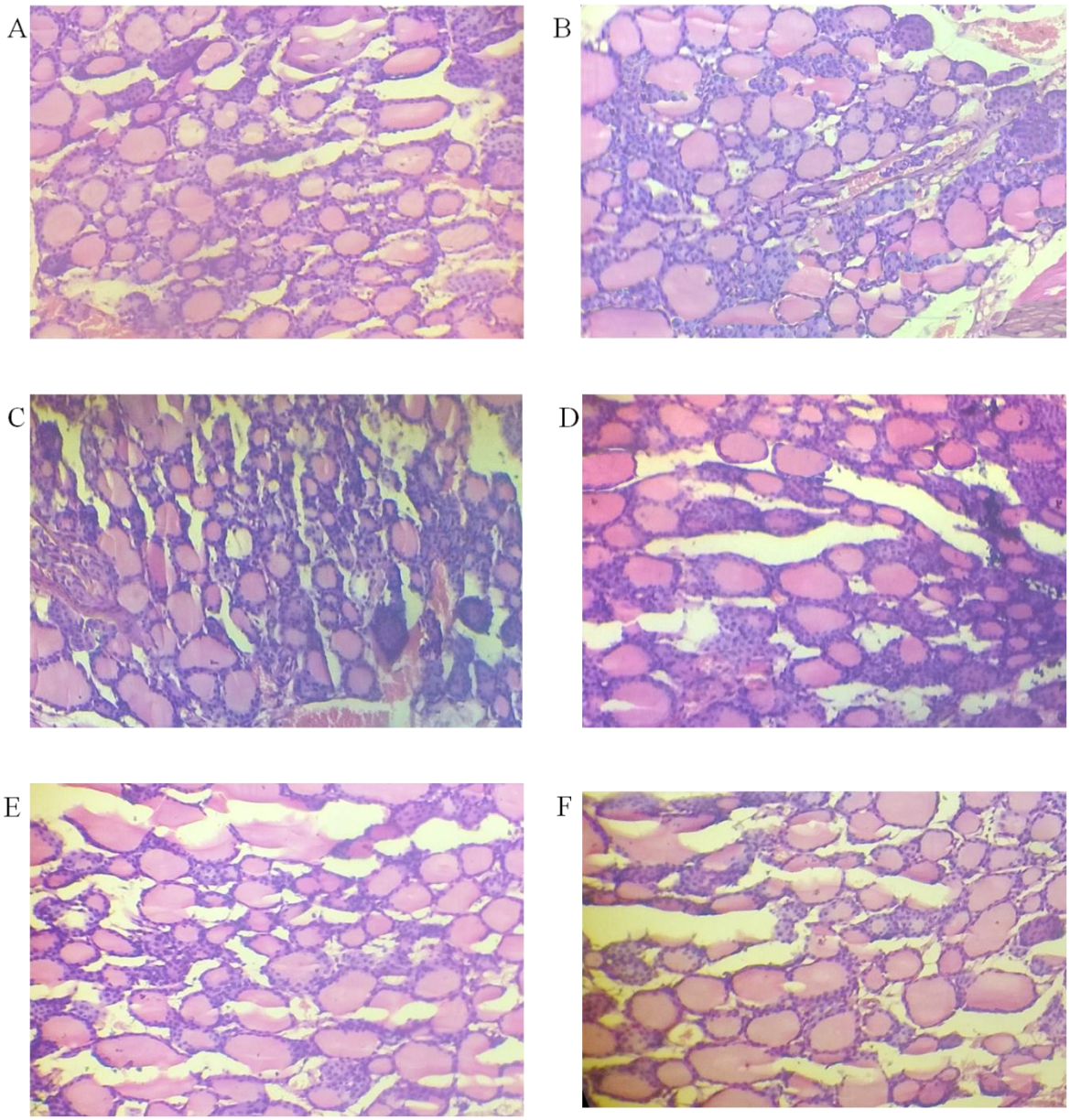

Figure 5.32 Histopathology analysis of thyroid glands. A) Negative control; B) Positive control (Grade-4); C) Treatment group-1, PEI 10 KDa and pAL119-mCTLA4-IGHG1 polyplexes (Grade-3); D) Treatment group-2, ω-amino-OA-PEI and pAL119-mCTLA4-IGHG1 polyplexes (Grade-2); E) Prevention group-1, PEI 10 KDa and pAL119-mCTLA4-IGHG1 polyplexes (Grade-2); F) Prevention group-2, ω-amino-OA-PEI and pAL119-mCTLA4-IGHG1 polyplexes (Grade-1).

Histopathology of thyroid glands provided semi-quantitative results based on grading of thyroid glands damage and inflammatory cell infiltration. Hence, Quantification of mCTLA4-IGHG1 mRNA was performed to predict and correlate mCTLA4-IGHG1 protein expression that can be induced after pAL119-mCTLA4-IGHG1 plasmid transformation. As mRNA expression occurs prior to protein synthesis and hence may give better correlation. $2^{-\Delta\Delta Cp}$ analysis was performed to

obtain fold change in expression of mCTLA4-IGHG1 transcript due to administration of PEI 10 KDa and pAL119-mCTLA4-IGHG1 polyplexes as well as ω-amino-OA-PEI and pAL119-mCTLA4-IGHG1 polyplexes. Melt curve analysis was performed which indicated melting temperature for mCTLA4-IGHG1 and GAPDH amplicon at 84°C and 86°C respectively.

The $2^{-\Delta\Delta Cp}$ analysis showed 2.43 and 5.63 fold increase in the expression levels of mCTLA4-IGHG1 in Treatment group-1 and Treatment group-2, respectively in comparison to Positive Control group. Similarly, $2^{-\Delta\Delta Cp}$ analysis showed 2.38 and 5.11 fold increase in the expression levels of mCTLA4-IGHG1 in Prevention group-1 and Prevention group-2, respectively in comparison to Positive Control group (Figure 5.33).

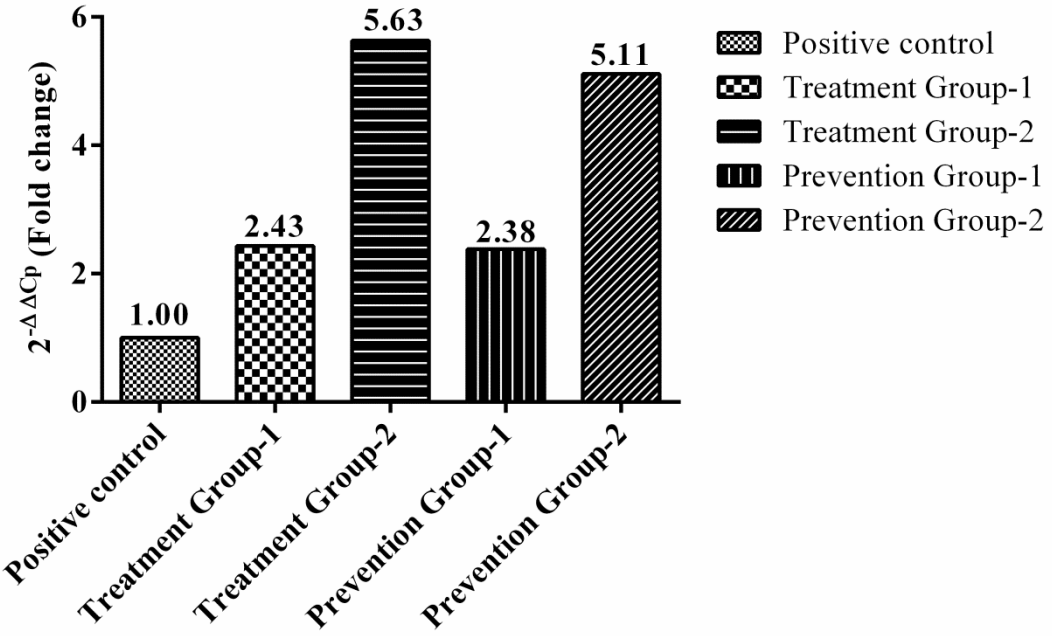

Figure 5.33 Expression fold change analysis of mCTLA4-IGHG1 mRNA. A) Positive control group; B) Treatment group-1, PEI 10 KDa and pAL119-mCTLA4-IGHG1 polyplexes; C) Treatment group-2, ω-amino-OA-PEI and pAL119-mCTLA4-IGHG1 polyplexes; D) Prevention group-1, PEI 10 KDa and pAL119-mCTLA4-IGHG1 polyplexes; E) Prevention group-2, ω-amino-OA-PEI and pAL119-mCTLA4-IGHG1 polyplexes, expressed as $2^{-\Delta\Delta Cp}$ value.

From results it can be concluded that increase in mCTLA4-IGHG1 transcript levels are in accordance with results obtained in histopathology study in form of decrease in lymphocytic cell infiltration and thyroid follicle damage as well as reduced thyroid

gland size as evident in both the Treatment groups and both prevention groups comparison to positive control group.

Therapeutic role of cytokine genes such as IL-10 has already been proved in EAT (68) and in other diseases such as autoimmune diabetes (69) and airway eosinophilia (70). Therapeutic role of death receptor and its ligand such as FAS ligand has also been proved in autoimmune thyroiditis (67) (71). However, this is the first time where beneficial role of CTLA4-IG gene has been proved in management of autoimmune thyroiditis in mice EAT model. CTLA4-IG gene delivery in form of pAL119-mCTLA4-IGHG1 using ω-amino-OA-PEI cationic polymer produced higher transcript levels in thyroid glands of treated EAT mice and suppressed induction of MTg based EAT when delivered before induction of EAT model. Hence, further clinical studies need to be performed so that role of CTLA4-IG protein can be extended in management of autoimmune hypothyroidism. Overall results also demonstrate that short chain aliphatic lipids substituted PEI based polymers are promising candidates for in vivo gene therapy applications.

IV. CONCLUSION

In summary, CTLA4-IG gene delivery in form of pAL119-mCTLA4-IGHG1 has beneficial role in treatment and prevention of EAT in mice model and short chain aliphatic lipid substituted LMW PEI 10KDa based polymers developed in present investigation by modification of PEI 10KDa using HA, OA, ω-amino-HA and ω-amino-OA were found to be efficient transfection vectors. The acceptable *in vitro* cytotoxicity profile, ability to retain *in vitro* as well as *in vivo* stability and transfection efficiency of polyplexes prepared from these modified polymers reveal their potential as promising candidates for *in vivo* gene therapy applications.

V. REFERENCES

1. Mulligan RC. The basic science of gene therapy. Science. 1993 May 14;260(5110):926-32.
2. Felgner PL, Gadek TR, Holm M, Roman R, Chan HW, Wenz M, et al. Lipofection: a highly efficient, lipid-mediated DNA-transfection procedure. Proceedings of the National Academy of Sciences of the United States of America. 1987;84(21):7413-7.
3. Ledley FD. Nonviral gene therapy: the promise of genes as pharmaceutical products. Hum Gene Ther. 1995 Sep;6(9):1129-44.
4. Wiethoff CM, Middaugh CR. Barriers to nonviral gene delivery. J Pharm Sci. 2003 Feb;92(2):203-17.
5. Boussif O, Lezoualc'h F, Zanta MA, Mergny MD, Scherman D, Demeneix B, et al. A versatile vector for gene and oligonucleotide transfer into cells in culture and in vivo: polyethylenimine. Proc Natl Acad Sci U S A. 1995 Aug 1;92(16):7297-301.
6. De Smedt SC, Demeester J, Hennink WE. Cationic polymer based gene delivery systems. Pharm Res. 2000 Feb;17(2):113-26.
7. Ziebarth JD, Wang Y. Understanding the protonation behavior of linear polyethylenimine in solutions through Monte Carlo simulations. Biomacromolecules. 2010 Jan 11;11(1):29.
8. Suh J, Paik HJ, Hwang BK. Ionization of Poly(ethylenimine) and Poly(allylamine) at Various pH′s. Bioorganic Chemistry. 1994 1994/09/01;22(3):318-27.
9. Nagaya J, Homma M, Tanioka A, Minakata A. Relationship between protonation and ion condensation for branched poly(ethylenimine). Biophysical Chemistry. 1996 1996/05/13;60(1):45-51.
10. Behr J-P. The proton sponge: a trick to enter cells the viruses did not exploit. CHIMIA International Journal for Chemistry. 1997;51(1-2):34-6.
11. Godbey WT, Wu KK, Mikos AG. Tracking the intracellular path of poly(ethylenimine)/DNA complexes for gene delivery. Proceedings of the National Academy of Sciences of the United States of America. 1999;96(9):5177-81.

12. Sonawane ND, Szoka FC, Jr., Verkman AS. Chloride accumulation and swelling in endosomes enhances DNA transfer by polyamine-DNA polyplexes. J Biol Chem. 2003 Nov 7;278(45):44826-31.
13. Morimoto K, Nishikawa M, Kawakami S, Nakano T, Hattori Y, Fumoto S, et al. Molecular weight-dependent gene transfection activity of unmodified and galactosylated polyethyleneimine on hepatoma cells and mouse liver. Mol Ther. 2003 Feb;7(2):254-61.
14. Hashemi M, Parhiz BH, Hatefi A, Ramezani M. Modified polyethyleneimine with histidine-lysine short peptides as gene carrier. Cancer Gene Ther. 2011 Jan;18(1):12-9.
15. Xu P, Van Kirk EA, Zhan Y, Murdoch WJ, Radosz M, Shen Y. Targeted charge-reversal nanoparticles for nuclear drug delivery. Angew Chem Int Ed Engl. 2007;46(26):4999-5002.
16. Zheng M, Zhong Y, Meng F, Peng R, Zhong Z. Lipoic acid modified low molecular weight polyethylenimine mediates nontoxic and highly potent in vitro gene transfection. Mol Pharm. 2011 Dec 5;8(6):2434-43.
17. Doody AM, Korley JN, Dang KP, Zawaneh PN, Putnam D. Characterizing the structure/function parameter space of hydrocarbon-conjugated branched polyethylenimine for DNA delivery in vitro. J Control Release. 2006 Nov 28;116(2):227-37.
18. Kim SH, Mok H, Jeong JH, Kim SW, Park TG. Comparative evaluation of target-specific GFP gene silencing efficiencies for antisense ODN, synthetic siRNA, and siRNA plasmid complexed with PEI-PEG-FOL conjugate. Bioconjug Chem. 2006 Jan-Feb;17(1):241-4.
19. Thomas M, Klibanov AM. Enhancing polyethylenimine's delivery of plasmid DNA into mammalian cells. Proc Natl Acad Sci U S A. 2002 Nov 12;99(23):14640-5.
20. Alshamsan A, Haddadi A, Incani V, Samuel J, Lavasanifar A, Uludag H. Formulation and delivery of siRNA by oleic acid and stearic acid modified polyethylenimine. Mol Pharm. 2009 Jan-Feb;6(1):121-33.
21. Neamnark A, Suwantong O, Bahadur RK, Hsu CY, Supaphol P, Uludag H. Aliphatic lipid substitution on 2 kDa polyethylenimine improves plasmid delivery and transgene expression. Mol Pharm. 2009 Nov-Dec;6(6):1798-815.

22. Incani V, Tunis E, Clements BA, Olson C, Kucharski C, Lavasanifar A, et al. Palmitic acid substitution on cationic polymers for effective delivery of plasmid DNA to bone marrow stromal cells. J Biomed Mater Res A. 2007 May;81(2):493-504.
23. Gebhart CL, Sriadibhatla S, Vinogradov S, Lemieux P, Alakhov V, Kabanov AV. Design and formulation of polyplexes based on pluronic-polyethyleneimine conjugates for gene transfer. Bioconjug Chem. 2002 Sep-Oct;13(5):937-44.
24. Ochietti B, Lemieux P, Kabanov AV, Vinogradov S, St-Pierre Y, Alakhov V. Inducing neutrophil recruitment in the liver of ICAM-1-deficient mice using polyethyleneimine grafted with Pluronic P123 as an organ-specific carrier for transgenic ICAM-1. Gene Ther. 2002 Jul;9(14):939-45.
25. Belenkov AI, Alakhov VY, Kabanov AV, Vinogradov SV, Panasci LC, Monia BP, et al. Polyethyleneimine grafted with pluronic P85 enhances Ku86 antisense delivery and the ionizing radiation treatment efficacy in vivo. Gene Ther. 2004 Nov;11(22):1665-72.
26. Bromberg L, Raduyk S, Hatton TA, Concheiro A, Rodriguez-Valencia C, Silva M, et al. Guanidinylated polyethyleneimine-polyoxypropylene-polyoxyethylene conjugates as gene transfection agents. Bioconjug Chem. 2009 May 20;20(5):1044-53.
27. Tian H, Xiong W, Wei J, Wang Y, Chen X, Jing X, et al. Gene transfection of hyperbranched PEI grafted by hydrophobic amino acid segment PBLG. Biomaterials. 2007 Jun;28(18):2899-907.
28. Mahato RI, Lee M, Han S, Maheshwari A, Kim SW. Intratumoral delivery of p2CMVmIL-12 using water-soluble lipopolymers. Mol Ther. 2001 Aug;4(2):130-8.
29. Han S, Mahato RI, Kim SW. Water-soluble lipopolymer for gene delivery. Bioconjug Chem. 2001 May-Jun;12(3):337-45.
30. Yockman JW, Maheshwari A, Han SO, Kim SW. Tumor regression by repeated intratumoral delivery of water soluble lipopolymers/p2CMVmIL-12 complexes. J Control Release. 2003 Feb 21;87(1-3):177-86.
31. Kim WJ, Chang CW, Lee M, Kim SW. Efficient siRNA delivery using water soluble lipopolymer for anti-angiogenic gene therapy. J Control Release. 2007 Apr 23;118(3):357-63.

32. Wang DA, Narang AS, Kotb M, Gaber AO, Miller DD, Kim SW, et al. Novel branched poly(ethylenimine)-cholesterol water-soluble lipopolymers for gene delivery. Biomacromolecules. 2002 Nov-Dec;3(6):1197-207.
33. Furgeson DY, Chan WS, Yockman JW, Kim SW. Modified linear polyethylenimine-cholesterol conjugates for DNA complexation. Bioconjug Chem. 2003 Jul-Aug;14(4):840-7.
34. Habeeb AFSA. Determination of free amino groups in proteins by trinitrobenzenesulfonic acid. Analytical Biochemistry. 1966;14(3):328-36.
35. Evans BC, Nelson CE, Yu SS, Beavers KR, Kim AJ, Li H, et al. Ex vivo red blood cell hemolysis assay for the evaluation of pH-responsive endosomolytic agents for cytosolic delivery of biomacromolecular drugs. J Vis Exp. 2013(73):e50166.
36. ASTM. Standard Practice for Assessment of Hemolytic Properties of Materials. West Conshohocken, PA: ASTM International; 2000.
37. Chung CT, Niemela SL, Miller RH. One-step preparation of competent Escherichia coli: transformation and storage of bacterial cells in the same solution. Proceedings of the National Academy of Sciences of the United States of America. 1989;86(7):2172-5.
38. Sambrook J, Fritsch EF, Maniatis T. Molecular cloning: a laboratory manual: Cold spring harbor laboratory press; 1989.
39. Gibney K, Sovadinova I, Lopez AI, Urban M, Ridgway Z, Caputo GA, et al. Poly(ethylene imine)s as antimicrobial agents with selective activity. Macromolecular bioscience. 2012;12(9):1279-89.
40. Hall HK. Correlation of the Base Strengths of Amines1. Journal of the American Chemical Society. 1957 1957/10/01;79(20):5441-4.
41. Brissault B, Kichler A, Guis C, Leborgne C, Danos O, Cheradame H. Synthesis of Linear Polyethylenimine Derivatives for DNA Transfection. Bioconjugate Chemistry. 2003 2003/05/01;14(3):581-7.
42. Gibney KA, Sovadinova I, Lopez AI, Urban M, Ridgway Z, Caputo GA, et al. Poly(ethylene imine)s as antimicrobial agents with selective activity. Macromol Biosci. 2012 Sep;12(9):1279-89.
43. Akinc A, Thomas M, Klibanov AM, Langer R. Exploring polyethylenimine-mediated DNA transfection and the proton sponge hypothesis. The journal of gene medicine. 2005;7(5):657-63.

44. von Harpe A, Petersen H, Li Y, Kissel T. Characterization of commercially available and synthesized polyethylenimines for gene delivery. J Control Release. 2000 Nov 3;69(2):309-22.
45. Guillot C, Ménoret S, Guillonneau C, Braudeau C, Castro MG, Lowenstein P, et al. Active suppression of allogeneic proliferative responses by dendritic cells after induction of long-term allograft survival by CTLA4Ig. Blood. 2003;101(8):3325-33.
46. Guillot C, Mathieu P, Coathalem H, Le Mauff B, Castro MG, Tesson L, et al. Tolerance to cardiac allografts via local and systemic mechanisms after adenovirus-mediated CTLA4Ig expression. The Journal of Immunology. 2000;164(10):5258-68.
47. Brunet JF, Denizot F, Luciani MF, Roux-Dosseto M, Suzan M, Mattei MG, et al. A new member of the immunoglobulin superfamily--CTLA-4. Nature. 1987 Jul 16-22;328(6127):267-70.
48. Ledbetter JA, Imboden JB, Schieven GL, Grosmaire LS, Rabinovitch PS, Lindsten T, et al. CD28 ligation in T-cell activation: evidence for two signal transduction pathways. Blood. 1990 Apr 01;75(7):1531-9.
49. Dall'Era M, Davis J. CTLA4Ig: a novel inhibitor of costimulation. Lupus. 2004;13(5):372-6.
50. Herrero-Beaumont G, Martinez Calatrava MJ, Castaneda S. Abatacept mechanism of action: concordance with its clinical profile. Reumatol Clin. 2012 Mar-Apr;8(2):78-83.
51. Moreland L, Bate G, Kirkpatrick P. Abatacept. Nat Rev Drug Discov. 2006 Mar;5(3):185-6.
52. Dastiridou A, Kalogeropoulos C, Brazitikos P, Symeonidis C, Androudi S. New biologic-response modifiers in ocular inflammatory disease: beyond anti-TNF treatment. Expert Rev Clin Pharmacol. 2012 Sep;5(5):543-55.
53. Linsley PS, Nadler SG. The clinical utility of inhibiting CD28-mediated costimulation. Immunol Rev. 2009 May;229(1):307-21.
54. Prasher DC, Eckenrode VK, Ward WW, Prendergast FG, Cormier MJ. Primary structure of the Aequorea victoria green-fluorescent protein. Gene. 1992;111(2):229-33.

55. Chalfie M, Tu Y, Euskirchen G, Ward WW, Prasher DC. Green fluorescent protein as a marker for gene expression. Science. [10.1126/science.8303295]. 1994;263(5148):802.
56. Erbacher P, Bettinger T, Belguise-Valladier P, Zou S, Coll JL, Behr JP, et al. Transfection and physical properties of various saccharide, poly(ethylene glycol), and antibody-derivatized polyethylenimines (PEI). J Gene Med. 1999 May-Jun;1(3):210-22.
57. Nguyen HK, Lemieux P, Vinogradov SV, Gebhart CL, Guerin N, Paradis G, et al. Evaluation of polyether-polyethyleneimine graft copolymers as gene transfer agents. Gene Ther. 2000 Jan;7(2):126-38.
58. Vinogradov SV, Bronich TK, Kabanov AV. Self-assembly of polyamine-poly(ethylene glycol) copolymers with phosphorothioate oligonucleotides. Bioconjug Chem. 1998 Nov-Dec;9(6):805-12.
59. Hagendorfer H, Kaegi R, Parlinska M, Sinnet B, Ludwig C, Ulrich A. Characterization of silver nanoparticle products using asymmetric flow field flow fractionation with a multidetector approach--a comparison to transmission electron microscopy and batch dynamic light scattering. Anal Chem. 2012 Mar 20;84(6):2678-85.
60. Bhattacharjee S. DLS and zeta potential – What they are and what they are not? Journal of Controlled Release. 2016;235:337-51.
61. Cerda-Cristerna BI, Flores H, Pozos-Guillen A, Perez E, Sevrin C, Grandfils C. Hemocompatibility assessment of poly(2-dimethylamino ethylmethacrylate) (PDMAEMA)-based polymers. J Control Release. 2011 Aug 10;153(3):269-77.
62. Moreau E, Ferrari I, Drochon A, Chapon P, Vert M, Domurado D. Interactions between red blood cells and a lethal, partly quaternized tertiary polyamine. J Control Release. 2000 Feb 14;64(1-3):115-28.
63. Fischer D, Li Y, Ahlemeyer B, Krieglstein J, Kissel T. In vitro cytotoxicity testing of polycations: influence of polymer structure on cell viability and hemolysis. Biomaterials. 2003 Mar;24(7):1121-31.
64. Moghimi SM, Symonds P, Murray JC, Hunter AC, Debska G, Szewczyk A. A two-stage poly(ethylenimine)-mediated cytotoxicity: implications for gene transfer/therapy. Mol Ther. 2005 Jun;11(6):990-5.

65. Lechardeur D, Verkman A, Lukacs GL. Intracellular routing of plasmid DNA during non-viral gene transfer. Advanced drug delivery reviews. 2005;57(5):755-67.
66. Kong YcM. Experimental autoimmune thyroiditis in the mouse. Current protocols in immunology. 2007:15.7. 1-.7. 21.
67. Batteux F, Lores P, Bucchini D, Chiocchia G. Transgenic expression of Fas ligand on thyroid follicular cells prevents autoimmune thyroiditis. J Immunol. 2000 Feb 15;164(4):1681-8.
68. Zhang Z-L, Lin B, Yu L-Y, Shen S-X, Zhu L-H, Wang W-P, et al. Gene therapy of experimental autoimmune thyroiditis mice by in vivo administration of plasmid DNA coding for human interleukin-10. Acta pharmacologica Sinica. 2003;24(9):885-90.
69. Zhang ZL, Shen SX, Lin B, Yu LY, Zhu LH, Wang WP, et al. Intramuscular injection of interleukin-10 plasmid DNA prevented autoimmune diabetes in mice. Acta Pharmacol Sin. 2003 Aug;24(8):751-6.
70. Nakagome K, Dohi M, Okunishi K, Komagata Y, Nagatani K, Tanaka R, et al. In vivo IL-10 gene delivery suppresses airway eosinophilia and hyperreactivity by down-regulating APC functions and migration without impairing the antigen-specific systemic immune response in a mouse model of allergic airway inflammation. J Immunol. 2005 Jun 01;174(11):6955-66.
71. Batteux F, Tourneur L, Trebeden H, Charreire J, Chiocchia G. Gene therapy of experimental autoimmune thyroiditis by in vivo administration of plasmid DNA coding for Fas ligand. The Journal of Immunology. 1999;162(1):603-8.